Thermodynamic Properties of F = 1 Spinor Bose-Einstein Condensates

Diplomarbeit von

Parvis Soltan-Panahi

Hauptgutachter: Prof. Dr. Hagen Kleinert

vorgelegt dem
Fachbereich Physik der
Freien Universität Berlin
im September 2006

Abstract

In this thesis, the functional integral approach of many-body theory is employed to investigate the thermodynamic properties of both homogeneous and harmonically trapped $F = 1$ spinor Bose-Einstein condensates. Special emphasis is given to the systems dependence on the total magnetization, which is preserved in spinor Bose-Einstein condensates. The treatment is divided into three parts.

The first part provides the physical and mathematical basis of this thesis. The main-emphasis is given to the derivation of the functional integral representation of the grand-canonical partition function and the introduction of the background method.

The second part treats an interaction-free $F = 1$ spinor gas, where the system exhibits most of its quantum mechanical nature. Due to the combination of spin degrees of freedom and the conservation of the total magnetization, the $F = 1$ spinor system possesses three different phases: a gas, a ferromagnetic, and an antiferromagnetic phase. The latter phase is distinct because of the occurrence of a double condensation. Within the framework of the grand-canonical ensemble, we calculate the critical temperatures of the phase transitions and their dependence on the total magnetization. Moreover, the finite-size scaling is studied. A further characterization of the phases is given by determining the occupation number of the three different Zeeman states of both the excited and the Bose-Einstein condensed particles. The treatment of the ideal spinor gas is completed by the calculation of the heat capacity as a function of temperature and magnetization.

In the third part the treatment is generalized to the case of a weakly interacting $F = 1$ spinor gas. Due to the high dilution of the quantum gas, we restrict our study to a two-particle delta potential, which is characterized by two s-wave scattering lengths, and discuss the associated Gross-Pitaevskii equations. Within first-order perturbation theory, we derive an analytical expression for the shift of the first critical temperature of a harmonically trapped $F = 1$ spinor gas as a function of magnetization. Our results agree well with a numerical solution of the Hartree-Fock-Popov approximation [65].

Contents

Chapter 1

Introduction

1.1 History

In 1924 S.N. Bose [1] and A. Einstein [2,3] made the prediction that a phase transition occurs at a finite critical temperature where bosonic particles with a non-vanishing rest mass would macroscopically occupy the same quantum state. This phenomenon, called Bose-Einstein condensation (BEC), happens when the quantum wave functions of the particles start to overlap. In 1995 – more than 70 years after its theoretical prediction – BEC was realized experimentally for dilute atomic gases of rubidium [4], lithium [5], and sodium [6]. The experimental success was made possible by combining the techniques of laser cooling [7–9] and evaporative cooling [10] in a magnetic trap. Both the laser cooling and the experimental realization of BEC were rewarded with the Nobel prize in 1997 and 2001, respectively.

Since its experimental realization, the field of BEC has grown rapidly to one of the most active fields in both experimental and theoretical physics. Its attraction originates from the fact that Bose-Einstein condensates provide a unique model system for studying quantum phenomena from scratch. Furthermore, it has developed to a highly interdisciplinary field. For example, the experimental success of controlling the interaction strength between particles via a so-called Feshbach resonance [11, 12], opened the way to a comprehensive study of two-particle interactions such as reversible atom–molecule formation for both bosonic and fermionic atoms [13–15], which essentially belongs to the field of atomic and molecular physics. Furthermore, it offered the possibility to study the crossover from a Bose-Einstein condensate to a Bardeen-Cooper-Schrieffer superfluid [16]. Another highly notable example is the confinement of Bose-Einstein condensed particles in an optical lattice [17–19], which is basically an artificial crystal of light and therefore an ideal model system for studying solid-state physics phenomena under controllable conditions.

Among a considerable number of other intriguing aspects of BEC like the construction of an atomic laser [20] or the realization of an array of Josephson junctions with a BEC [21], the subject of Bose-Einstein condensates with atomic spin degrees of freedom, the so-called *spinor condensates* [22–24], are experiencing an enormously growing attention today. Its

emergence dates back to the year 1997, where a Bose-Einstein condensate was confined by optical means for the first time [25]. So far, spinor condensates with spin 1 have been realized in ^{23}Na [25] and in ^{87}Rb [26, 27]. The more complex spin 2 state has also been prepared for ^{87}Rb [27], whereas a promising candidate for a spin 3 spinor condensate is ^{52}Cr [28].

Spinor condensates can be considered as multi-component systems, which are described by a vector order parameter. In contrast to scalar BECs and mixtures of bosonic particles [29,30] the Zeeman components of spinor condensates are not subjected to the conservation of the number of particles. On the contrary, they show rich dynamic by exchanging particles among themselves. Therefore, spinor condensates exhibit a large number of quantum phenomena that do not occur in single-component or mixtures of single-component Bose-Einstein condensates. For instance, they allow the study of quantum magnetism such as spin dynamics [26, 27, 31], spin waves [32, 33], or spin mixing [34, 35]. Mostly, these effects are caused by coherent collisional processes between two atoms where the spin of each particle is changed while the total magnetization is preserved. This and its dependence on the quadratic Zeeman effect caused by a weak external magnetic field has been shown for both a spinor condensate with a macroscopic number of particles [36, 37] and an effective two-particle spinor condensate [38]. The latter was realized by embedding a macroscopic spinor condensate in an optical lattice, where each lattice site was on average occupied by only two particles.

1.2 Experiment

To realize Bose-Einstein condensation, the thermal de Broglie wavelength

$$\lambda = \sqrt{\frac{2\pi\hbar^2}{Mk_BT}}\ , \tag{1.1}$$

where M denotes the mass of the bosonic atoms, has to become comparable to the mean interatomic distances in the degenerate quantum gas. Therefore, the experimental setup has to be arranged in such a way that either the density of the quantum gas is sufficiently high or, accordingly, the temperature very low. The former possibility is ruled out due to the interaction between the atoms, which at high densities causes the formation of molecules or the transition to a liquid or even to a solid. On the contrary, to avoid the latter effects, the particle density has to be of the order of around $10^{14} - 10^{15}\,\mathrm{cm}^{-3}$, which is 4-5 magnitudes lower than the density of air under standard conditions. On the other hand, keeping the density of the gas as low as just stated yields a critical temperature of around 100 nK, which is far below the temperatures that are achieved by using conventional cooling techniques which are mainly based on the Joule-Thomson effect. Therefore, atoms have to be cooled differently.

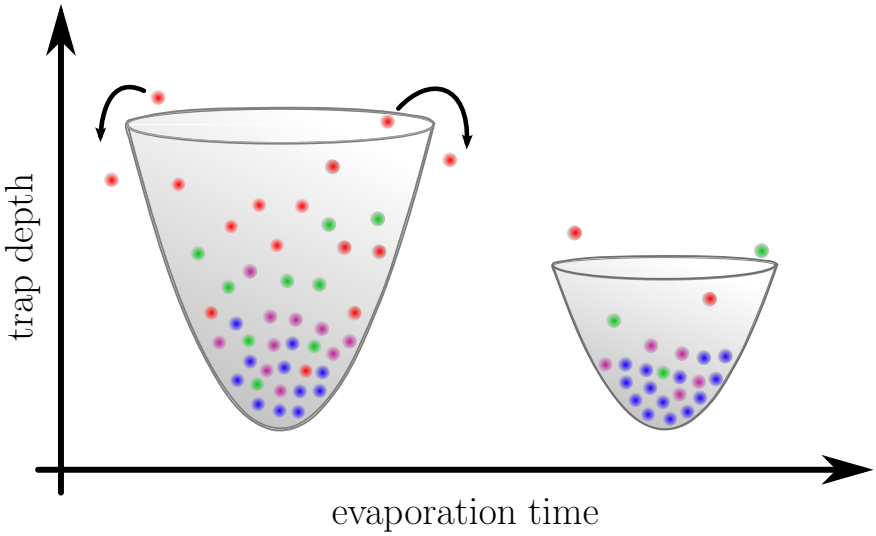

Figure 1.1: Evaporative cooling. The atoms are confined in an harmonic magnetic potential. With the help of radio-frequency radiation, the potential is practically cut at a certain trap depth and particles with higher energies than this depth leave the trap. Elastic collisional processes cause restoring the equilibrium state and a net cooling is achieved. During the evaporation time, the trap depth is lowered little by little causing a further decrease of temperature. With this method, one reaches temperatures down to 500 pK [39].

1.2.1 Cooling Techniques

Essentially, there are two cooling steps for reaching BEC. In the first step the cooling is performed using laser beams whose wavelengths are adjusted in such a way that, based on the Doppler effect, only atoms moving towards the laser absorb a photon and consequently slow down in this direction. This is because of the conservation of total momentum. After re-emitting the photon in a random direction a net cooling is achieved. Using this method one achieves temperatures of around 100 μK, which is still three magnitudes above the critical temperature of BEC.

To overcome this temperature difference, another cooling method, the so-called evaporative cooling, is applied. The idea of evaporative cooling is as simple as cooling a cup of coffee by blowing on it. Already this example indicates, that a kind of "cup" is needed to confine the degenerate quantum gas. This is achieved by applying a strong harmonic magnetic field that causes a trapping of magnetic atoms in a particular atomic Zeeman state. The cooling is then achieved by applying a radio-frequency radiation that induces a Zeeman spin flip of atoms with higher kinetic energy. Due to the fact that the trap is sensitive to the spin state of the atoms, the spin flipped atoms drop out of the trap. To ensure that only high energetic particles perform a spin flip, one takes advantage that the energy spacing of the Zeeman states depends on the external harmonic magnetic field and therefore on the position of the atoms in the trap. The radio frequency is tuned in such a way, that only particles in a

given distance to the center of the magnetic field, are in resonance and therefore leave the trap, i.e., the radio frequency field acts like cutting the magnetic potential at given height. The particular loss of high energetic atoms finally leads to Bose-Einstein condensation. A schematic picture of evaporative cooling is given in Figure 1.1.

Today, one can reach temperatures down to 500 pK [39] using a combination of these methods. However, the cooling techniques demand atoms with quite particular properties. First of all, in order to be cooled by laser light, the atoms must have an appropriate electronic transition. Furthermore, the employment of magnetic traps requires atoms with a strong magnetic dipole moment. The evaporative cooling is also only possible if the particles exchange their energy by elastic collisions, whereas inelastic collisions lead to molecule formation and to trap losses. Thus, the ratio between elastic and inelastic interaction plays a crucial role. The atoms which turned out best to match these conditions, are the alkali atoms. With the exception of francium all of them have been Bose-Einstein condensed. In their ground state of alkali atoms all electrons but one occupy closed shells and therefore do not contribute to the total electronic spin. The remaining electron is situated in the s-orbital of the atom and consequently does not have an orbital angular momentum, but an intrinsic spin of $S = 1/2$. On the other hand, the nucleus of the atom also carries a spin I that couples with the total electronic spin J. Thus, in case of an alkali atom the total atomic spin is given by $F = |I \pm 1/2|$ which is $2F + 1$ times degenerated. In most experiments the alkali atoms have a nuclear spin of $I = 3/2$ and therefore the ground state is split into the hyperfine states $F = 1$ and $F = 2$, where the former has the lower energy. In Figure 1.2 the hyperfine splitting of the electronic ground state of ^{87}Rb is schematically shown, which is typical for alkali atoms with $I = 3/2$.

1.2.2 Imaging Technique

The proper experiment starts with the achievement of Bose-Einstein condensation. With the help of electromagnetic radiation sources the experimentalist directly manipulates the atoms in the confining trap. During the experiment, the Bose-Einstein condensed cloud cannot be seen directly. However, imaging pictures are obtained by switching off the trap and measuring the spatial density distribution of the atomic cloud after free ballistic expansion. This is done by illuminating the atomic cloud by resonant light. The atoms absorb light and cast a shadow on a measurement device. Even though the resulting picture is the *spatial* density profile of the expanding cloud, it reflects the *momentum* density distribution of the trapped quantum gas. This is because particles with high momenta expand faster than particles with low momenta. Therefore, they are rather found at the edge of the expanded cloud whereas particles with low momenta are rather situated in the center.

1.2.3 Spinor Bose-Einstein Condensates

Due to the Zeeman splitting, the ground state of a magnetically trapped atom is not degenerate anymore. On the contrary, only particles in Zeeman states with negative magnetic

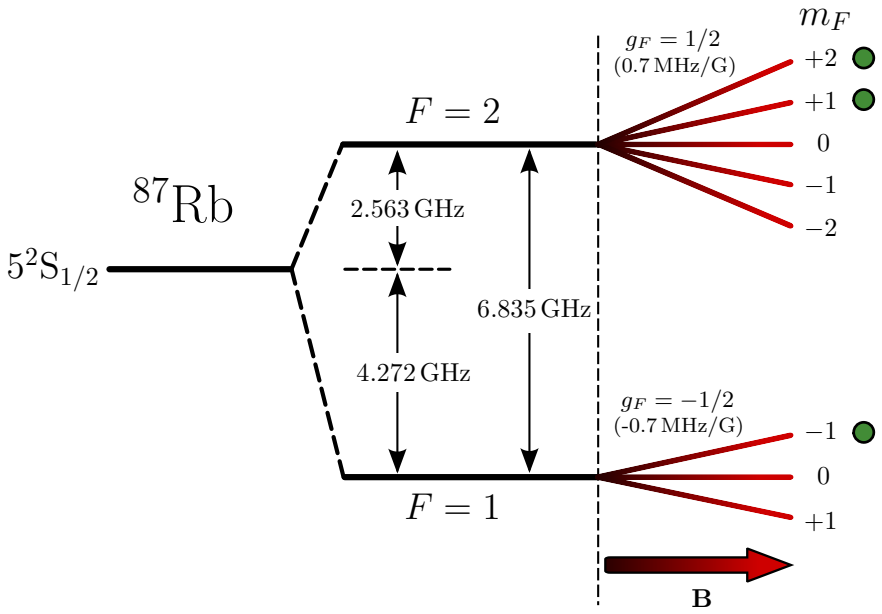

Figure 1.2: Hyperfine splitting of the electronic ground state of ^{87}Rb, which is exemplary for alkali atoms with nuclear spin $I = 3/2$. The three times degenerated $F = 1$ state represents the lowest energy state. An external magnetic field breaks the degeneracy and causes a Zeeman splitting. The Landé g_F factors denote the Zeeman splitting of the respective states. The green dots indicate states, which can be trapped magnetically. Experimental values are taken from Ref. [40].

dipole moment can be trapped experimentally. This is caused of the fact that a magnetic field with a local maximum cannot be created in a current-free region. Differently speaking, the spin degree of freedom is practically frozen out by the magnetic trap. The Zeeman states, which are magnetically trappable are shown in Figure 1.2 and denoted by a green dot. As a consequence of this Zeeman selection, magnetically trapped Bose-Einstein condensates behave exactly like spinless condensates would behave. In order to preserve the spin degrees of freedom and to create spinor Bose-Einstein condensates, the atoms have to be trapped independent from their Zeeman states. This is done with a so-called optical trap [41], which consists of laser beams that induce a dipole moment to the atoms. The atoms with the induced dipole moments in turn interact with the intensity gradient of the light field leading to their trapping. The optical trap can even confine atoms with a vanishing magnetic dipole moment. However, usually BEC is first evaporatively created in a magnetic trap and then loaded into an optical trap. Experimentally, the population of the different Zeeman states can arbitrarily be adjusted. After carrying out the respective manipulations of the atoms, the optical trap is switched off and the condensate falls freely. In order to distinguish between the different Zeeman components a Stern-Gerlach configuration, i.e., a strong inhomogeneous magnetic field is applied that spatially separates the Zeeman components. The probing of the atomic cloud is then again performed by the absorption imaging method as already described above.

1.3 Outline

This thesis is divided into three parts.

In the **first part** we give a summary of the necessary mathematical and physical content this thesis is based on. In **Chapter 2**, we briefly derive the grand-canonical partition function in its functional integral representation. Moreover, we explicitly calculate the generating grand-canonical partition function for an ideal $F = 1$ spinor system. The first part finishes in **Chapter 3** by introducing the background method, which provides the mathematical tool for studying phase transitions in BECs.

In the **second part** of this thesis, we treat the case of an ideal $F = 1$ spinor gas. We start in **Chapter 4** with deriving the effective action of a homogeneous and harmonically trapped spinor gas. For the case of the harmonically trapped system, we also elaborate the finite-size scaling. On the basis of the latter and of the background method, we then derive in **Chapter 5** the Gross-Pitaevskii equations of a $F = 1$ spinor system and discuss the respective solutions. Based on this, we calculate the first and the second critical temperature in **Chapter 6** as a function of total magnetization. In order to characterize the three occurring phases, we determine in **Chapter 7** the occupation number of the three Zeeman states for both the excited and the Bose-Einstein condensed particles. We finish this part with **Chapter 8**, which contains the calculation of the heat capacity with emphasis on the behavior at the points of phase transitions.

In **Part three** we extend our study to the case of a weakly interacting $F = 1$ spinor gas. We start with **Chapter 9** by introducing the two-particle interaction potential, which is described by two scalar quantities only. In **Chapter 10**, we treat the Gross-Pitaevskii equations of the interacting spinor system and adopt a Thomas-Fermi approximation to calculate their solutions. In **Chapter 11**, the main emphasis is given to the determination of an analytical expression for the first critical temperature. We use first-order perturbation theory and compare our result with the Hartree-Fock-Popov approximation carried out by others.

Part I

Mathematical and Physical Preliminaries

Chapter 2

Field Theoretic Description of Quantum Statistics

In this chapter we give a brief introduction into the methods and notations that are used throughout this thesis.

2.1 Second Quantization

Time-independent, non-relativistic, one-particle systems are described by the *Schrödinger equation*

$$\left[-\frac{\hbar^2}{2M}\Delta + V(\mathbf{x})\right]\varphi_{\mathbf{n}}(\mathbf{x}) = E_{\mathbf{n}}\varphi_{\mathbf{n}}(\mathbf{x}), \tag{2.1}$$

where $V(\mathbf{x})$ is an external potential and $\varphi_{\mathbf{n}}(\mathbf{x})$ the one-particle wave function with the energy $E_{\mathbf{n}}$. The eigenfunctions may be chosen in such a way that they fulfill the orthonormality condition

$$\int d^3x\, \varphi^*_{\mathbf{n}}(\mathbf{x})\varphi_{\mathbf{n}'}(\mathbf{x}) = \delta_{\mathbf{n}\mathbf{n}'}. \tag{2.2}$$

Moreover, because the Schrödinger Hamiltonian is Hermitian, its eigenfunctions obey a completeness relation (see Ref. [42])

$$\sum_{\mathbf{n}} \varphi^*_{\mathbf{n}}(\mathbf{x})\varphi_{\mathbf{n}}(\mathbf{x}') = \delta(\mathbf{x}-\mathbf{x}'). \tag{2.3}$$

The above formulation of quantum mechanics can be generalized to an arbitrary number of particles. We simply have to replace on the left-hand side of Eq. (2.1) the one-particle Hamiltonian by the sum of all one-particle Hamilton functions and additional terms due to the two, three, or higher particle interactions. However, for a larger number of particles it is very inconvenient to use the latter formulation of quantum mechanics. Many-particle physics is most conveniently described in terms of the so-called *second quantization*, which is basically a compact formulation of the first quantized Schrödinger quantum mechanics. In

the so-called *Fock space* of a many-particle system the Hamilton operator is given by[1] [43]

$$\begin{aligned}\hat{H} &= \int d^3x\, \hat{\phi}_a^\dagger(\mathbf{x}) \left[-\frac{\hbar^2}{2M}\Delta + V(\mathbf{x})\right] \hat{\phi}_a(\mathbf{x}) \\ &+ \int d^3x \int d^3x'\, \hat{\phi}_a^\dagger(\mathbf{x}) \hat{\phi}_{a'}^\dagger(\mathbf{x}') V_{aba'b'}^{(\mathrm{int})}(\mathbf{x},\mathbf{x}') \hat{\phi}_b(\mathbf{x}) \hat{\phi}_{b'}(\mathbf{x}'), \end{aligned} \tag{2.4}$$

where $V_{aba'b'}^{(\mathrm{int})}(\mathbf{x},\mathbf{x}')$ denotes the two-particle interaction potential[2], which fulfills the symmetry conditions

$$V_{aba'b'}^{(\mathrm{int})}(\mathbf{x},\mathbf{x}') = V_{aba'b'}^{(\mathrm{int})}(\mathbf{x}',\mathbf{x}) = V_{a'b'ab}^{(\mathrm{int})}(\mathbf{x}',\mathbf{x}). \tag{2.5}$$

The first equal sign is due to Newton's law actio=reactio, whereas the second one arises from the indistinguishability of identical particles. In Eq. (2.4) we have introduced the field operators

$$\hat{\phi}_a(\mathbf{x}) = \sum_{\mathbf{n}} \hat{\phi}_{\mathbf{n}a} \varphi_{\mathbf{n}}(\mathbf{x}), \qquad \hat{\phi}_a^\dagger(\mathbf{x}) = \sum_{\mathbf{n}} \hat{\phi}_{\mathbf{n}a}^\dagger \varphi_{\mathbf{n}}^*(\mathbf{x}). \tag{2.6}$$

Here, the annihilation operator $\hat{\phi}_{\mathbf{n}a}$ with

$$\hat{\phi}_{\mathbf{n}a} \,|\ldots, N_{\mathbf{n}a}, \ldots\rangle = \sqrt{N_{\mathbf{n}a}}\; |\ldots, N_{\mathbf{n}a} - 1, \ldots\rangle \tag{2.7}$$

and the creation operator $\hat{\phi}_{\mathbf{n}a}^\dagger$ with

$$\hat{\phi}_{\mathbf{n}a}^\dagger \,|\ldots, N_{\mathbf{n}a}, \ldots\rangle = \sqrt{N_{\mathbf{n}a} + 1}\; |\ldots, N_{\mathbf{n}a} + 1, \ldots\rangle \tag{2.8}$$

annihilate or create a particle in the state $|\mathbf{n}, a\rangle$, respectively. From Eq. (2.6) it follows, that Eqs. (2.7) and (2.8) also hold for the field operators $\hat{\phi}_a^\dagger(\mathbf{x})$, $\hat{\phi}_a(\mathbf{x})$ and therefore they create and annihilate particles at the place $\mathbf{x}$ in the state $|a\rangle$. In Eqs. (2.7) and (2.8), the ket vectors $|\ldots, N_{\mathbf{n}a}, \ldots\rangle$ denote a state in occupation number representation, which fulfills the orthonormality condition

$$\langle \ldots, N_{\mathbf{n}a}, \ldots | \ldots, N'_{\mathbf{n}a}, \ldots\rangle = \prod_{a=-1}^{1} \prod_{\mathbf{n}} \delta_{N_{\mathbf{n}a}, N'_{\mathbf{n}a}}. \tag{2.9}$$

The annihilation and creation operators obey the commutator relationship[3]

$$[\hat{\phi}_{\mathbf{n}a}, \hat{\phi}_{\mathbf{n}'b}^\dagger]_- = \delta_{ab}\delta_{\mathbf{n}\mathbf{n}'}, \tag{2.10}$$

$$[\hat{\phi}_{\mathbf{n}a}, \hat{\phi}_{\mathbf{n}'b}]_- = [\hat{\phi}_{\mathbf{n}a}^\dagger, \hat{\phi}_{\mathbf{n}'b}^\dagger]_- = 0. \tag{2.11}$$

[1] For indices referring to the spin degree of freedom, we use in the whole thesis *Einstein's summation convention*, i.e., repeated indices are understood to be summed over -1, 0, 1. We do not perform the sum if at least one index appears in brackets. Any exception from this rule will explicitly be mentioned in the text.

[2] Based on the experimental realization of Bose-Einstein condensates, we neglect any interaction between more than two particles.

[3] We remark that, strictly speaking, (2.7) and (2.8) follow from commutator relationships of the annihilation and creation operators.

Correspondingly, using the latter commutation relationships and Eqs. (2.3), (2.6) yields the commutators of the field operators

$$[\hat{\phi}_a(\mathbf{x}), \hat{\phi}_b^\dagger(\mathbf{x}')]_- = \delta_{ab}\,\delta(\mathbf{x}-\mathbf{x}'), \tag{2.12}$$

$$[\hat{\phi}_a(\mathbf{x}), \hat{\phi}_b(\mathbf{x}')]_- = [\hat{\phi}_a^\dagger(\mathbf{x}), \hat{\phi}_b^\dagger(\mathbf{x}', t)]_- = 0. \tag{2.13}$$

Now, we write down the operator of the total number of particles

$$\hat{N} = \hat{N}_1 + \hat{N}_0 + \hat{N}_{-1}, \tag{2.14}$$

where we have defined the operator of the total number of particles in the Zeeman state $|a\rangle$ by

$$\hat{N}_a = \int d^3x\, \hat{\phi}_a^\dagger(\mathbf{x})\hat{\phi}_a(\mathbf{x}) \quad \text{(no sum)}. \tag{2.15}$$

We also define the dimensionless total magnetization

$$\hat{\mathbf{M}} = \int d^3x\, \hat{\phi}_a^\dagger(\mathbf{x})\mathbf{F}_{ab}\hat{\phi}_b(\mathbf{x}), \tag{2.16}$$

where $\mathbf{F} = (F^x, F^y, F^z)^T$ is the matrix representation of the operator of angular momentum

$$F^x = \frac{1}{\sqrt{2}}\begin{pmatrix} 0 & 1 & 0 \\ 1 & 0 & 1 \\ 0 & 1 & 0 \end{pmatrix}, \quad F^y = \frac{i}{\sqrt{2}}\begin{pmatrix} 0 & -1 & 0 \\ 1 & 0 & -1 \\ 0 & 1 & 0 \end{pmatrix}, \quad F^z = \begin{pmatrix} 1 & 0 & 0 \\ 0 & 0 & 0 \\ 0 & 0 & -1 \end{pmatrix}. \tag{2.17}$$

The matrices F^x, F^y, and F^z fulfill the fundamental commutation relationship of angular momentum

$$[F^i, F^j] = i\epsilon_{ijk}F_k, \qquad \epsilon_{ijk} = \begin{cases} +1 & \text{for} \quad (i,j,k) \text{ even permutation of } (1,2,3), \\ -1 & \text{for} \quad (i,j,k) \text{ odd permutation of } (1,2,3), \\ 0 & \text{for} \qquad\qquad \text{otherwise.} \end{cases} \tag{2.18}$$

Consequently, pairwise different spin matrices, do not have a complete eigensystem in common. Physically this means, that only one of them can be measured independently. It is therefore sufficient to choose one particular axis as the quantization axis. Most conveniently, we choose the z-axis as quantization axis and define the operator of total magnetization as

$$\hat{M} \equiv \hat{M}_z = \int d^3x\, \hat{\phi}_a^\dagger(\mathbf{x})F_{ab}^z\hat{\phi}_b(\mathbf{x}). \tag{2.19}$$

Using (2.15), (2.17) and (2.19) yields

$$\hat{M} = \hat{N}_1 - \hat{N}_{-1}, \tag{2.20}$$

From the latter we observe that the magnetization is dimensionless. This is done for convenience. In this notation, if all particles occupy the Zeeman state $|1\rangle$ or $|-1\rangle$, then we have according to Eqs. (2.14) and (2.20) the identity $\hat{M} = \hat{N}$ or $\hat{M} = -\hat{N}$, respectively.

2.2 Coherent States

In the last section we have introduced the complete and orthonormal basis $\{|\ldots, N_{\mathbf{n}a}, \ldots\rangle\}$. Now, we will present another convenient complete basis, the so-called basis of coherent states, which turn out to be crucial for the derivation of the functional integral representation of quantum statistics. A state $|\psi\rangle$ is called coherent state, if it is an eigenvector of the annihilation operator, i.e.,

$$\hat{\phi}_{\mathbf{n}a}\,|\psi\rangle = \psi_{\mathbf{n}a}\,|\psi\rangle\,, \qquad \langle\psi|\,\hat{\phi}^\dagger_{\mathbf{n}a} = \langle\psi|\,\psi^*_{\mathbf{n}a}, \tag{2.21}$$

where $\psi_{\mathbf{n}a}$ is an ordinary, complex number and the vector $\langle\psi|$ the adjoint of $|\psi\rangle$. In analogy to Eq. (2.6) we define the complex functions

$$\psi_a(\mathbf{x}) = \sum_{\mathbf{n}} \psi_{\mathbf{n}a}\varphi_{\mathbf{n}}(\mathbf{x}), \qquad \psi^*_a(\mathbf{x}) = \sum_{\mathbf{n}} \psi^*_{\mathbf{n}a}\varphi^*_{\mathbf{n}}(\mathbf{x}). \tag{2.22}$$

Note that $\psi_a(\mathbf{x})$ can be a completely arbitrary function, because the functions $\varphi_{\mathbf{n}}(\mathbf{x})$ fulfill the completeness relation (2.3) and may therefore represent any function. From Eqs. (2.6) and (2.21) we deduce

$$\hat{\phi}_a(\mathbf{x})\,|\psi\rangle = \psi_a(\mathbf{x})\,|\psi\rangle\,, \qquad \langle\psi|\,\hat{\phi}^\dagger_a(\mathbf{x}) = \langle\psi|\,\psi^*_a(\mathbf{x}). \tag{2.23}$$

Therefore, a coherent state $|\psi\rangle$ to the annihilation operator $\hat{\phi}_{\mathbf{n}a}$ is also a coherent state to the respective field annihilation operator $\hat{\phi}_a(\mathbf{x})$.

Explicitly, a coherent state is given by (see Ref. [44])

$$|\psi\rangle = \exp\left\{\int d^3x\,\psi_a(\mathbf{x})\hat{\phi}^\dagger_a(\mathbf{x})\right\}|0\rangle\,, \tag{2.24}$$

where $|0\rangle$ is the vacuum state of the system in the occupation number representation. To show that (2.24) is a coherent state, we multiply the annihilation field operator $\hat{\phi}_a(\mathbf{x})$ from the left side, perform a Taylor expansion of the exponential function and make use of Eqs. (2.12), (2.13), (2.23). Another proof is given in Appendix A.1. Note that according to (2.24) it is possible to create an infinite number of coherent states to the annihilation operator $\hat{\phi}_{\mathbf{n}a}$.

The coherent states do not fulfill the orthogonality condition. As proven in Appendix A.2, their scalar product is given by

$$\langle\psi|\psi'\rangle = e^{(\psi|\psi')}, \tag{2.25}$$

where we have defined

$$(\psi|\psi') = \int d^3x\,\psi^*_a(\mathbf{x})\psi'_a(\mathbf{x}). \tag{2.26}$$

We immediately deduce from Eqs. (2.22), (2.23), and (2.25) that any functional operator $\hat{O}[\hat{\phi}^\dagger_a, \hat{\phi}_a]$ in its normal ordered form, i.e., all creation operators $\hat{\phi}^\dagger_a(\mathbf{x})$ are on the left side

and all annihilation operators $\hat{\phi}_a(\mathbf{x})$ are correspondingly on the right side, have the following matrix elements

$$\langle\psi|\,\hat{O}[\hat{\phi}^\dagger,\hat{\phi}]\,|\psi'\rangle = O[\psi^*,\psi']e^{(\psi|\psi')}. \tag{2.27}$$

Instead of $\hat{O}[\hat{\phi}_1^\dagger,\hat{\phi}_0^\dagger,\hat{\phi}_{-1}^\dagger,\hat{\phi}_1,\hat{\phi}_0,\hat{\phi}_{-1}]$ we wrote more conveniently $\hat{O}[\hat{\phi}^\dagger,\hat{\phi}]$. For functional expressions, we will use this notation throughout this thesis. We emphasize that the functional $O[\psi^*,\psi]$ on the right-hand side of (2.27) is not an operator anymore.

The most important property of the coherent states is that they obey a closure relation, which is proved in Appendix A.3 to be

$$\left[\prod_{a=-1}^{1}\int\mathcal{D}\psi_a^*\int\mathcal{D}\psi_a\right]e^{-(\psi|\psi)}\,|\psi\rangle\,\langle\psi| = \mathbb{1}, \tag{2.28}$$

where $\mathbb{1}$ denotes the unity operator of the Fock space. The measure in the latter equation is defined as

$$\prod_{a=-1}^{1}\int\mathcal{D}\psi_a^*\int\mathcal{D}\psi_a \equiv \prod_{a=-1}^{1}\prod_{\mathbf{n}}\int\frac{d\psi_{\mathbf{n}a}^*}{\sqrt{2\pi}}\int\frac{d\psi_{\mathbf{n}a}}{\sqrt{2\pi}}. \tag{2.29}$$

Efficiently, the new measure denotes, that we have to sum up any arbitrary function $\psi_a(\mathbf{x})$, which is seen from Eqs. (2.22), (2.24), and (2.26). Therefore, the definition in (2.29) is not only a convenient abbreviation, but it offers a new perspective to the coherent states.

The trace of an operator $\hat{O}$ is defined as

$$\operatorname{Tr}\hat{O} = \left(\sum_{N_{\mathbf{0}}=0}^{\infty}\cdots\sum_{N_{\mathbf{n}}=0}^{\infty}\cdots\right)\langle N_{\mathbf{0}},\ldots,N_{\mathbf{n}},\ldots|\,\hat{O}\,|N_{\mathbf{0}},\ldots,N_{\mathbf{n}},\ldots\rangle\,. \tag{2.30}$$

With the help of the complete relation (2.28) this reads in the coherent state representation

$$\operatorname{Tr}\hat{O} = \left[\prod_{a=-1}^{1}\int\mathcal{D}\psi_a^*\int\mathcal{D}\psi_a\right]e^{-(\psi|\psi)}\,\langle\psi|\,\hat{O}\,|\psi\rangle\,. \tag{2.31}$$

2.3 Partition Function

The central quantity to describe the equilibrium properties of a quantum mechanical system is the grand-canonical partition function [45]

$$\mathcal{Z} = \operatorname{Tr}\left[e^{-\beta(\hat{H}-\mu\hat{N}-\eta\hat{M})}\right], \tag{2.32}$$

where $\beta = 1/(k_BT)$, μ is the chemical potential, and η denotes the magnetic chemical potential that is introduced in order to fix the magnetization of the system. We emphasize that η is *not* a magnetic field, but a Lagrangian, which, like the Lagrangian μ, is a function

of temperature. Both μ and η have to be adjusted in such a way that the total number of particles and the total magnetization is kept fixed.

In quantum statistics, the mean-value of a physical observable associated with the operator $\hat{O}$ is given by

$$\left\langle \hat{O} \right\rangle = \frac{\mathrm{Tr}\left[\hat{O}\, e^{-\beta(\hat{H}-\mu\hat{N}-\eta\hat{M})}\right]}{\mathrm{Tr}\left[e^{-\beta(\hat{H}-\mu\hat{N}-\eta\hat{M})}\right]}. \tag{2.33}$$

Furthermore, the grand-canonical free energy is defined with the help of the partition function (2.32) as

$$\mathcal{F} = -\frac{1}{\beta}\log\mathcal{Z}. \tag{2.34}$$

Using Eqs. (2.32)–(2.34) yields the total number of particles

$$N \equiv \left\langle \hat{N} \right\rangle = -\frac{\partial\mathcal{F}}{\partial\mu} \tag{2.35}$$

and the total magnetization[4]

$$M \equiv \left\langle \hat{M} \right\rangle = -\frac{\partial\mathcal{F}}{\partial\eta}. \tag{2.36}$$

At this point we define the normalized total number of particles in the Zeeman state $|a\rangle$ and the normalized total magnetization

$$\mathcal{N}_a \equiv \frac{\left\langle \hat{N}_a \right\rangle}{N}, \qquad \mathcal{M} \equiv \frac{M}{N}, \qquad \mathcal{N} \equiv \frac{N}{N} = 1. \tag{2.37}$$

The notation $\mathcal{N}$ is introduced for clearness and will sometimes be used for explicitly implicating that the respective value is due to the total number of particles.

2.4 Functional Integral

In the last sections we have briefly introduced the physical framework of this thesis. With the help of the coherent states, discussed in Section 2.2, we will do now the step from the operator formulation of many-particle quantum statistics to the field theoretical functional integral formulation [44,46]. This is a generalization of Feynman's path integral approach to quantum mechanics [47]. We start our discussion by applying the coherent state representation of the tract (2.31) to the partition function in (2.32):

$$\mathcal{Z} = \left[\prod_{a=-1}^{1}\int\mathcal{D}\psi_a^*\int\mathcal{D}\psi_a\right] e^{-(\psi|\psi)}\left\langle\psi\right| e^{-\beta(\hat{H}-\mu\hat{N}-\eta\hat{M})}\left|\psi\right\rangle. \tag{2.38}$$

[4]The symbol for magnetization must not be mixed up with the one for mass of the atom, which is also denoted by M.

The latter equation indicates that we have to calculate the matrix elements of the kind $\langle\psi_P|\, e^{-\beta(\hat{H}-\mu\hat{N}-\eta\hat{M})}\,|\psi_0\rangle$, where we have set $|\psi_P\rangle = |\psi_0\rangle \equiv |\psi\rangle$. Note that relation (2.27) cannot be applied to the latter matrix elements, because, due to the exponential expression, the normal ordering condition is not fulfilled. At this point we recognize that the Boltzmann factor $e^{-\beta(\hat{H}-\mu\hat{N}-\eta\hat{M})}$ corresponds to the quantum mechanical time evolution operator $\hat{U}(t,0) = e^{-i(\hat{H}-\mu\hat{N}-\eta\hat{M})t/\hbar}$ evaluated at $t = -i\hbar\beta$. This motivates the definition of the *imaginary time* $\tau \equiv it$. The transition from real to imaginary time is called *Wick rotation*. Since in the whole thesis we only treat thermodynamic properties with no further time dependence, we will sometimes refer the imaginary time simply as time.

To calculate the matrix elements we use that $\hat{H}$, $\hat{N}$, and $\hat{M}$ commute among each other. This allows us to split the (imaginary) time interval $[0, \hbar\beta]$ into P pieces with $\Delta\tau = \hbar\beta/P$

$$\langle\psi_P|\, e^{-\beta(\hat{H}-\mu\hat{N}-\eta\hat{M})}\,|\psi_0\rangle = \langle\psi_P|\, e^{-\Delta\tau(\hat{H}-\mu\hat{N}-\eta\hat{M})/\hbar}\, e^{-\Delta\tau(\hat{H}-\mu\hat{N}-\eta\hat{M})/\hbar} \cdots e^{-\Delta\tau(\hat{H}-\mu\hat{N}-\eta\hat{M})/\hbar}\,|\psi_0\rangle\,. \tag{2.39}$$

Substituting between two time steps, respectively, the closure relation (2.28) leads to

$$\langle\psi_P|\, e^{-\beta(\hat{H}-\mu\hat{N}-\eta\hat{M})}\,|\psi_0\rangle = \left[\prod_{p=1}^{P-1}\prod_{a=-1}^{1}\int \mathcal{D}\psi_{ap}^{*}\int \mathcal{D}\psi_{ap}\; e^{-(\psi_p|\psi_p)}\right]\prod_{p'=1}^{P}\langle\psi_{p'}|\, e^{-\Delta\tau(\hat{H}-\mu\hat{N}-\eta\hat{M})/\hbar}\,|\psi_{p'-1}\rangle\,. \tag{2.40}$$

The reason for splitting the original matrix element in Eq. (2.38) into P matrix elements is the following. In order to get rid of the creation and annihilation operators in (2.38), we like to use the identity (2.27), which is only valid for operators, where all creation operators $\hat{\phi}_a^{\dagger}(\mathbf{x})$ are on the left side and all annihilation operators $\hat{\phi}_a(\mathbf{x})$ are situated on the right side. This is the case for the Hamiltonian (2.4), the particle number operators (2.14), (2.15), and the operator of total magnetization (2.19), but this is not true for the Boltzmann factor occurring in (2.38), because its Taylor expansion contains terms of the order $\hat{H}^2$ and higher. However, we expand the Boltzmann factor into a Taylor series yielding

$$e^{-\Delta\tau(\hat{H}-\mu\hat{N}-\eta\hat{M})/\hbar} = \left[1 - \frac{\Delta\tau}{\hbar}(\hat{H}-\mu\hat{N}-\eta\hat{M}) + \frac{1}{2}\frac{(\Delta\tau)^2}{\hbar^2}(\hat{H}-\mu\hat{N}-\eta\hat{M})^2 + \ldots\right] \tag{2.41}$$

and observe that in the $P \to \infty$ limit, terms of the order $(\Delta\tau)^2$ are negligible. Therefore, according to (2.41), Eq. (2.27) can be applied on the right-hand sided matrix element of Eq. (2.40). Using Eqs. (2.4), (2.14), (2.19), (2.23), and (2.27) we get in first order of $\Delta\tau$

$$\langle\psi_{p'}|\, e^{-\Delta\tau(\hat{H}-\mu\hat{N}-\eta\hat{M})\hbar}\,|\psi_{p'-1}\rangle = \exp\left\{(\psi_{p'}|\psi_{p'-1}) - \Delta\tau\tilde{H}[\psi_{p'}^{*},\psi_{p'-1}]/\hbar\right\}, \tag{2.42}$$

with the functional expression

$$\begin{aligned}\tilde{H}[\psi^*_{p'},\psi_{p'-1}] &\equiv H[\psi^*_{p'},\psi_{p'-1}]-\mu N[\psi^*_{p'},\psi_{p'-1}]-\eta M[\psi^*_{p'},\psi_{p'-1}] \\ &= \int d^3x\,\psi^*_{ap'}(\mathbf{x})\left\{\left[-\frac{\hbar^2}{2M}\Delta+V(\mathbf{x})-\mu\right]\delta_{ab}-\eta F^z_{ab}\right\}\psi_{b(p'-1)}(\mathbf{x}) \\ &\quad+\int d^3x\int d^3x'\,\psi^*_{ap'}(\mathbf{x})\psi^*_{a'p'}(\mathbf{x}')V^{(\mathrm{int})}_{aba'b'}(\mathbf{x},\mathbf{x}')\psi_{b(p'-1)}(\mathbf{x})\psi_{b'(p'-1)}(\mathbf{x}'),\end{aligned} \tag{2.43}$$

where we are not supposed to sum over p'. Note that no operator appears in the latter functional expression anymore.

Substituting (2.42) in (2.40) yields after some manipulations

$$\begin{aligned}\langle\psi_P|\,e^{-\beta(\hat{H}-\mu\hat{N}-\eta\hat{M})}\,|\psi_0\rangle &= e^{(\psi_P|\psi_P)}\left[\prod_{p=1}^{P-1}\prod_{a=-1}^{1}\int\mathcal{D}\psi^*_{ap}\int\mathcal{D}\psi_{ap}\right] \\ &\times\exp\left\{-\frac{1}{\hbar}\sum_{p'=1}^{P}\Delta\tau\left[\hbar\int d^3x\,\psi^*_{ap'}(\mathbf{x})\frac{\psi_{ap'}(\mathbf{x})-\psi_{a(p'-1)}(\mathbf{x})}{\Delta\tau}+\tilde{H}[\psi^*_{p'},\psi_{p'-1}]\right]\right\}.\end{aligned} \tag{2.44}$$

We set $\psi_a(\mathbf{x},\tau_p)\equiv\psi_{ap}(\mathbf{x})$ with $\tau_p\equiv p\hbar\beta/P$ and take in Eq. (2.44) the continuum limit $P\to\infty$ yielding

$$\begin{aligned}&\langle\psi_P|\,e^{-\beta(\hat{H}-\mu\hat{N}-\eta\hat{M})}\,|\psi_0\rangle \\ &\qquad= e^{\left(\psi(\hbar\beta)\middle|\psi(\hbar\beta)\right)}\left[\prod_{a=-1}^{1}\int_{\psi^*(0)=\psi^*_0}^{\psi^*(\hbar\beta)=\psi^*_P}\mathcal{D}\psi^*_a\int_{\psi(0)=\psi_0}^{\psi(\hbar\beta)=\psi_P}\mathcal{D}\psi_a\right]e^{-\mathcal{A}[\psi^*,\psi]/\hbar},\end{aligned} \tag{2.45}$$

where we have introduced the Euclidean action

$$\mathcal{A}[\psi^*,\psi]=\mathcal{A}^{(0)}[\psi^*,\psi]+\mathcal{A}^{(\mathrm{int})}[\psi^*,\psi]. \tag{2.46}$$

The first contribution corresponds to a non-interacting $F=1$ spinor gas

$$\mathcal{A}^{(0)}[\psi^*,\psi]=\int_0^{\hbar\beta}d\tau\int d^3x\,\psi^*_a(\mathbf{x},\tau)\left\{\left[\hbar\frac{\partial}{\partial\tau}-\frac{\hbar^2}{2M}\Delta+V(\mathbf{x})-\mu\right]\delta_{ab}-\eta F^z_{ab}\right\}\psi_b(\mathbf{x},\tau) \tag{2.47}$$

and the second is due to the interaction of the particles:

$$\mathcal{A}^{(\mathrm{int})}[\psi^*,\psi]=\frac{1}{2}\int_0^{\hbar\beta}d\tau\int d^3x\int d^3x'\,V^{(\mathrm{int})}_{aba'b'}(\mathbf{x},\mathbf{x}')\psi^*_a(\mathbf{x},\tau)\psi_b(\mathbf{x},\tau)\psi^*_{a'}(\mathbf{x}',\tau)\psi_{b'}(\mathbf{x}',\tau). \tag{2.48}$$

In Eq. (2.45) the functional integration has to be carried out over all fields $\psi_a(\mathbf{x},\tau)$, $\psi^*_a(\mathbf{x},\tau)$ with the boundary conditions

$$\psi_a(\mathbf{x},0)=\psi_{a0}(\mathbf{x}),\qquad\psi_a(\mathbf{x},\hbar\beta)=\psi_{aP}(\mathbf{x}) \tag{2.49}$$

and the corresponding one for the complex conjugated.

Note that strictly speaking, we have to add to the imaginary time dependency of the complex conjugated fields $\psi^*(\mathbf{x},\tau)$ in Eq. (2.47), (2.48) an infinitesimal positive quantity σ. This arises from the fact that ψ^* in the time-sliced version is always one time step in advance to ψ, which can be seen from (2.43), (2.44). This is because the operators $\hat{H}$, $\hat{N}$, $\hat{M}$ are always time-ordered, i.e., the creation operators are always on the left side and the annihilation operator on the right side. However, in most cases we can neglect this additional infinitesimal constant and we therefore omit writing this additional constant, but we keep this in mind for Appendix C.1, where we calculate the Green's function for equal imaginary time.

Setting $\psi_{a0}(\mathbf{x}) = \psi_{aP}(\mathbf{x})$ and substituting Eq. (2.45) in (2.38) finally yields the field theoretical grand-canonical partition function

$$\boxed{\mathcal{Z} = \left[\prod_{a=-1}^{1} \oint \mathcal{D}\psi_a^* \oint \mathcal{D}\psi_a\right] e^{-\mathcal{A}[\psi^*,\psi]/\hbar},} \tag{2.50}$$

where the loop at the integral sign denotes that we have to functional integrate all fields, which are periodic in τ such that

$$\psi_a(\mathbf{x},0) = \psi_a(\mathbf{x},\hbar\beta), \qquad \psi_a^*(\mathbf{x},0) = \psi_a^*(\mathbf{x},\hbar\beta), \qquad a = 1,0,-1 \tag{2.51}$$

is fulfilled.

2.5 Generating Grand-Canonical Partition Function

In this section we explicitly calculate the generating grand-canonical partition function of an ideal $F = 1$ spinor gas. In this particular case, the functional (2.50) can be solved analytically. The solution of the generating functional will be used throughout the thesis and is therefore very important.

In analogy to the result (2.50) of the last section, we write the generating grand-canonical partition function as the functional integral

$$\mathcal{Z}^{(0)}[j^*,j] = \left[\prod_{a=-1}^{1} \oint \mathcal{D}\psi_a^* \oint \mathcal{D}\psi_a\right] e^{-\mathcal{A}^{(0)}[\psi^*,\psi;j^*,j]/\hbar}, \tag{2.52}$$

where the generating action functional is given by

$$\mathcal{A}^{(0)}[\psi^*,\psi;j^*,j] = \mathcal{A}^{(0)}[\psi^*,\psi] - \int_0^{\hbar\beta} d\tau \int d^3x \Big\{ j_a^*(\mathbf{x},\tau)\psi_a(\mathbf{x},\tau) + \psi_a^*(\mathbf{x},\tau) j_a(\mathbf{x},\tau) \Big\}. \tag{2.53}$$

Here, we have introduced arbitrary current fields $j_a^*(\mathbf{x},\tau)$, $j_a(\mathbf{x},\tau)$, which couple linearly to the Bose fields $\psi_a(\mathbf{x},\tau)$ and $\psi_a^*(\mathbf{x},\tau)$, respectively. The action functional $\mathcal{A}^{(0)}[\psi^*,\psi]$ is

the same as in (2.47). For vanishing current fields, the generating grand-canonical partition function coincides with (2.50) for vanishing two-particle interaction.

In order to calculate the functional integral (2.52) we perform a Fourier-Matsubara decomposition of the fields

$$\psi_a(\mathbf{x},\tau) = \sum_{m=-\infty}^{\infty}\sum_{\mathbf{n}} \psi_{\mathbf{n}ma}\,\varphi_{\mathbf{n}}(\mathbf{x}) f^{(m)}(\tau) \tag{2.54}$$

$$\psi_a^*(\mathbf{x},\tau) = \sum_{m=-\infty}^{\infty}\sum_{\mathbf{n}} \psi_{\mathbf{n}ma}^*\varphi_{\mathbf{n}}^*(\mathbf{x}) f^{*(m)}(\tau). \tag{2.55}$$

Here, $\{\varphi_{\mathbf{n}}(\mathbf{x})\}$ is the complete orthonormal set of functions that fulfills the eigenvalue equation (2.1). Furthermore, we have introduced the Matsubara functions

$$f^{(m)}(\tau) = e^{-i\omega_m\tau}, \qquad f^{*(m)}(\tau) = e^{i\omega_m\tau} \tag{2.56}$$

with the Matsubara frequencies

$$\omega_m = \frac{2\pi}{\hbar\beta}\,m, \qquad m = 0, \pm1, \pm2, \dots\ . \tag{2.57}$$

The set of Matsubara functions $\{f^{(m)}(\tau)\}$ provide a complete, orthogonal basis in the space of $\hbar\beta$-periodic function. In other words, any function of τ with the period $\hbar\beta$, can be represented as a linear combination of Matsubara functions. Note that according to the periodicity condition in (2.51) all in here considered fields are periodic in τ and therefore have a Fourier-Matsubara representation (2.54), (2.55).

Using Eqs. (2.56) and (2.57) it is easily shown that the Matsubara functions are orthogonal:

$$\int_0^{\hbar\beta} d\tau\, f^{(m)}(\tau) f^{*(m')}(\tau) = \int_0^{\hbar\beta} d\tau\, e^{i(\omega_m-\omega_{m'})\tau} = \hbar\beta\delta_{mm'}. \tag{2.58}$$

Now, we prove the completeness relation for the Matsubara functions. Explicitly substituting the Matsubara frequencies (2.57) in (2.56) and performing the sum over m yields

$$\sum_{m=-\infty}^{\infty} f^{(m)}(\tau) f^{*(m)}(\tau') = \sum_{m=-\infty}^{\infty} e^{-i2\pi m(\tau-\tau')/(\hbar\beta)}. \tag{2.59}$$

With the help of the Poisson summation formula (B.1) the latter equation reads

$$\sum_{m=-\infty}^{\infty} f^{(m)}(\tau) f^{*(m)}(\tau') = \hbar\beta \sum_{n=-\infty}^{\infty} \delta\left(\tau-\tau'-n\hbar\beta\right), \tag{2.60}$$

which shows that the Matsubara functions are complete in the $\hbar\beta$-periodic space. In this thesis, we restrict ourself to the limits $\tau, \tau' \in [0, \hbar\beta)$ and therefore the right-hand side of

Eq. (2.60) reduces to $\hbar\beta\,\delta(\tau-\tau')$.

Substituting the Fourier-Matsubara transformed fields (2.54), (2.55) in Eqs. (2.47), (2.53) and considering the orthogonality properties (2.2), (2.58) and the spin matrix F^z in (2.17) yields for the generating action

$$\mathcal{A}[\psi^*,\psi;j^*,j]=\hbar\sum_{m=-\infty}^{\infty}\sum_{\mathbf{n}}\sum_{a=-1}^{1}\left(\beta\psi^*_{\mathbf{n}ma}E_{\mathbf{n}ma}\psi_{\mathbf{n}ma}+\psi_{\mathbf{n}ma}c^*_{\mathbf{n}ma}+\psi^*_{\mathbf{n}ma}c_{\mathbf{n}ma}\right) \tag{2.61}$$

where we have used the short-hand notation

$$c_{\mathbf{n}ma} = -\int_0^{\hbar\beta}d\tau\int d^3x\, j_a(\mathbf{x},\tau)\varphi^*_{\mathbf{n}}(\mathbf{x})f^{*(m)}(\tau)/\hbar, \tag{2.62}$$

$$c^*_{\mathbf{n}ma} = -\int_0^{\hbar\beta}d\tau\int d^3x\, j^*_a(\mathbf{x},\tau)\varphi_{\mathbf{n}}(\mathbf{x})f^{(m)}(\tau)/\hbar, \tag{2.63}$$

and the eigenvalue

$$E_{\mathbf{n}ma}=-i\hbar\omega_m+E_{\mathbf{n}}-\mu-\eta a,\qquad a=1,0,-1 \tag{2.64}$$

of the eigenvalue problem

$$\left[\hbar\frac{\partial}{\partial\tau}-\frac{\hbar^2}{2M}\Delta+V(\mathbf{x})-\mu-\eta a\right]\varphi_{\mathbf{n}}(\mathbf{x})f^{(m)}(\tau)=E_{\mathbf{n}ma}\,\varphi_{\mathbf{n}}(\mathbf{x})f^{(m)}(\tau). \tag{2.65}$$

Due to the change of the functional variables in (2.54), (2.55), the measure of the functional integral over all periodic fields reads

$$\prod_{a=-1}^{1}\oint\mathcal{D}\psi^*_a\oint\mathcal{D}\psi_a=\prod_{m=-\infty}^{\infty}\prod_{\mathbf{n}}\prod_{a=-1}^{1}\int\frac{d\psi^*_{\mathbf{n}ma}}{\sqrt{2\pi}}\int\frac{d\psi_{\mathbf{n}ma}}{\sqrt{2\pi}}, \tag{2.66}$$

where the factor $(2\pi)^{-1}$ originates from the closure relation of the coherent states (2.28), (2.29). Inserting (2.61), (2.66) in the functional expression for the generating grand-canonical partition function (2.52) leads to

$$\begin{aligned}\mathcal{Z}^{(0)}[j^*,j] &= \left[\prod_{m=-\infty}^{\infty}\prod_{\mathbf{n}}\prod_{a=-1}^{1}\int\frac{d\psi^*_{\mathbf{n}ma}}{\sqrt{2\pi}}\int\frac{d\psi_{\mathbf{n}ma}}{\sqrt{2\pi}}\right] \\ &\quad\times\exp\left\{-\sum_{m=-\infty}^{\infty}\sum_{\mathbf{n}}\sum_{a=-1}^{1}\left(\beta\psi^*_{\mathbf{n}ma}E_{\mathbf{n}ma}\psi_{\mathbf{n}ma}+\psi_{\mathbf{n}ma}c^*_{\mathbf{n}ma}+\psi^*_{\mathbf{n}ma}c_{\mathbf{n}ma}\right)\right\},\end{aligned} \tag{2.67}$$

which reads more conveniently

$$\begin{aligned}\mathcal{Z}^{(0)}[j^*,j] &= \prod_{m=-\infty}^{\infty}\prod_{\mathbf{n}}\prod_{a=-1}^{1}\int\frac{d\psi^*_{\mathbf{n}ma}}{\sqrt{2\pi}}\int\frac{d\psi_{\mathbf{n}ma}}{\sqrt{2\pi}} \\ &\quad\times\exp\Big\{-\beta\psi^*_{\mathbf{n}ma}E_{\mathbf{n}ma}\psi_{\mathbf{n}ma}-\psi_{\mathbf{n}ma}c^*_{\mathbf{n}ma}-\psi^*_{\mathbf{n}ma}c_{\mathbf{n}ma}\Big\}.\end{aligned} \tag{2.68}$$

The latter integrals are of the following type

$$I = \int \frac{d\psi^*}{\sqrt{2\pi}} \int \frac{d\psi}{\sqrt{2\pi}}\, e^{-(\psi^* A\psi + \psi c^* + \psi^* c)}. \tag{2.69}$$

Introducing the substitutions

$$\psi = \psi_1 + i\psi_2, \qquad c = c_1 + ic_2, \qquad \psi_1, \psi_2, c_1, c_2 \in \mathbb{R} \tag{2.70}$$

equation (2.69) transforms to the product of two integrals of ordinary Gaussian form:

$$\begin{aligned} I &= \frac{1}{\pi} \int_{-\infty}^{\infty} d\psi_1\, e^{-(A\psi_1^2 + 2c_1\psi_1)} \int_{-\infty}^{\infty} d\psi_2\, e^{-(A\psi_2^2 + 2c_2\psi_2)} \\ &= \frac{e^{c^* A^{-1} c}}{A}, \qquad \mathrm{Re}\, A > 0\,. \end{aligned} \tag{2.71}$$

Comparing (2.69) with (2.68) leads to the identifications $A = \beta E_{\mathbf{n}ma}$, $c = c_{\mathbf{n}ma}$, $c^* = c^*_{\mathbf{n}ma}$. Using the latter and Eqs. (2.62)–(2.64), (2.68), and (2.71) yields the generating partition function of the $F = 1$ spinor gas

$$\boxed{\mathcal{Z}^{(0)}[j^*, j] = \mathcal{Z}^{(0)} \exp\left\{ \frac{1}{\hbar^2} \int_0^{\hbar\beta} d\tau \int_0^{\hbar\beta} d\tau' \int d^3x \int d^3x'\, j_a^*(\mathbf{x}, \tau) G_{ab}^{(0)}(\mathbf{x}, \tau; \mathbf{x}', \tau') j_b(\mathbf{x}', \tau') \right\}} \tag{2.72}$$

with the partition function for vanishing current fields

$$\mathcal{Z}^{(0)} = \prod_{m=-\infty}^{\infty} \prod_{\mathbf{n}} \prod_{a=-1}^{1} \frac{1}{\beta\left(-i\hbar\omega_m + E_{\mathbf{n}} - \mu - a\eta\right)}, \qquad E_{\mathbf{n}} - \mu - a\eta > 0 \tag{2.73}$$

and the *Green's function* of the ideal $F = 1$ spinor system

$$G_{ab}^{(0)}(\mathbf{x}, \tau; \mathbf{x}', \tau') = \frac{1}{\beta} \sum_{\mathbf{n}} \sum_{m=-\infty}^{\infty} \frac{\varphi_{\mathbf{n}}(\mathbf{x}) \varphi_{\mathbf{n}}^*(\mathbf{x}') e^{-i\omega_m(\tau - \tau')}}{-i\hbar\omega_m + E_{\mathbf{n}} - \mu - a\eta}\, \delta_{ab}. \tag{2.74}$$

Here, we have explicitly inserted the Matsubara functions (2.56). Note that the Green's function (2.74) satisfies the equation

$$\left\{ \left[\hbar \frac{\partial}{\partial\tau} - \frac{\hbar^2}{2M}\Delta + V(\mathbf{x}) - \mu \right] \delta_{ac} - \eta F_{ac}^z \right\} G_{cb}^{(0)}(\mathbf{x}, \tau; \mathbf{x}', \tau') = \hbar\, \delta_{ab}\, \delta(\mathbf{x} - \mathbf{x}')\, \delta(\tau - \tau'), \tag{2.75}$$

which is shown with the help of the completeness relations (2.3), (2.60) and Eqs. (2.64), (2.65). Therefore, $G_{ab}^{(0)}$ is, indeed, the Green's function.

Chapter 3

Background Method

Bose-Einstein condensation belongs to the field of critical phenomena [45, 48]. There, the thermodynamic properties are investigated close to a critical temperature, where a phase transition occurs. The different phases involved in a phase transition, usually differ in their symmetry properties. A famous example is the ferromagnetic phase transition in metals. There, below a certain critical temperature, called the Curie temperature, the system spontaneously magnetizes, whereas above the Curie temperature the system is not magnetized at all. The magnetization defines a preferred direction in space and therefore the rotational invariance is destroyed. The loss of the symmetry has to be accounted for introducing another describing parameter, the so-called *order parameter*. In a ferromagnetic system the order parameter is given by the expectation value of the magnetization. In the case of spinor Bose-Einstein condensation, the order parameter is given by the expectation value of the fields

$$\Psi_a(\mathbf{x},\tau) \equiv \langle \psi_a(\mathbf{x},\tau) \rangle \,, \qquad a = 1, 0, -1. \tag{3.1}$$

Note that the order parameter has a vectorial form with three components. For spinor Bose-Einstein condensates, the modulus square $|\Psi_a(\mathbf{x},\tau)|^2$ describes the particle density of the condensed particles in the Zeeman state $|a\rangle$.

In order to take account the critical properties of spinor Bose-Einstein condensates, we introduce a convenient method, called *background method* [47–50], to treat the spinor system below and above the critical temperature. The starting point of the background method is the decomposition of the fields into a background field $\Psi_a(\mathbf{x},\tau)$ and a fluctuation field $\delta\psi_a(\mathbf{x},\tau)$

$$\begin{aligned} \psi_a^*(\mathbf{x},\tau) &= \Psi_a^*(\mathbf{x},\tau) + \delta\psi_a^*(\mathbf{x},\tau), \\ \psi_a(\mathbf{x},\tau) &= \Psi_a(\mathbf{x},\tau) + \delta\psi_a(\mathbf{x},\tau), \qquad a = 1, 0, -1. \end{aligned} \tag{3.2}$$

The fluctuation fields $\delta\psi_a(\mathbf{x},\tau)$ denote all fields that are spatially orthogonal to the background fields, i.e., they fulfill the condition [51]

$$\int d^3x \, \Psi_a^*(\mathbf{x},\tau)\delta\psi_a(\mathbf{x},\tau) = 0. \tag{3.3}$$

Substituting the decomposition of the fields (3.2) into the Euclidean action (2.46)–(2.48) yields

$$\mathcal{A}[\Psi^*+\delta\psi^*,\Psi+\delta\psi]=\mathcal{A}[\Psi^*,\Psi]+\mathcal{A}^{(1)}[\delta\psi^*,\delta\psi]+\mathcal{A}^{(2)}[\delta\psi^*,\delta\psi]+\mathcal{A}^{(\mathrm{cor})}[\delta\psi^*,\delta\psi], \quad (3.4)$$

where the first term on the right-hand side is the Euclidean action evaluated at the background fields

$$\begin{aligned}\mathcal{A}[\Psi^*,\Psi] \;=& \int_0^{\hbar\beta}d\tau\int d^3x\,\Psi_a^*(\mathbf{x},\tau)\left\{\left[\hbar\frac{\partial}{\partial\tau}-\frac{\hbar^2}{2M}\Delta+V(\mathbf{x})\right]\delta_{ab}-\eta F_{ab}^z\right\}\Psi_b(\mathbf{x},\tau) \quad (3.5)\\ &+\frac{1}{2}\int_0^{\hbar\beta}d\tau\int d^3x\int d^3x'\,V^{(\mathrm{int})}_{aba'b'}(\mathbf{x},\mathbf{x}')\Psi_a^*(\mathbf{x},\tau)\Psi_b(\mathbf{x},\tau)\Psi_{a'}^*(\mathbf{x}',\tau)\Psi_{b'}(\mathbf{x}',\tau).\end{aligned}$$

The the linear contribution to the action reads

$$\begin{aligned}\mathcal{A}^{(1)}[\delta\psi^*,\delta\psi]=&\int_0^{\hbar\beta}d\tau\int d^3x\,\Psi_a^*(\mathbf{x},\tau)\left\{\left[\hbar\frac{\partial}{\partial\tau}-\frac{\hbar^2}{2M}\Delta+V(\mathbf{x})\right]\delta_{ab}-\eta F_{ab}^z\right\}\delta\psi_b(\mathbf{x},\tau)\\ &+\delta\psi_a^*(\mathbf{x},\tau)\left\{\left[\hbar\frac{\partial}{\partial\tau}-\frac{\hbar^2}{2M}\Delta+V(\mathbf{x})\right]\delta_{ab}-\eta F_{ab}^z\right\}\Psi_b(\mathbf{x},\tau)+\int_0^{\hbar\beta}d\tau\int d^3x\int d^3x'\\ &\times V^{(\mathrm{int})}_{aba'b'}(\mathbf{x},\mathbf{x}')\Psi_a^*(\mathbf{x},\tau)\Psi_b(\mathbf{x},\tau)\Big[\Psi_{a'}^*(\mathbf{x}',\tau)\,\delta\psi_{b'}(\mathbf{x}',\tau)+\Psi_{b'}(\mathbf{x}',\tau)\,\delta\psi_{a'}^*(\mathbf{x}',\tau)\Big], \quad (3.6)\end{aligned}$$

using (2.5) the quadratic contribution is

$$\begin{aligned}\mathcal{A}^{(2)}[\delta\psi^*,\delta\psi]=&\int_0^{\hbar\beta}d\tau\int d^3x\,\delta\psi_a^*(\mathbf{x},\tau)\left\{\left[\hbar\frac{\partial}{\partial\tau}-\frac{\hbar^2}{2M}\Delta+V(\mathbf{x})\right]\delta_{ab}-\eta F_{ab}^z\right\}\delta\psi_b(\mathbf{x},\tau)\\ &+\frac{1}{2}\int_0^{\hbar\beta}d\tau\int d^3x\int d^3x'\,V^{(\mathrm{int})}_{aba'b'}(\mathbf{x},\mathbf{x}')\Big\{2\Psi_a^*(\mathbf{x},\tau)\Psi_b(\mathbf{x},\tau)\delta\psi_{a'}^*(\mathbf{x}',\tau)\delta\psi_{b'}(\mathbf{x}',\tau)\\ &+2\Psi_a^*(\mathbf{x},\tau)\Psi_{b'}(\mathbf{x}',\tau)\delta\psi_{a'}^*(\mathbf{x}',\tau)\delta\psi_b(\mathbf{x},\tau)+\Psi_a^*(\mathbf{x},\tau)\Psi_{a'}^*(\mathbf{x}',\tau)\delta\psi_b(\mathbf{x},\tau)\delta\psi_{b'}(\mathbf{x}',\tau)\\ &+\Psi_b(\mathbf{x},\tau)\Psi_{b'}(\mathbf{x}',\tau)\delta\psi_a^*(\mathbf{x},\tau)\delta\psi_{a'}^*(\mathbf{x}',\tau)\Big\} \quad (3.7)\end{aligned}$$

and, finally, the cubic and quartic contributions are given by

$$\begin{aligned}\mathcal{A}^{(\mathrm{cor})}[\delta\psi^*,\delta\psi]=&\frac{1}{2}\int_0^{\hbar\beta}d\tau\int d^3x\int d^3x'\,V^{(\mathrm{int})}_{aba'b'}(\mathbf{x},\mathbf{x}')\Big\{2\delta\psi_{a'}^*(\mathbf{x}',\tau)\delta\psi_{b'}(\mathbf{x}',\tau) \quad (3.8)\\ &\times\Big[\Psi_a^*(\mathbf{x},\tau)\delta\psi_b(\mathbf{x},\tau)+\Psi_b(\mathbf{x},\tau)\delta\psi_a^*(\mathbf{x},\tau)\Big]+\delta\psi_a^*(\mathbf{x},\tau)\delta\psi_b(\mathbf{x},\tau)\delta\psi_{a'}^*(\mathbf{x}',\tau)\delta\psi_{b'}(\mathbf{x}',\tau)\Big\},\end{aligned}$$

where we have used the symmetry condition (2.5) of the interaction potential. The background method now consists in neglecting terms of linear order in the fluctuation fields $\delta\psi_a$,

$\delta\psi_a^*$, i.e., the functional $\mathcal{A}^{(1)}$ is set to zero. By virtue of the background method the action reads

$$\mathcal{A}[\Psi^* + \delta\psi^*, \Psi + \delta\psi] = \mathcal{A}[\Psi^*, \Psi] + \mathcal{A}^{(2)}[\delta\psi^*, \delta\psi] + \mathcal{A}^{(\mathrm{cor})}[\delta\psi^*, \delta\psi]. \tag{3.9}$$

Substituting (3.9) in (2.50) and performing a change of the functional integration variables

$$\prod_{a=-1}^{1} \oint \mathcal{D}\psi_a^* \oint \mathcal{D}\psi_a \to \prod_{a=-1}^{1} \oint \mathcal{D}\delta\psi_a^* \oint \mathcal{D}\delta\psi_a \tag{3.10}$$

yields the partition function

$$\mathcal{Z} = \left[\prod_{a=-1}^{1} \oint \mathcal{D}\delta\psi_a^* \oint \mathcal{D}\delta\psi_a\right] e^{-\mathcal{A}[\Psi^*+\delta\psi^*, \Psi+\delta\psi]/\hbar}. \tag{3.11}$$

Note that the functional integral in Eq. (3.11) has to be carried out over all fluctuating fields, i.e., over all periodic fields which fulfills the orthogonality condition (3.3).

As the Euclidean action $\mathcal{A}[\Psi^*, \Psi]$ does not depend on the fluctuation fields, we write for Eq. (3.11)

$$\mathcal{Z} = e^{-\mathcal{A}[\Psi^*, \Psi]/\hbar} \left[\prod_{a=-1}^{1} \oint \mathcal{D}\delta\psi_a^* \oint \mathcal{D}\delta\psi_a\right] e^{-\left(\mathcal{A}^{(2)}[\delta\psi^*, \delta\psi] + \mathcal{A}^{(\mathrm{cor})}[\delta\psi^*, \delta\psi]\right)/\hbar}. \tag{3.12}$$

Instead of working directly with the partition function, one uses in field theory the so-called *effective action*[1]

$$\Gamma[\Psi^*, \Psi] = -\frac{1}{\beta} \log \mathcal{Z}, \tag{3.13}$$

which can be decomposed as

$$\Gamma[\Psi^*, \Psi] = \Gamma^{(0)}[\Psi^*, \Psi] + \Gamma^{(1)}[\Psi^*, \Psi] + \Gamma^{(2)}[\Psi^*, \Psi]. \tag{3.14}$$

Here, the zeroth order term of the effective action in the fluctuation fields reads

$$\Gamma^{(0)}[\Psi^*, \Psi] = \frac{\mathcal{A}[\Psi^*, \Psi]}{\hbar\beta}, \tag{3.15}$$

the second order contribution of the fluctuation fields

$$\Gamma^{(1)}[\Psi^*, \Psi] = -\frac{1}{\beta} \log \left[\prod_{a=-1}^{1} \oint \mathcal{D}\delta\psi_a^* \oint \mathcal{D}\delta\psi_a\right] e^{-\mathcal{A}^{(2)}[\delta\psi^*, \delta\psi]/\hbar}, \tag{3.16}$$

and the higher order term is given by

$$\Gamma^{(2)}[\Psi^*, \Psi] = -\frac{1}{\beta} \log \frac{\left[\prod_{a=-1}^{1} \oint \mathcal{D}\delta\psi_a^* \oint \mathcal{D}\delta\psi_a\right] e^{-\left(\mathcal{A}^{(2)}[\delta\psi^*, \delta\psi] + \mathcal{A}^{(\mathrm{cor})}[\delta\psi^*, \delta\psi]\right)/\hbar}}{\left[\prod_{a=-1}^{1} \oint \mathcal{D}\delta\psi_a^* \oint \mathcal{D}\delta\psi_a\right] e^{-\mathcal{A}^{(2)}[\delta\psi^*, \delta\psi]/\hbar}}. \tag{3.17}$$

[1] For a constant background field Ψ the effective action is also called *effective potential*.

The contributions $\Gamma^{(0)}$, $\Gamma^{(1)}$, and $\Gamma^{(2)}$ are of zeroth, first, and second order in $\hbar$ [50]. It is shown in Ref. [49,50], that a non-vanishing expectation values of the fields, i.e., $\langle\psi_a(\mathbf{x},\tau)\rangle \neq 0$, requires that the effective action $\Gamma[\Psi^*,\Psi]$ extremizes with respect to the background fields Ψ_a^*, Ψ_a. Considering, only the lowest order, this corresponds to the extremization of the zeroth-order effective action $\Gamma^{(0)}$ given in Eq. (3.15), which is equivalent to extremizing the Euclidean action (3.5):

$$\left.\frac{\delta\mathcal{A}[\Psi^*,\Psi]}{\delta\Psi_a^*(\mathbf{x},\tau)}\right|_{\Psi^*=\Psi^*_{\rm extr}}^{\Psi=\Psi_{\rm extr}} = \left.\frac{\delta\mathcal{A}[\Psi^*,\Psi]}{\delta\Psi_a(\mathbf{x},\tau)}\right|_{\Psi^*=\Psi^*_{\rm extr}}^{\Psi=\Psi_{\rm extr}} = 0, \qquad a=1,0,-1, \tag{3.18}$$

which yields the following equation

$$0=\left\{\left[\hbar\frac{\partial}{\partial\tau}-\frac{\hbar^2}{2M}\Delta+V(\mathbf{x})-\mu\right]\delta_{ab}-\eta F^z_{ab}+\int d^3x'\,V^{(\rm int)}_{aba'b'}(\mathbf{x},\mathbf{x}')\Psi^*_{a'}(\mathbf{x}',\tau)\Psi_{b'}(\mathbf{x}',\tau)\right\}\Psi_b(\mathbf{x},\tau) \tag{3.19}$$

and correspondingly

$$0=\left\{\left[-\hbar\frac{\partial}{\partial\tau}-\frac{\hbar^2}{2M}\Delta+V(\mathbf{x})-\mu\right]\delta_{ab}-\eta F^z_{ab}+\int d^3x'\,V^{(\rm int)}_{baa'b'}(\mathbf{x},\mathbf{x}')\Psi^*_{a'}(\mathbf{x}',\tau)\Psi_{b'}(\mathbf{x}',\tau)\right\}\Psi^*_b(\mathbf{x},\tau). \tag{3.20}$$

These are the *Gross-Pitaevskii equations* of $F=1$ spinor Bose gas, which originally have been derived for a scalar Bose gas in Ref. [54,55]. We will discuss them in detail later for both a non-interacting spinor gas in Chapter 5 and a weakly interacting spinor gas in Chapter 10.

Part II

Ideal Spinor Gas

Chapter 4

Effective Action

In this section we calculate the effective action of an ideal $F = 1$ spinor gas. The effective action provides the basis for studying the thermodynamic properties of a physical system and is therefore of special importance. We consider two cases. In the first case we treat a homogeneous system, i.e., no external potential is applied. In the second case we calculate the effective action for a system, where an arbitrary harmonic trap is used. The first case is mainly of theoretical interest, as a homogeneous spinor gas cannot yet be created experimentally. However, there have been attempts to realize a homogeneous Bose-Einstein condensate in lower dimensions [52]. In most present-day experiments the harmonic trap is of special interest. Therefore, the treatment of a harmonically trapped spinor gas makes it in principle possible to verify our results experimentally. On the other hand, both systems exhibit to some extent quite different physics, which makes it worthwhile to compare them with one another.

4.1 General Case

We first calculate the general expression of the effective action. Using Eqs. (2.46)–(2.48) yields for the action of a non-interacting spinor gas

$$\mathcal{A}[\psi^*,\psi] = \int_0^{\hbar\beta} d\tau \int d^3x\, \psi_a^*(\mathbf{x},\tau) \left\{ \left[\hbar\frac{\partial}{\partial\tau} - \frac{\hbar^2}{2M}\Delta + V(\mathbf{x}) - \mu \right] \delta_{ab} - \eta F^z_{ab} \right\} \psi_b(\mathbf{x},\tau), \quad (4.1)$$

where the matrix of angular momentum F^z was defined in (2.17).

Substituting Eq. (4.1) in Eqs. (3.14)–(3.17) leads to the effective action

$$\Gamma[\Psi^*,\Psi] = \Gamma^{(0)}[\Psi^*,\Psi] + \Gamma^{(1)}, \quad (4.2)$$

where the tree-level effective action $\Gamma^{(0)}[\Psi^*,\Psi]$ is given in (3.15) and the first-order contribution of the effective action reads

$$\Gamma^{(1)} = -\frac{1}{\beta}\log\left[\prod_{a=-1}^{1} \oint \mathcal{D}\delta\psi_a^* \oint \mathcal{D}\delta\psi_a \right] e^{-\mathcal{A}[\delta\psi^*,\delta\psi]/\hbar}. \quad (4.3)$$

Note that the latter does not depend on the background fields anymore, which follows from Eqs. (3.7), (3.15). Furthermore, the action $\mathcal{A}^{(2)}[\delta\psi^*, \delta\psi]$ in (3.16) coincides with (4.1) evaluated on the fluctuation fields $\delta\psi^*$, $\delta\psi$.

As current fields are not present, the functional integral (4.3) is nearly identical to the analytically solved functional integral (2.52). The only difference is that (2.52) is performed over all periodic fields, whereas (4.3) has to be performed over all periodic *fluctuation fields*, i.e., over all period fields, which are orthogonal to the background fields Ψ^*, Ψ due to (3.3). Note, we will show in the next chapter that the background field is proportional to the ground state wave function $\varphi_{\mathbf{0}}(\mathbf{x})$ that solves the one-particle Schrödinger equation (2.1). In complete analogy to (2.54) and (2.55) the fluctuation fields are given as

$$\delta\psi_a(\mathbf{x},\tau) = \sum_{m=-\infty}^{\infty} \sum_{\substack{\mathbf{n}\\ \mathbf{n}\neq\mathbf{0}}} \delta\psi_{\mathbf{n}ma}\, \varphi_{\mathbf{n}}(\mathbf{x}) e^{-i\omega_m\tau} \tag{4.4}$$

$$\delta\psi_a^*(\mathbf{x},\tau) = \sum_{m=-\infty}^{\infty} \sum_{\substack{\mathbf{n}\\ \mathbf{n}\neq\mathbf{0}}} \delta\psi_{\mathbf{n}ma}^* \varphi_{\mathbf{n}}^*(\mathbf{x}) e^{i\omega_m\tau}, \tag{4.5}$$

where $\varphi_{\mathbf{n}}$ is a solution of the Schrödinger equation (2.1), $\delta\psi^*_{\mathbf{n}ma}$ is a complex coefficient, and ω_m the Matsubara frequency (2.57). Note that the fluctuations, as defined above, fulfill the condition (3.3), where we have used $\Psi_a(\mathbf{x}) = \text{const} \times \varphi_{\mathbf{0}}(\mathbf{x})$ and the orthogonality relation (2.2).

Accordingly, the measure of the functional integral over all periodically fluctuating fields reads

$$\prod_{a=-1}^{1} \oint \mathcal{D}\delta\psi_a^* \oint \mathcal{D}\delta\psi_a = \prod_{m=-\infty}^{\infty} \prod_{\substack{\mathbf{n}\\ \mathbf{n}\neq\mathbf{0}}} \prod_{a=-1}^{1} \int \frac{d\delta\psi^*_{\mathbf{n}ma}}{\sqrt{2\pi}} \int \frac{d\delta\psi_{\mathbf{n}ma}}{\sqrt{2\pi}}. \tag{4.6}$$

Therefore, performing the replacements

$$\prod_{\mathbf{n}} \longmapsto \prod_{\substack{\mathbf{n}\\ \mathbf{n}\neq\mathbf{0}}}, \qquad \sum_{\mathbf{n}} \longmapsto \sum_{\substack{\mathbf{n}\\ \mathbf{n}\neq\mathbf{0}}} \tag{4.7}$$

the calculation of the functional integral (4.3) turns out to be completely the same as the one performed in Section 2.5 for vanishing current fields.

Using Eqs. (2.52), (2.73), (4.3), and the latter replacement yields the fluctuation correction

$$\Gamma^{(1)} = \frac{1}{\beta} \sum_{a=-1}^{1} \sum_{\substack{\mathbf{n}\\ \mathbf{n}\neq\mathbf{0}}} \sum_{m=-\infty}^{\infty} \log\Big[\beta\left(-i\hbar\omega_m + E_{\mathbf{n}} - \mu - a\eta\right)\Big], \tag{4.8}$$

where $E_{\mathbf{n}}$ denote the eigenvalues determined by Eq. (2.1). Note that the convergence of the Gaussian integral leads to the condition

$$E_{\mathbf{n}} - \mu - a\eta \geq 0 \quad \text{for all } \mathbf{n}, a. \tag{4.9}$$

We perform the m sum in (4.8) by using Appendix B.3 that finally leads to

$$\Gamma^{(1)} = \frac{1}{\beta}\sum_{a=-1}^{1}\sum_{\substack{\mathbf{n}\\ \mathbf{n}\neq\mathbf{0}}}\log\left\{1-e^{-\beta(E_{\mathbf{n}}-\mu-a\eta)}\right\}. \tag{4.10}$$

Using Eqs. (3.15), (4.1), (4.2), and (4.10) we obtain for the total effective action

$$\boxed{\Gamma[\Psi^*,\Psi]=\frac{\mathcal{A}[\Psi^*,\Psi]}{\hbar\beta}+\frac{1}{\beta}\sum_{a=-1}^{1}\sum_{\substack{\mathbf{n}\\ \mathbf{n}\neq\mathbf{0}}}\log\left\{1-e^{-\beta(E_{\mathbf{n}}-\mu-a\eta)}\right\}.} \tag{4.11}$$

Note that Eq. (4.11) is valid for an arbitrary trap configuration which enters the effective action in form of the one-particle energy eigenvalues $E_{\mathbf{n}}$.

In order to further evaluate the latter for a given trap configuration, we have to determine the one-particle energy eigenvalues $E_{\mathbf{n}}$, i.e., we have to solve the one-particle Schrödinger equation (2.1).

4.2 Homogeneous Spinor Gas

We explicitly calculate the effective action (4.11) for a vanishing trap, i.e., $V(\mathbf{x})\equiv 0$. In this case, the eigenvalue equation (2.1) is solved by a plane wave with an appropriate normalization

$$\varphi_{\mathbf{k}}(\mathbf{x})=\frac{1}{\sqrt{V}}e^{i\mathbf{k}\mathbf{x}}, \tag{4.12}$$

where V denotes the volume, which the particles occupy. The wave vector $\mathbf{k}$ is a function of the quantum number $\mathbf{n}$, whose explicit form is given below. We impose to the eigenfunctions $\varphi_{\mathbf{k}}(\mathbf{x})$ periodic boundary conditions[1]

$$\varphi_{\mathbf{k}}(\mathbf{x}+L\mathbf{e}_i)=\varphi_{\mathbf{k}}(\mathbf{x}),\qquad i=x,y,z, \tag{4.13}$$

where $\mathbf{e}_i$ denote the unit vectors and $L=\sqrt[3]{V}$ the edge-length of the confining volume, which is taken to be a cubic box. The energy eigenvalues then read

$$E_{\mathbf{k}}=\frac{\hbar^2\mathbf{k}^2}{2M}, \tag{4.14}$$

where the wave vector $\mathbf{k}$ is given by

$$\mathbf{k}=\frac{2\pi}{\sqrt[3]{V}}\mathbf{n},\qquad (\mathbf{n})_i\equiv n_i=0,\pm1,\pm2,\ldots. \tag{4.15}$$

[1]The choice of the boundary condition to let vanish ψ at the border of the box, i.e., assuming a box with $V(\mathbf{x})=\infty$ for $\mathbf{x}\in\partial V$, where ∂V denotes the border of the box, would give rise to a non-uniform behavior of the condensates ground state. The uniformity is restored by including two-body interactions as is discussed in Ref. [69].

In the thermodynamic limit, i.e., for $V \to \infty$ while keeping the particle density N/V constant, the spacing between neighboring energy eigenvalues $E_{\mathbf{n}}$ becomes infinitesimally small. Therefore, we perform the replacement

$$\sum_{\substack{\mathbf{k} \\ \mathbf{k}\neq\mathbf{0}}} \longmapsto V \int \frac{d^3k}{(2\pi)^{3/2}}. \tag{4.16}$$

Substituting (4.14) and (4.16) into (4.10) yields

$$\Gamma^{(1)} = -\frac{V}{\beta} \sum_{a=-1}^{1} \sum_{n=1}^{\infty} \frac{1}{n} \int \frac{d^3k}{(2\pi)^{3/2}}\, e^{-n\beta[\epsilon(\mathbf{k})-\mu-a\eta]}, \tag{4.17}$$

where we have used the Taylor series of the logarithmic function

$$\log(1-z) = -\sum_{n=1}^{\infty} \frac{z^n}{n}\ . \tag{4.18}$$

Furthermore, in Eq. (4.17) the free-particle dispersion relation is given by

$$\epsilon(\mathbf{k}) \equiv \frac{\hbar^2\mathbf{k}^2}{2M}. \tag{4.19}$$

The integral (4.17) is of a Gaussian type and is immediately evaluated:

$$\Gamma^{(1)} \;=\; -\frac{V}{\beta\lambda^3} \sum_{a=-1}^{1} \zeta_{5/2}\Big(e^{\beta(\mu+a\eta)}\Big). \tag{4.20}$$

Here, we have used the thermal de Broglie wave length (1.1) and the polylogarithmic function

$$\zeta_\nu(z) = \sum_{n=1}^{\infty} \frac{z^n}{n^\nu}. \tag{4.21}$$

We define the fugacity as

$$z \equiv e^{\beta(\mu-E_{\mathbf{0}})}, \tag{4.22}$$

where $E_{\mathbf{0}}$ denotes the ground state energy of the system, which vanishes for the homogeneous case. Analogously we define the magnetic fugacity

$$z_\eta \equiv e^{\beta\eta}. \tag{4.23}$$

Using Eqs. (4.11) and (4.20)–(4.23), the effective action of the homogeneous spinor gas finally reads

$$\Gamma[\Psi^*,\Psi] = \frac{\mathcal{A}[\Psi^*,\Psi]}{\hbar\beta} - \frac{V}{\beta\lambda^3}\Big[\zeta_{5/2}(zz_\eta) + \zeta_{5/2}(z) + \zeta_{5/2}(z/z_\eta)\Big], \tag{4.24}$$

where the tree-level action $\mathcal{A}[\Psi^*,\Psi]$ is given in Eq. (4.1). Note that all information of interest about this system summarized in the effective action. It will be the starting point for deriving all thermodynamic properties of the homogeneous ideal spinor gas.

4.3 Harmonically Trapped Spinor Gas

In the last section we have derived the effective action of a homogeneous spinor gas. Now, we discuss in a similar way the harmonically trapped spinor gas. The potential of an arbitrary harmonic trap is given by

$$V(\mathbf{x}) = \frac{M}{2}\omega_i^2 x_i^2, \tag{4.25}$$

where ω_1, ω_2, ω_3 denote the trap frequencies in different spatial directions. Using this potential, the solution of the Schrödinger equation (2.1) is well known from quantum mechanics (see Ref. [53]). The energy eigenvalues are given by

$$E_{\mathbf{n}} = \frac{3}{2}\hbar\bar{\omega} + \hbar\omega_i n_i, \qquad n_1, n_2, n_3 = 0, 1, 2, \dots , \tag{4.26}$$

where we use for the arithmetic mean of the trap frequencies the short-hand notation

$$\bar{\omega} = (\omega_1 + \omega_2 + \omega_3)/3. \tag{4.27}$$

Note that according to (4.26), the ground-state energy of the harmonically trapped spinor gas is given by $E_{\mathbf{0}} = 3\hbar\bar{\omega}/2$.

Substituting the energy eigenvalues (4.26) into the fluctuation contribution of the effective action (4.10) gives

$$\Gamma^{(1)} = -\frac{1}{\beta}\sum_{a=-1}^{1}\sum_{n=1}^{\infty}\frac{1}{n}\, e^{n\beta(\mu+a\eta-E_{\mathbf{0}})}\left(\sum_{n_1,n_2,n_3=0}^{\infty} e^{-n\beta\hbar\omega_i n_i} - 1\right). \tag{4.28}$$

The second term on the right-hand of the latter equation is introduced, because $\Gamma^{(1)}$ does not contain terms originating from the ground state.

The n_i–sums are of the geometric type and can be performed analytically:

$$\Gamma^{(1)} = -\frac{1}{\beta}\sum_{a=-1}^{1}\sum_{n=1}^{\infty}\frac{1}{n}\left[\frac{e^{n\beta(\mu+a\eta-E_{\mathbf{0}})}}{(1-e^{-n\beta\hbar\omega_1})(1-e^{-n\beta\hbar\omega_2})(1-e^{-n\beta\hbar\omega_3})} - 1\right]. \tag{4.29}$$

However, it is not necessary to take the exact form of $\Gamma^{(1)}$. We will always work in the regime where we can adopt the semiclassical approximation, i.e., we assume the thermal energy to be much smaller than the level spacing between the one-particle energy eigenvalues:

$$\beta\hbar\omega_i \ll 1, \quad i = 1, 2, 3\ . \tag{4.30}$$

Substituting the Taylor expansion of the exponential function

$$e^{-n\beta\hbar\omega_i} = 1 - n\beta\hbar\omega_i + \frac{1}{2}(n\beta\hbar\omega_i)^2 + \dots \quad i = 1, 2, 3 \tag{4.31}$$

in (4.29) yields in first order of $\beta\hbar\omega_i$

$$\Gamma^{(1)} = -\frac{1}{\beta(\beta\hbar\tilde{\omega})^3}\sum_{a=-1}^{1}\sum_{n=1}^{\infty}\frac{e^{n\beta(\mu+a\eta-E_{\mathbf{0}})}}{n^4}\left\{1+\frac{3}{2}n\beta\hbar\bar{\omega}+\mathcal{O}(\beta^2\hbar^2\omega_i^2)\right\}. \tag{4.32}$$

where we have introduced the geometric mean frequency

$$\tilde{\omega} = (\omega_1\omega_2\omega_3)^{1/3}. \tag{4.33}$$

We note that the ground-state correction on the right-hand side of Eqs. (4.28) and (4.29) is of the order $(\beta\hbar\omega_i)^3$.

With the help of the polylogarithmic function (4.21) and the abbreviations (4.22) we obtain for the first order of the semiclassical approximation

$$\Gamma^{(1)} = -\frac{1}{\beta(\beta\hbar\tilde{\omega})^3}\Big\{\zeta_4(zz_\eta)+\zeta_4(z)+\zeta_4(z/z_\eta)+\frac{3}{2}\beta\hbar\bar{\omega}\left[\zeta_3(zz_\eta)+\zeta_3(z)+\zeta_3(z/z_\eta)\right]\Big\}, \tag{4.34}$$

so that the effective action (4.11) reads in first order

$$\begin{aligned}\Gamma[\Psi^*,\Psi] &= \frac{\mathcal{A}[\Psi^*,\Psi]}{\hbar\beta}-\frac{1}{\beta(\beta\hbar\tilde{\omega})^3}\Big\{\zeta_4(zz_\eta)+\zeta_4(z)+\zeta_4(z/z_\eta)\\ &\quad+\frac{3}{2}\beta\hbar\bar{\omega}\left[\zeta_3(zz_\eta)+\zeta_3(z)+\zeta_3(z/z_\eta)\right]\Big\}.\end{aligned} \tag{4.35}$$

In analogy to Eq. (4.24) this equation provides the basis for studying the harmonically trapped ideal spinor condensate up to the first order in $\beta\hbar\bar{\omega}$.

In the further chapters we will always discuss both the homogeneous $F = 1$ spinor gas and the harmonically trapped spinor gas. As we will see in the following chapters, the treatment of both cases are quite similar. In order to have a compact notation, we summarize Eqs. (4.24) and (4.35) as

$$\boxed{\begin{aligned}\Gamma[\Psi^*,\Psi] &= \frac{\mathcal{A}[\Psi^*,\Psi]}{\hbar\beta}-\frac{C_\nu}{\beta}\Big\{\zeta_{\nu+1}(zz_\eta)+\zeta_{\nu+1}(z)+\zeta_{\nu+1}(z/z_\eta)\\ &\quad+\frac{3}{2}\,\delta_{3\nu}\beta\hbar\bar{\omega}\Big[\zeta_3(zz_\eta)+\zeta_3(z)+\zeta_3(z/z_\eta)\Big]\Big\},\end{aligned}} \tag{4.36}$$

where the different traps are characterized by

$$\nu = \begin{cases} 3/2 & \text{No trap,}\\ 3 & \text{Harmonic trap.}\end{cases} \tag{4.37}$$

The coefficient $C_{3/2}$ belonging to the homogeneous spinor gas reads

$$C_{3/2} = \frac{V}{\lambda^3}, \tag{4.38}$$

whereas the coefficient belonging to the harmonically trapped spinor gas is

$$C_3 = \frac{1}{(\beta\hbar\tilde{\omega})^3} \ . \tag{4.39}$$

Note that according to its definition C_ν is not a constant, but a function of temperature T.

Physically, the first term on the right-hand side of Eq. (4.36) is the contribution due to the macroscopic occupation of the ground-state, whereas the second term represents the contribution of particles being in excited states.

Chapter 5

Gross-Pitaevskii Equations

In the last section we have derived for two different trap configurations the effective action of an ideal $F = 1$ spinor gas. As mentioned before, extremizing the effective action with respect to the background fields $\Psi(\mathbf{x}, \tau)$ and $\Psi^*(\mathbf{x}, \tau)$ yields the grand-canonical free energy of the system. This is the most important global quantity of a thermodynamical system, as it allows to calculate all interesting quantities like heat capacity, entropy, magnetic susceptibility, etc. In this section we discuss the explicit form of the background fields $\Psi(\mathbf{x}, \tau)$ and $\Psi^*(\mathbf{x}, \tau)$ and their physical meaning. As we will see below, the background fields only become important below the transition temperature to the Bose-Einstein phase. The equations, which determine the background fields, are known as Gross-Pitaevskii equations [54, 55] and have already been derived for the general case in Chapter 3.

5.1 Motivation

We start by motivating the physical meaning of the background fields.

According to Eq. (2.35) the total number of particles N in the spinor gas is given by the partial derivative of the grand-canonical free energy with respect to the chemical potential. Analogously, if we work with the effective action (3.13), the total number of particles is given by

$$N = -\frac{\partial \Gamma[\Psi^*, \Psi]}{\partial \mu}\bigg|_{\Psi^* = \Psi^*_{\text{extr}}}^{\Psi = \Psi_{\text{extr}}}. \tag{5.1}$$

Note that in the effective action approach, we first have to perform the partial derivative and then substitute the extremized background fields.

Substituting the general result of the effective action (4.11) in (5.1) yields with the Euclidean action (4.1)

$$N = \frac{1}{\hbar\beta}\int_0^{\hbar\beta} d\tau \int d^3x\, \Psi_a^*(\mathbf{x}, \tau)\Psi_a(\mathbf{x}, \tau)\Big|_{\Psi^* = \Psi^*_{\text{extr}}}^{\Psi = \Psi_{\text{extr}}} + \sum_{a=-1}^{1} \sum_{\substack{\mathbf{n} \\ \mathbf{n} \neq \mathbf{0}}} \frac{1}{e^{\beta(E_{\mathbf{n}} - \mu - a\eta)} - 1}. \tag{5.2}$$

The second term on the right-hand side of (5.2) is the Bose-Einstein distribution, whereas the first term on the right-hand side is the total number of particles in the condensate fraction. This can directly be seen by taking the limit $T \to 0$, i.e. $\beta \to \infty$, and considering the condition $E_{\mathbf{0}} - \mu - a\eta$:

$$N = \lim_{\beta\to\infty} \frac{1}{\hbar\beta} \int_0^{\hbar\beta} d\tau \int d^3x\, \Psi_a^*(\mathbf{x},\tau)\Psi_a(\mathbf{x},\tau)\Big|_{\Psi^*=\Psi^*_{\mathrm{extr}}}^{\Psi=\Psi_{\mathrm{extr}}}. \tag{5.3}$$

Neglecting the dependence on the imaginary time corresponds to the case of a time-independent system. In this thesis we exclusively consider stationary solutions of the order parameter, i.e., solutions with vanishing time dependence. We then get for the total number of particles

$$N = \int d^3x\, \Psi_a^*(\mathbf{x})\Psi_a(\mathbf{x})\Big|_{\Psi^*=\Psi^*_{\mathrm{extr}}}^{\Psi=\Psi_{\mathrm{extr}}}. \tag{5.4}$$

Clearly, $|\Psi_a(\mathbf{x})|^2$ is the condensates particle density in the a^{th} Zeeman state. According to thermodynamics the occupied state at $T = 0$ is the ground state.

5.2 Derivation of Gross-Pitaevskii Equations

As mentioned before the Gross-Pitaevskii equations are obtained by extremizing the effective action with respect to the background fields. However, according to Eq. (4.11), this is equivalent to extremizing the action of the system, hence

$$\frac{\delta\mathcal{A}[\Psi^*,\Psi]}{\delta\Psi_a^*(\mathbf{x},\tau)}\Big|_{\Psi^*=\Psi^*_{\mathrm{extr}}}^{\Psi=\Psi_{\mathrm{extr}}} = 0. \tag{5.5}$$

Substituting Eq. (4.1) in (5.5) yields the Gross-Pitaevskii equations

$$\left\{\Big[\hbar\frac{\partial}{\partial\tau} - \frac{\hbar^2}{2M}\Delta + V(\mathbf{x}) - \mu\Big]\delta_{ab} - \eta F^z_{ab}\right\}\Psi_b(\mathbf{x},\tau) = 0, \qquad a = -1, 0, 1. \tag{5.6}$$

For convenience we have neglected the notation $\Psi_{b,\mathrm{extr}}$ and used instead simply Ψ_b. We will use this notation throughout the work.

As discussed above, we consider only time-independent background fields. Furthermore, we have motivated in the last section that the background fields have to be identified with the ground-state wave function, i.e., they fulfill the one-particle Schrödinger equation

$$\left[-\frac{\hbar^2}{2M}\Delta + V(\mathbf{x})\right]\Psi_a(\mathbf{x}) = E_{\mathbf{0}}\Psi_a(\mathbf{x}) \tag{5.7}$$

with the ground-state energy eigenvalue $E_{\mathbf{0}}$.

Using the latter equation and the fact that the matrix on the left-hand side of (5.6) is diagonal, we obtain three independent Gross-Pitaevskii equations

$$\Big(E_{\mathbf{0}} - \mu - a\eta\Big)\Psi_a(\mathbf{x}) = 0, \qquad a = 1, 0, -1\,. \tag{5.8}$$

We choose the background field to be real and set

$$\Psi_a(\mathbf{x}) = \sqrt{N_a^{\mathrm{C}}}\,\varphi_{\mathbf{0}}(\mathbf{x}), \qquad a = 1, 0, -1 \tag{5.9}$$

with $\varphi_{\mathbf{0}}(\mathbf{x})$ defined in (2.1)–(2.3). Moreover, the real number N_a^{C} represents the total number of particles in the electronic quantum ground Zeeman state $|a\rangle$.

We deduce from (5.9) that in a spinor Bose-Einstein condensate the spatial particle distribution of every Zeeman state differs only by a normalization factor. Finally, substituting (5.9) in (5.8) gives us the Gross-Pitaevskii equations in an algebraic form

$$\boxed{\Big(E_{\mathbf{0}} - \mu - a\eta\Big)N_a^{\mathrm{C}} = 0, \qquad a = -1, 0, 1.} \tag{5.10}$$

Together with the effective action (4.36), the Gross-Pitaevskii equations (5.10) provide the fundamental basis for studying phase transitions of a spinor gas to a spinor Bose-Einstein condensate. As we will see in the next section, different solutions of (5.10) correspond for a given magnetization to different phases at different temperatures.

5.3 Solution of Gross-Pitaevskii Equations

In the last section we have derived the algebraic Gross-Pitaevskii equations

$$\Big(E_{\mathbf{0}} - \mu - \eta\Big)N_1^{\mathrm{C}} = 0, \tag{5.11}$$

$$\Big(E_{\mathbf{0}} - \mu\Big)N_0^{\mathrm{C}} = 0, \tag{5.12}$$

$$\Big(E_{\mathbf{0}} - \mu + \eta\Big)N_{-1}^{\mathrm{C}} = 0. \tag{5.13}$$

This set of equations has to be fulfilled for all temperatures at any given magnetization M. The dependence on the temperature and magnetization of Eqs. (5.11)–(5.13) enters via the chemical potential μ and the magnetic chemical potential η, which have to be adjusted in such a way, that the conservation of the total number of particles (5.1) and the total magnetization

$$M = -\frac{\partial\Gamma[\Psi^*, \Psi]}{\partial\eta}\bigg|_{\Psi^* = \Psi^*_{\mathrm{extr}}}^{\Psi = \Psi_{\mathrm{extr}}} \tag{5.14}$$

is fulfilled.

Using Eqs. (4.1), (4.36), (5.6), and (5.9) we obtain for (5.1) and (5.14)

$$N = N^{\mathrm{C}} + C_\nu \Big\{ \zeta_\nu(zz_\eta) + \zeta_\nu(z) + \zeta_\nu(z/z_\eta) + \frac{3}{2}\,\delta_{3\nu}\beta\hbar\bar{\omega}\Big[\zeta_2(zz_\eta) + \zeta_2(z) + \zeta_2(z/z_\eta)\Big]\Big\}, \quad (5.15)$$

$$M = N_1^{\mathrm{C}} - N_{-1}^{\mathrm{C}} + C_\nu \Big\{ \zeta_\nu(zz_\eta) - \zeta_\nu(z/z_\eta) + \frac{3}{2}\,\delta_{3\nu}\beta\hbar\bar{\omega}\Big[\zeta_2(zz_\eta) - \zeta_2(z/z_\eta)\Big]\Big\}, \quad (5.16)$$

where C_ν is a function of temperature defined in (4.38), (4.39). Furthermore, we have introduced the total number of particles being in the condensed state

$$N^{\mathrm{C}} = N_1^{\mathrm{C}} + N_0^{\mathrm{C}} + N_{-1}^{\mathrm{C}}. \quad (5.17)$$

We emphasize that Eqs. (5.11)–(5.13), (5.15), and (5.16) have always to be fulfilled. In order to solve these five equation simultaneously, we need five free quantities which enter the latter equations. Our free quantities are given by the condensates densities N_1^{C}, N_0^{C}, N_{-1}^{C}, and both fugacities z and z_η.

The convenient structure of the algebraic Gross-Pitaevskii equations Eqs. (5.11)–(5.13) suggests taking the most obvious solution, namely,

$$N_1^{\mathrm{C}} = N_0^{\mathrm{C}} = N_{-1}^{\mathrm{C}} = 0. \quad (5.18)$$

Physically, this solution corresponds to the case, that no particles are Bose-Einstein condensed, i.e., this corresponds to a *gas phase*. Substituting (5.18) into (5.15), (5.16) yields the total number of particles

$$N = C_\nu \Big\{ \zeta_\nu(zz_\eta) + \zeta_\nu(z) + \zeta_\nu(z/z_\eta) + \frac{3}{2}\delta_{3\nu}\beta\hbar\bar{\omega}\Big[\zeta_2(zz_\eta) + \zeta_2(z) + \zeta_2(z/z_\eta)\Big]\Big\} \quad (5.19)$$

and the total magnetization

$$M = C_\nu \Big\{ \zeta_\nu(zz_\eta) - \zeta_\nu(z/z_\eta) + \frac{3}{2}\delta_{3\nu}\beta\hbar\bar{\omega}\Big[\zeta_2(zz_\eta) - \zeta_2(z/z_\eta)\Big]\Big\} \quad (5.20)$$

in the gas phase. From the definition of the magnetic fugacity (4.23) and the monotony of the polylogarithmic function (4.21), which is depicted in Figure 5.1, we can deduce from Eq. (5.20) for the gas phase

$$\begin{aligned} M > 0 &\iff \eta > 0, \\ M = 0 &\iff \eta = 0, \\ M < 0 &\iff \eta < 0. \end{aligned} \quad (5.21)$$

For convenience, we restrict ourselves in this thesis to the case $M \geq 0$, where we have $\eta > 0$ according to (5.21). The case of a negative magnetization is treated by simply redefining the

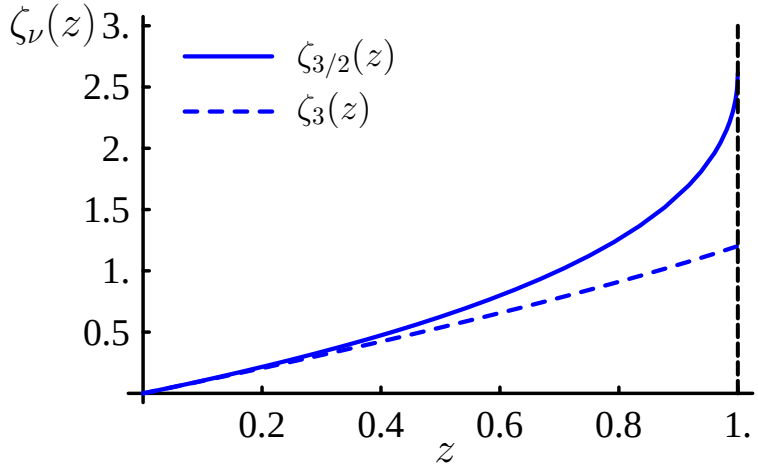

Figure 5.1: Behavior of the polylogarithmic function (4.21) which is continuous in its domain. For $z > 1$ it diverges for any ν. Moreover, for $\nu > 1$ it has a well defined value at $z = 1$.

arbitrarily chosen z-axis in the opposite direction. The magnetization is then again positive.

We search now solutions, which differ from (5.18), namely, we work out the first phase transition of the system. Therefore, we consider Eq. (4.9), which states

$$E_{\mathbf{0}} - \mu - \eta \geq 0. \tag{5.22}$$

Here, $E_{\mathbf{0}}$ is the ground state energy of the system. The phase transition occurs if one of the order parameters N_a^{C} in Eqs. (5.11)–(5.13) changes from zero to a finite value. Considering a positive magnetization, we get with (5.21) and (5.22) as the only possible solution of the Gross-Pitaevskii equations (5.11)–(5.13):

$$N_0^{\mathrm{C}} = N_{-1}^{\mathrm{C}} = 0, \tag{5.23}$$

$$E_{\mathbf{0}} - \mu - \eta = 0. \tag{5.24}$$

As seen from the latter equations, the number of particles N_1^{C}, which denotes the particles in the BEC state $|a = 1\rangle$, is not restricted anymore by the Gross-Pitaevskii equations, whereas the remaining BEC states $|0\rangle$ and $|-1\rangle$ are not occupied at all. Therefore, the condensate fraction is fully polarized and we call the temperature/magnetization domain, where (5.23), (5.24) is fulfilled, *ferromagnetic phase*. Furthermore, we refer to the critical temperature, where the phase transition from the gas phase to the ferromagnetic phase occurs, as the *first critical temperature* T_{c_1}. The ferromagnetic phase has interesting physical properties. For example, particles in the Bose-Einstein condensed state may have a magnetization, which is quite different from the magnetization of the thermal cloud.

In order to determine the unknown particle number N_1^{C} and the remaining fugacity, we substitute the condition of the ferromagnetic phase (5.23), (5.24) in (5.15), (5.16) yielding

the total number of particles

$$N = N_1^{\mathrm{C}} + C_\nu \Big\{ \zeta(\nu) + \zeta_\nu(z) + \zeta_\nu(z^2) + \frac{3}{2}\,\delta_{3\nu}\,\beta\hbar\bar{\omega}\Big[\zeta(2) + \zeta_2(z) + \zeta_2(z^2)\Big]\Big\}, \tag{5.25}$$

and the total magnetization

$$M = N_1^{\mathrm{C}} + C_\nu \Big\{ \zeta(\nu) - \zeta_\nu(z^2) + \frac{3}{2}\,\delta_{3\nu}\,\beta\hbar\bar{\omega}\Big[\zeta(2) - \zeta_2(z^2)\Big]\Big\}. \tag{5.26}$$

Here, we have $z z_\eta = 1$, which follows from (4.22), (4.23), and (5.24). Moreover, we have introduced the Riemann zeta function $\zeta(\nu) \equiv \zeta_\nu(1)$.

So far, we have discussed two solutions of the algebraic Gross-Pitaevskii equations (5.11)–(5.13). Now, we search for an additional phase. Substituting (5.24) in (5.12), (5.13) yields the following Gross-Pitaevskii equations

$$\eta N_0^{\mathrm{C}} = 0, \tag{5.27}$$
$$\eta N_{-1}^{\mathrm{C}} = 0, \tag{5.28}$$

As discussed above, in the ferromagnetic phase the latter equations are fulfilled with Eq. (5.23). To enter a new phase, one of the components of the order parameter in Eqs. (5.27) and (5.28) has to take a non-zero value. This is only possible if the condition

$$\eta = 0 \tag{5.29}$$

is fulfilled, so that we obtain from (5.24)

$$E_{\mathbf{0}} - \mu = 0. \tag{5.30}$$

At this point, we strongly emphasize that η is *not* a magnetic field, but a Lagrangian parameter, which was introduced in order to fix the total magnetization of the system. Therefore, it is possible to set η equal zero as done in (5.29).

From (5.27)–(5.29) we see that for $\eta = 0$ both the $|a = 0\rangle$ and the $|a = -1\rangle$ Zeeman state of the condensed fraction may take a non-zero value. Under the given conditions, none of the latter states is preferred, so that we assume that both Zeeman ground states get occupied at the same critical temperature, i.e., it occurs a *double condensation* [56]. Substituting the conditions (5.29) and (5.30) in Eqs. (5.15), (5.16) yields for the total number of particles

$$N = N_1^{\mathrm{C}} + N_0^{\mathrm{C}} + N_{-1}^{\mathrm{C}} + 3C_\nu\,\zeta(3)\left[1 + \frac{3}{2}\,\delta_{3\nu}\beta\hbar\bar{\omega}\frac{\zeta(2)}{\zeta(3)}\right] \tag{5.31}$$

and for the total magnetization

$$M = N_1^{\mathrm{C}} - N_{-1}^{\mathrm{C}}. \tag{5.32}$$

The latter equation clearly indicates that the total magnetization is only due to Bose-Einstein condensed particles. Conversely speaking, the thermal cloud is not magnetized at all and therefore we call this phase *antiferromagnetic phase*. Moreover, we refer the transition temperature, where the second phase transition occurs, the *second critical temperature* T_{c_2}.

In Figure 5.2 we have schematically summarized the phases with the respective solutions of the Gross-Pitaevskii equations.

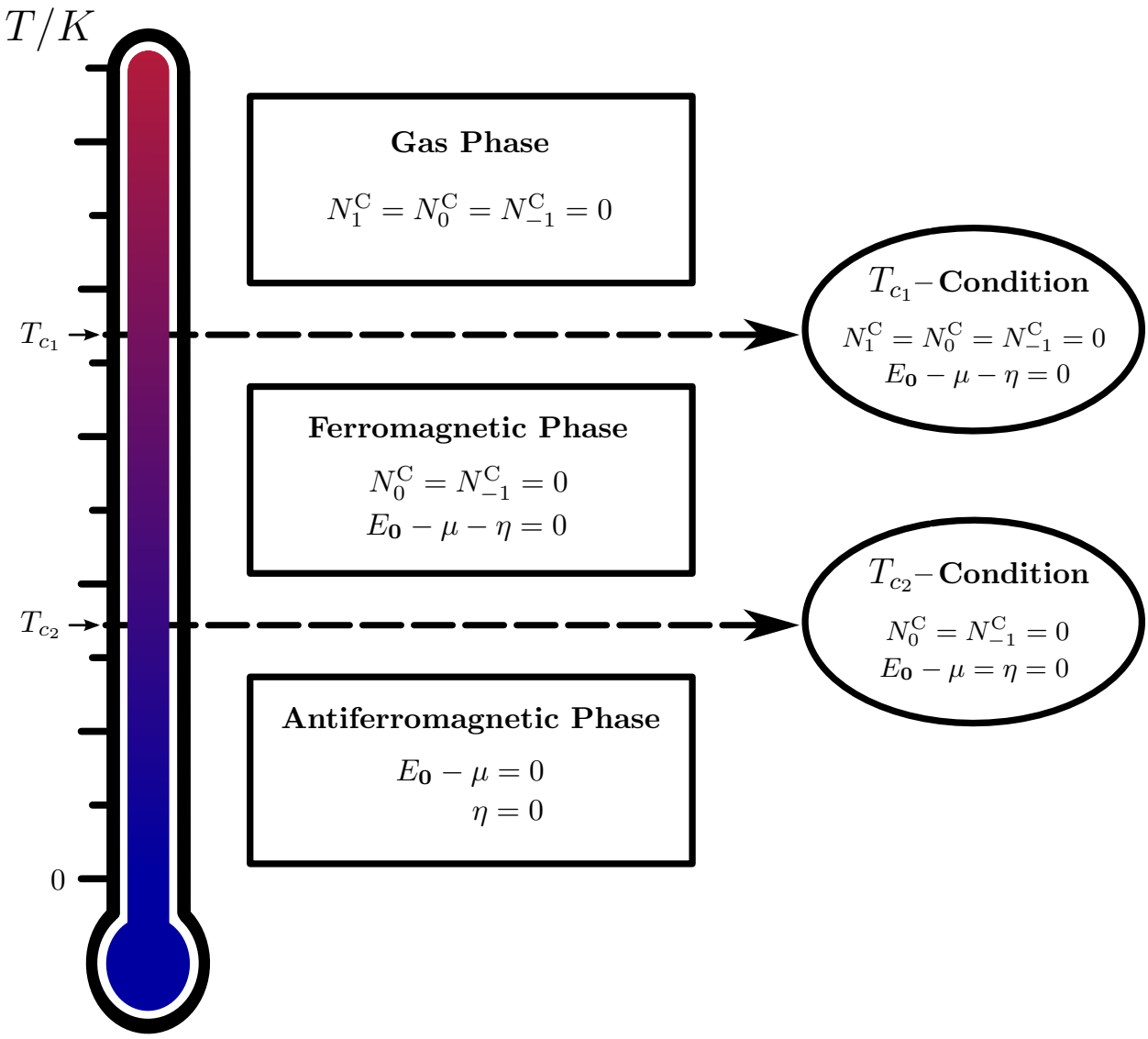

Figure 5.2: The ideal $F = 1$ spinor gas exhibits three different phases. The phases and the corresponding conditions to the order parameters and the fugacities are summarized in the boxes. The transition point between two phases, both of the respective conditions have to be fulfilled simultaneously, which is indicated in the circle.

Chapter 6

Critical Temperatures

In the last chapter we have derived the solutions of the Gross-Pitaevskii equations (5.11)–(5.13). We have shown that they correspond to three phases: a gas phase, a ferromagnetic phase, and an antiferromagnetic phase, which are summarized schematically in Figure 5.2. The occurrence of the corresponding transition temperatures have only been discussed qualitatively. In this chapter, we will calculate the first and the second critical temperature, which turn out to be dependent on the total magnetization of the $F = 1$ spinor gas.

6.1 First Critical Temperature

We start with the calculation of the first critical temperature. In order to have a dimensionless temperature scaling, we first calculate the critical temperature of a full polarized spinor gas where we neglect any finite-size effects.

6.1.1 Full Polarized Spinor Gas

According to (5.19) and (5.20) we get in zeroth order of the semiclassical approximation for the total number of particles in the gas phase

$$N = C_\nu \Big[\zeta_\nu(z z_\eta) + \zeta_\nu(z) + \zeta_\nu(z/z_\eta)\Big] \tag{6.1}$$

and the total magnetization

$$M = C_\nu \Big[\zeta_\nu(z z_\eta) - \zeta_\nu(z/z_\eta)\Big]. \tag{6.2}$$

Subtracting (6.2) from (6.1) yields

$$N - M = C_\nu \Big[\zeta_\nu(z) + 2\zeta_\nu(z/z_\eta)\Big]. \tag{6.3}$$

In case of a full polarized spinor gas we have $M \to N$. Therefore, assuming a constant temperature, we get with Eqs. (4.38) and (4.39) the condition that the bracket on the right-hand side of (6.3) vanishes. Moreover, using the monotony of the polylogarithmic function

and Eq. (6.2) we deduce that for positive M we have the condition $z_\eta > 1$. Using the latter arguments, we obtain from (6.1) for the case of a full polarized spinor gas the relation

$$N = C_\nu \, \zeta_\nu(z z_\eta). \tag{6.4}$$

If we reach the first critical temperature T_0, we have to fulfill the $T_{c_1}-$condition $z z_\eta = 1$ given in Figure 5.2. According to (6.4) we then have

$$N = C_\nu \, \zeta(\nu)\Big|_{T=T_0}. \tag{6.5}$$

Note that C_ν as defined in Eqs. (4.38), (4.39) is a function of temperature. Substituting Eqs. (4.38) and (4.39) into Eq. (6.5) we obtain in zeroth order for the full polarized spinor gas for the homogeneous case

$$T_0 = \frac{2\pi\hbar^2}{k_B M}\left[\frac{N}{V\zeta(3/2)}\right]^{2/3} \tag{6.6}$$

and for the harmonically trapped system

$$T_0 = \frac{\hbar\bar{\omega}}{k_B}\left[\frac{N}{\zeta(3)}\right]^{1/3}. \tag{6.7}$$

In the further work we always will scale temperatures with respect to (6.6) and (6.7) and denote this as

$$\mathcal{T}_\bullet \equiv \frac{T_\bullet}{T_0}. \tag{6.8}$$

So far, we have only calculated the first critical temperature of a full polarized spinor gas, which was rather for formal reasons. Now, we turn to the calculation of the first critical temperature for an arbitrary magnetization. Substituting from Figure 5.2 the $T_{c_1}-$condition, i.e., $N_0 = N_{-1} = 0$, $z z_\eta = 1$ in Eqs. (5.15) and (5.16) yields

$$\mathcal{N} = \frac{\mathcal{T}_{c_1}^\nu}{\zeta(\nu)}\left\{\zeta(\nu) + \zeta_\nu(z) + \zeta_\nu(z^2) + \frac{3}{2}\frac{\delta_{3\nu}}{\mathcal{T}_{c_1}}\frac{\bar{\omega}}{\tilde{\omega}}\left[\frac{\zeta(3)}{N}\right]^{1/3}\Big[\zeta(2) + \zeta_2(z) + \zeta_2(z^2)\Big]\right\}, \tag{6.9}$$

$$\mathcal{M} = \frac{\mathcal{T}_{c_1}^\nu}{\zeta(\nu)}\left\{\zeta(\nu) - \zeta_\nu(z^2) + \frac{3}{2}\frac{\delta_{3\nu}}{\mathcal{T}_{c_1}}\frac{\bar{\omega}}{\tilde{\omega}}\left[\frac{\zeta(3)}{N}\right]^{1/3}\Big[\zeta(2) - \zeta_2(z^2)\Big]\right\}, \tag{6.10}$$

where we have divided Eqs. (5.15) and (5.16) by Eq. (6.5) and adopted the notation (2.37). Furthermore, we have used Eqs. (6.7) and (6.8) to rewrite the second order term $\beta\hbar\bar{\omega}$ as

$$\beta\hbar\bar{\omega} = \beta_0\hbar\bar{\omega}\frac{T_0}{T} = \frac{\bar{\omega}}{\tilde{\omega}}\left[\frac{\zeta(3)}{N}\right]^{1/3}\frac{1}{\mathcal{T}}. \tag{6.11}$$

From the latter we deduce that the first-order correction represents a finite-size scaling. Note that the first-order correction also vanishes in the high-temperature limit as clearly can be

seen from (6.11). Let us return to the calculation. In order to get an expression for the first critical temperature $\mathcal{T}_{c_1}$, we rewrite (6.9) as

$$\mathcal{T}_{c_1} = \left[\frac{\zeta(\nu)}{\zeta(\nu)+\zeta_\nu(z)+\zeta_\nu(z^2)}\right]^{1/\nu} \left\{1 + \frac{3}{2}\frac{\delta_{3\nu}}{\mathcal{T}_{c_1}}\frac{\bar{\omega}}{\tilde{\omega}}\left[\frac{\zeta(3)}{N}\right]^{1/3}\frac{\zeta(2)+\zeta_2(z)+\zeta_2(z^2)}{\zeta(3)+\zeta_3(z)+\zeta_3(z^2)}\right\}^{-1/3}. \tag{6.12}$$

Iterating the latter and expanding it into a Taylor series up to the first order in $N^{-1/3}$ yields the first critical temperature

$$\boxed{\mathcal{T}_{c_1} = \left[\frac{\zeta(\nu)}{\zeta(\nu)+\zeta_\nu(z)+\zeta_\nu(z^2)}\right]^{1/\nu} \left\{1 - \frac{\delta_{3\nu}}{2}\frac{\bar{\omega}}{\tilde{\omega}}\frac{1}{N^{1/3}}\frac{\zeta(2)+\zeta_2(z)+\zeta_2(z^2)}{\left[\zeta(3)+\zeta_3(z)+\zeta_3(z^2)\right]^{2/3}}\right\}.} \tag{6.13}$$

In order to obtain the first critical temperature (6.13) as a function of the magnetization $\mathcal{M}$, we perform the same manipulation as done above with Eq. (6.10). With the help of Eq. (6.13) we then get up to the first order in $N^{-1/3}$

$$\boxed{\begin{aligned}\mathcal{M} &= \frac{\zeta(\nu)-\zeta_\nu(z^2)}{\zeta(\nu)+\zeta_\nu(z)+\zeta_\nu(z^2)} + \frac{3}{2}\frac{\bar{\omega}}{\tilde{\omega}}\frac{\delta_{3\nu}}{N^{1/3}}\left\{\frac{\zeta(2)-\zeta_2(z^2)}{\left[\zeta(3)+\zeta_3(z)+\zeta_3(z^2)\right]^{2/3}}\right. \\ &\quad \left. - \frac{\left[\zeta(3)-\zeta_3(z^2)\right]\left[\zeta(2)+\zeta_2(z)+\zeta_2(z^2)\right]}{\left[\zeta(3)+\zeta_3(z)+\zeta_3(z^2)\right]^{5/3}}\right\}.\end{aligned}} \tag{6.14}$$

Here, we again emphasize that the magnetization $\mathcal{M}$ is a constant. In principle, using Eq. (6.14), one could explicitly calculate z as a function of $\mathcal{M}$ and substitute in (6.13). However, the determination of the fugacity is analytically not possible. Therefore, we will consider the fugacity z as a parameter which ranges from 0 to 1, corresponding to a full polarized and non-polarized spinor gas, respectively, and plot the critical temperature parametrically. This is shown in Figure 6.1 for both the homogeneous trapped spinor gas and the harmonically trapped spinor gas. In case of the harmonically trapped spinor gas we have chosen the particle number 10.000 and ∞ and have set $\bar{\omega} = \tilde{\omega}$.

6.2 Second Critical Temperature

The second critical temperature is calculated in complete analogy as done above. Substituting from Figure 5.2 the T_{c_2}–conditions, i.e. $N_0^{\mathrm{C}} = N_{-1}^{\mathrm{C}} = 0$ and $z = z_\eta = 1$, into (5.25) and (5.26) yields

$$\mathcal{N} = \mathcal{N}_1^{\mathrm{C}} + 3\frac{\mathcal{T}_{c_2}^\nu}{\zeta(\nu)}\left\{\zeta(\nu) + \frac{3}{2}\frac{\delta_{3\nu}}{\mathcal{T}_{c_2}}\frac{\bar{\omega}}{\tilde{\omega}}\left[\frac{\zeta(3)}{N}\right]^{1/3}\zeta(2)\right\}, \tag{6.15}$$

$$\mathcal{M} = \mathcal{N}_1^{\mathrm{C}}. \tag{6.16}$$

The latter has been divided by Eq. (6.5) and we have used the abbreviation (2.37). We observe again the property of the antiferromagnetic phase that the whole polarization is in the condensate fraction as can be seen from (6.16).

From (6.15) and (6.16) we can explicitly calculate $\mathcal{T}_{c_2}$ as a function of $\mathcal{M}$. We subtract (6.16) from (6.15) and solve for the second critical temperature

$$\mathcal{T}_{c_2} = \left[\frac{\zeta(\nu)}{3}\right]^{1/\nu} (1-\mathcal{M})^{1/\nu} \left\{\zeta(\nu) + \frac{3}{2}\frac{\delta_{3\nu}}{\mathcal{T}_{c_2}}\frac{\bar{\omega}}{\tilde{\omega}}\left[\frac{\zeta(3)}{N}\right]^{1/3}\zeta(2)\right\}^{-1/\nu}. \tag{6.17}$$

Iterating the latter and performing a Taylor series up to the order $N^{-1/3}$ leads to the following expression for the second critical temperature

$$\boxed{\mathcal{T}_{c_2} = \left(\frac{1-\mathcal{M}}{3}\right)^{1/\nu} - \frac{\delta_{3\nu}}{2}\frac{\bar{\omega}}{\tilde{\omega}}\frac{\zeta(2)}{\zeta(3)}\left[\frac{\zeta(3)}{N}\right]^{1/3}.} \tag{6.18}$$

Note that for the case of a harmonically trapped spinor gas the latter is only valid where

$$(1-\mathcal{M})^{1/3} \gg \frac{3^{1/3}}{2}\frac{\bar{\omega}}{\tilde{\omega}}\frac{\zeta(2)}{\zeta(3)}\left[\frac{\zeta(3)}{N}\right]^{1/3} \tag{6.19}$$

is fulfilled. Otherwise, T_{c_2} would becomes negative, which is obviously wrong. Note that this is not the case if we directly use Eq. (6.17). However, as the typical experimental values for the total number of particles are $10^5 - 10^7$ particles, Eq. (6.18) is a good approximation for a wide range of magnetizations $\mathcal{M}$.

In Figure 6.1 (b) we plot the critical temperatures for a finite number of particles. In the following we discuss our results for the first and the second critical temperature. To this end we observe that for a vanishing magnetization the first and the second critical tend to the same value, i.e.,

$$\lim_{\mathcal{M}\to 0}(\mathcal{T}_{c_1} - \mathcal{T}_{c_2}) = 0. \tag{6.20}$$

This can also directly be seen from the Gross-Pitaevskii equations (5.11)–(5.13). According to Eq. (5.21) the magnetic chemical potential takes in the gas phase at zero magnetization the value $\eta = 0$. Substituting this into the Gross-Pitaevskii equations leads to the occurrence of a triple condensation, which is due to the degeneracy of all Zeeman states.

6.3 Discussion

We discuss the critical temperatures of the homogeneous and harmonically trapped spinor system. For both trapping configurations, we see from Figure 6.1 that the critical temperatures depend strongly on the total magnetization of the spinor gas. The first critical

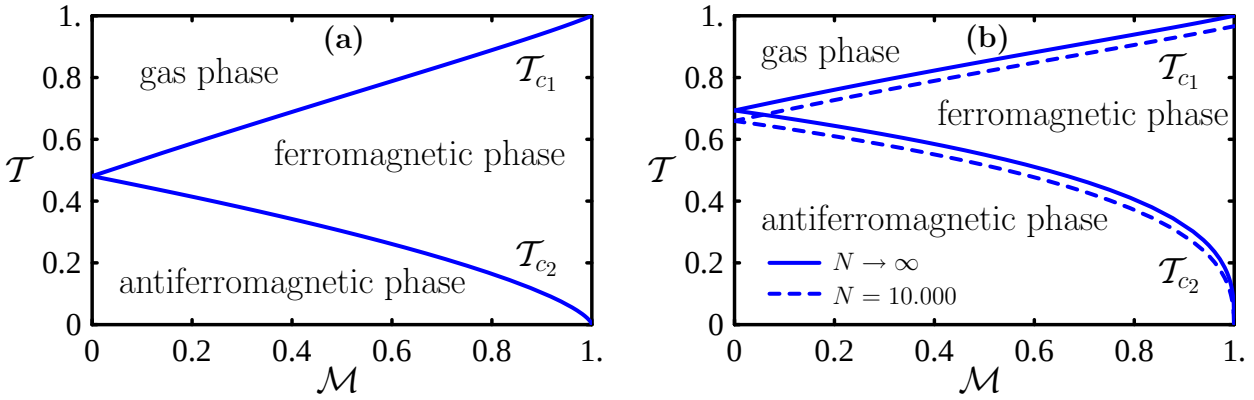

Figure 6.1: Critical temperatures of **(a)** homogeneous and **(b)** harmonically trapped spinor gas with $\bar{\omega} = \tilde{\omega}$.

temperature depends approximatively linear on the magnetization. By definition the first critical temperature reaches unity temperature for the full polarized case. Consequently, the first critical temperature decreases for lower magnetization. Furthermore, we see that $\mathcal{T}_{c_1}$ of the homogeneous spinor gas is much more sensitive to a change of the magnetization than the one of the harmonically trapped system.

As mentioned above, for zero magnetization the first critical temperature (6.13) and the second critical temperature (6.18) coincide. Therefore, the non-polarized spinor gas has only two phases and the ferromagnetic phase does not show up. Investigating further the characteristic properties of the $\mathcal{T}_{c_2}$ curve, we recognize that, in contrast to the behavior of $\mathcal{T}_{c_1}$, the second critical temperature decreases for a larger magnetization. For the case of a full polarized spinor system $\mathcal{T}_{c_2}$ takes the value zero. In other words, for a full polarized spinor gas the antiferromagnetic phase is missing, whereas for magnetizations ranging between one and zero we always have three phases.

We discuss the effect of a finite number of particles for the case $\bar{\omega} = \tilde{\omega}$ which is realized, for instance, in an isotropic trap. In Figure 6.1 (b) we plot the critical temperatures for $N = 10.000$ and $N \to \infty$ particles, where we have set $\bar{\omega} = \tilde{\omega}$. From Figure 6.1 (b) we see that for a smaller amount of particles those critical temperatures are decreased.

Chapter 7

Particle Numbers

In the last chapter we have derived the critical temperatures of a $F = 1$ spinor gas. In contrast to a scalar Bose gas, where we have only one critical temperature and two phases, the $F = 1$ spinor gas system has two critical temperatures and therefore three phases. In this chapter we derive the particle occupation number of the different Zeeman states as a function of the temperature for a given total magnetization. From this we will get a deeper physical understanding of the $F = 1$ spinor properties below $\mathcal{T}_{c_1}$.

7.1 Identification of Zeeman States

In order to determine the occupation number of each Zeeman state, we first have to identify the underlying equations. We start with considering a spinor gas in the gas phase, i.e., for temperatures above $\mathcal{T}_{c_1}$. Dividing Eqs. (5.19) and (5.20) by Eq. (6.5) and using (6.11) leads to

$$\mathcal{N} = \frac{\mathcal{T}^\nu}{\zeta(\nu)}\Bigg\{\zeta_\nu(zz_\eta)+\zeta_\nu(z)+\zeta_\nu(z/z_\eta)+\frac{3}{2}\,\frac{\delta_{3\nu}}{\mathcal{T}}\,\frac{\bar{\omega}}{\tilde{\omega}}\left[\frac{\zeta(3)}{N}\right]^{1/3}\Big[\zeta_2(zz_\eta)+\zeta_2(z)+\zeta_2(z/z_\eta)\Big]\Bigg\} \tag{7.1}$$

and

$$\mathcal{M} = \frac{\mathcal{T}^\nu}{\zeta(\nu)}\Bigg\{\zeta_\nu(zz_\eta)-\zeta_\nu(z/z_\eta)+\frac{3}{2}\,\frac{\delta_{3\nu}}{\mathcal{T}}\,\frac{\bar{\omega}}{\tilde{\omega}}\left[\frac{\zeta(3)}{N}\right]^{1/3}\Big[\zeta_2(zz_\eta)-\zeta_2(z/z_\eta)\Big]\Bigg\}. \tag{7.2}$$

Note that according to (2.37) we have $\mathcal{N} = 1$. However, we use this notation to emphasize that physically the left-hand side of Eq. (7.1) corresponds to the total number of particles. In the high-temperature limit $\mathcal{T} \to \infty$ the factor $\mathcal{T}^\nu$ in Eqs. (7.1) and (7.2) tends to infinity. In order to keep the left-hand side of Eqs. (7.1) and (7.2) constant, the second factors on the right-hand side of the latter equations have to tend to zero for high temperatures. According to Eqs. (4.22) and (4.23) we always have $z(\mathcal{T}), z_\eta(\mathcal{T}) > 0$. Furthermore, taking into account, that the zeta function is a monotonously increasing function (see Figure 5.1), we get with Eqs. (7.1) and (7.2) the following behavior of the fugacities in the high-temperature limit:

$$\lim_{\mathcal{T}\to\infty} z(\mathcal{T}) \;\longrightarrow\; 0, \tag{7.3}$$

$$\lim_{\mathcal{T}\to\infty} z(\mathcal{T})\, z_\eta(\mathcal{T}) \longrightarrow 0, \tag{7.4}$$

$$\lim_{\mathcal{T}\to\infty} z(\mathcal{T})\, z_\eta(\mathcal{T})^{-1} \longrightarrow 0. \tag{7.5}$$

Using Eqs. (4.21), (7.1), (7.3)–(7.5) we may write for Eq. (7.2) in the high-temperature limit

$$\mathcal{M} \overset{\mathcal{T}\gg\mathcal{T}_{c_1}}{\longrightarrow} \frac{z_\eta - z_\eta^{-1}}{z_\eta + 1 + z_\eta^{-1}}. \tag{7.6}$$

Note that the first-order contribution no longer appears in Eq. (7.6) due to the condition $\mathcal{T} \gg \mathcal{T}_{c_1}$. Therefore, in the high-temperature limit, the value of the magnetic fugacity z_η is the same for both the homogeneous spinor gas and the harmonically trapped one. Furthermore, we can deduce from Eq. (7.6) the following dependence of the magnetic fugacity on the magnetization

$$\lim_{\mathcal{T}\to\infty} z_\eta(\mathcal{T}) = \frac{1}{2}\frac{1}{1-\mathcal{M}}\left\{\mathcal{M} + \sqrt{4-3\mathcal{M}^2}\right\} \tag{7.7}$$

and its reciprocal

$$\lim_{\mathcal{T}\to\infty} z_\eta^{-1}(\mathcal{T}) = \frac{1}{2}\frac{1}{1+\mathcal{M}}\left\{-\mathcal{M} + \sqrt{4-3\mathcal{M}^2}\right\}. \tag{7.8}$$

Hence, we observe the symmetry

$$\lim_{\mathcal{T}\to\infty} z_\eta = \lim_{\mathcal{T}\to\infty} z_\eta^{-1}\Big|_{M\to -M}. \tag{7.9}$$

This finding motivates to study three special cases. At first, we study a system which is fully polarized in z-direction, i.e., $\mathcal{M} = +1$. The second limit is a system which has the opposite polarization of the first one, i.e. $\mathcal{M} = -1$. The last limit is a system with no polarization where $\mathcal{M} = 0$. From Eqs. (7.7) and (7.9) we conclude then the following behavior for the magnetic fugacity

$$\lim_{\mathcal{T}\to\infty} z_\eta^{\pm 1}(\mathcal{T}) \to \begin{cases} \infty & \mathcal{M} = \pm 1, \\ 1 & \mathcal{M} = 0, \\ 0 & \mathcal{M} = \mp 1. \end{cases} \tag{7.10}$$

We substitute the latter in Eq. (7.1) and deduce, that for the high-temperature limit the total number of particles are given by

$$\mathcal{N} \to \frac{\mathcal{T}^\nu}{\zeta(\nu)} \begin{cases} \zeta_\nu(z z_\eta) & \mathcal{M} = 1, \\ 3\,\zeta_\nu(z) & \mathcal{M} = 0, \\ \zeta_\nu(z/z_\eta) & \mathcal{M} = -1, \end{cases} \tag{7.11}$$

where, again, the first-order contribution could be neglected.

If the spinor gas is fully polarized in $\pm z$-direction, then every particle has to occupy the

Zeeman state $|a = \pm 1\rangle$. On the other hand, if the spinor gas in not polarized at all but still in thermal equilibrium, we expect each Zeeman state to be occupied by the same number of particles. Relating this to our results summarized in Eq. (7.11) motivates us to identify the particle number being in the excited a$^{\text{th}}$ Zeeman state as follows

$$\boxed{\mathcal{N}_a^{\mathrm{T}} = \frac{\mathcal{T}^\nu}{\zeta(\nu)} \begin{cases} \zeta_\nu(z z_\eta) + 3\,\delta_{3\nu}\beta\hbar\bar{\omega}\,\zeta_2(z z_\eta)/2 & a = 1, \\ \zeta_\nu(z) + 3\,\delta_{3\nu}\beta\hbar\bar{\omega}\,\zeta_2(z)/2 & a = 0, \\ \zeta_\nu(z/z_\eta) + 3\,\delta_{3\nu}\beta\hbar\bar{\omega}\,\zeta_2(z/z_\eta)/2 & a = -1, \end{cases}} \tag{7.12}$$

where the superscript T denotes the thermal particles. In general, the total number of particles being in the a$^{\text{th}}$ Zeeman state is given by a sum of particles being Bose-Einstein condensed and the thermal particles

$$\mathcal{N}_a = \mathcal{N}_a^{\mathrm{C}} + \mathcal{N}_a^{\mathrm{T}}. \tag{7.13}$$

With Eqs. (7.12) and (7.13) we are now able to make predictions for the particle number in every Zeeman state, which is of particular experimental interest. In a spinor condensate experiment it is, in principle, possible to measure via Stern-Gerlach separation the particle occupation number of the different Zeeman states [25]. This opens the possibility to verify the predictions which will be made in upcoming sections.

7.2 Particles in Gas Phase

We briefly discuss the occupation numbers of the different Zeeman states in the gas phase. We will see that the fluctuation of the occupation number is very small for $\mathcal{T} > \mathcal{T}_{c_1}$. Furthermore, we show that the first-order corrections become negligible in the high-temperature limit.

We see from Eq. (7.12) that, in order to determine the occupation number of the a$^{\text{th}}$ Zeeman state, we first have to calculate the fugacity and the magnetic fugacity. Using the coupled set of Eqs. (7.1) and (7.2), we obtain z and z_η as a function of the temperature and the magnetization. Unfortunately, this cannot be done in an analytic way. In order to obtain an exact result, which is also valid for temperatures near $\mathcal{T}_{c_1}$, we carry out the calculation numerically with the program MATHEMATICA. The calculation itself turns out to be quite uncomplicated and needs no further explanation.

In Figure 7.1 the particle number of different Zeeman states of an homogeneous and harmonically trapped spinor gas, respectively, is plotted for a total magnetization $\mathcal{M} = 0.25$. In order to see the correct behavior of the particle numbers near the first transition temperature we use the numerical data for the fugacity and magnetic fugacity. The particle numbers of every Zeeman state tend to a constant value for high temperatures, i.e., the spinor gas behaves like a classical gas. On the other hand, at temperatures close to the first transition

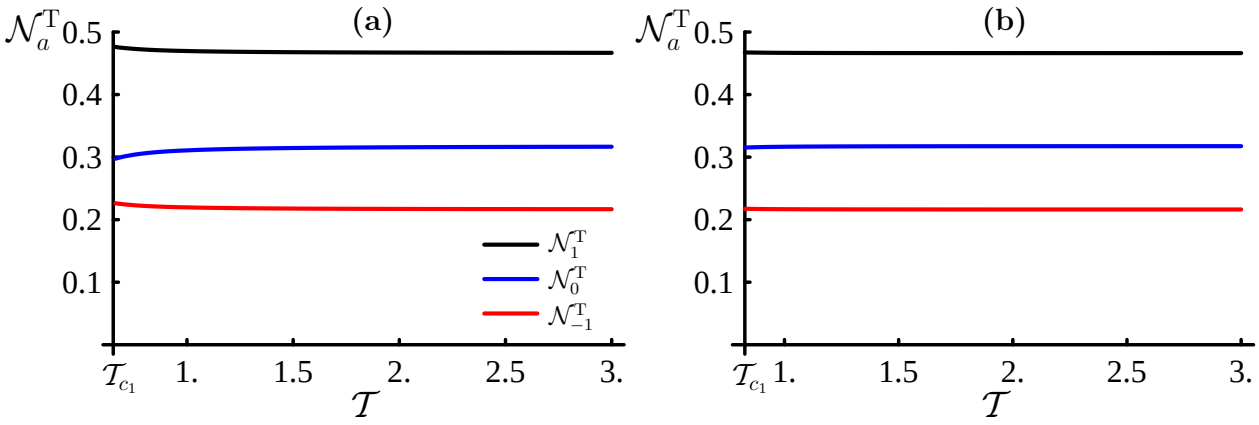

Figure 7.1: Occupation number of Zeeman states for **(a)** homogeneous and **(b)** harmonically trapped spinor gas with $\mathcal{M} = 0.25$. For (b), the finite-size corrections are completely negligible. It is seen that for temperature closely above the first critical temperature, the occupation number is nearly a constant in temperature.

point the particle numbers start to arrange themselves in a different way. For a homogeneous spinor gas this can be clearly seen in Figure 7.1 (a).

7.3 High-Temperature Limit

It is also possible to obtain an analytical result for both the fugacity and the magnetic fugacity in the high-temperature limit. To this end, we write Eqs. (7.1) and (7.2) differently by adding and subtracting them from each other. We then obtain

$$x = (1+\mathcal{M})^{-1}\left[2\zeta_\nu(zz_\eta) + \zeta_\nu(z)\right] \tag{7.14}$$

and

$$x = (1-\mathcal{M})^{-1}\left[\zeta_\nu(z) + 2\zeta_\nu(z/z_\eta)\right]. \tag{7.15}$$

Here, we have defined the dimensionless parameter

$$x \equiv \zeta(\nu)\mathcal{T}^{-\nu}, \tag{7.16}$$

which is small for $\mathcal{T} \gg 1$. Together with (7.3) and (7.10), this motivates to introduce the following Taylor expansion for the fugacity

$$z(x) \;=\; \alpha_0 + \alpha_1 x + \alpha_2 x^2 + \ldots, \tag{7.17}$$

and the magnetic fugacity

$$z_\eta(x) \;=\; a_0 + a_1 x + a_2 x^2 + \ldots. \tag{7.18}$$

Therein the parameter (7.16) is used as a smallness parameter which can also be interpreted in a physical way. To this end we restrict ourself to a homogeneous spinor gas. Using

Eqs. (4.38), (5.19), (5.20), and (6.5) we may write for the total number of particles in the homogeneous case

$$N = \frac{V}{\lambda^3}\,\zeta(3/2)\mathcal{T}^{-3/2}. \tag{7.19}$$

Comparing x as defined in (7.16) with the latter yields the following relation

$$x = \frac{N}{V}\lambda^3. \tag{7.20}$$

Hence, x is the density of the spinor gas multiplied by the third power of the average thermal length. But this is nothing but the average number of particles occupying a volume which is equal to the average size a particle itself. If x approaches unity, then the overlap of the wave functions of different particles in the system is no longer negligible. In this case we expect deviations from the classically predicted behavior which are due to quantum mechanical effects.

We will calculate the first two contributions to the fugacity z and to the magnetic fugacity z_η. The zeroth order of both functions has already been calculated in the last section. With Eqs. (7.3) and (7.7) we get for α_0 in (7.17) and a_0 in (7.18)

$$\alpha_0 = 0, \tag{7.21}$$

$$a_0 = \frac{1}{2}\,\frac{1}{1-\mathcal{M}}\left(\mathcal{M} + \sqrt{4-3\mathcal{M}^2}\right). \tag{7.22}$$

Alternatively, we can calculate a_0 in the following way. According to Eq. (7.6) the magnetization reads for high temperatures

$$\mathcal{M} = \lim_{\mathcal{T}\to\infty} \frac{z_\eta - z_\eta^{-1}}{z_\eta + 1 + z_\eta^{-1}}. \tag{7.23}$$

On the other hand, from Eqs. (7.14) and (7.18) we deduce

$$\lim_{\mathcal{T}\to\infty} z_\eta = a_0. \tag{7.24}$$

Substituting the latter into the former equation yields

$$\mathcal{M} = \frac{a_0 - a_0^{-1}}{a_0 + 1 + a_0^{-1}}. \tag{7.25}$$

Note, the magnetization is constant for all temperatures. Therefore, Eq. (7.25) is always valid. Solving Eq. (7.25) for a_0 yields the same as in Eq. (7.22).

To calculate the remaining coefficients α_i and a_i we use the polylogarithmic function (4.21) to rewrite Eqs. (7.14) and (7.15) in the following way

$$x = \frac{1}{1+\mathcal{M}}\left(2zz_\eta + 2\frac{z^2 z_\eta^2}{2^\nu} + \ldots + z + \frac{z^2}{2^\nu} + \ldots\right), \tag{7.26}$$

$$x = \frac{1}{1-\mathcal{M}}\left(z + \frac{z^2}{2^\nu} + \ldots + 2zz_\eta^{-1} + 2\frac{z^2 z_\eta^{-2}}{2^\nu} + \ldots\right). \tag{7.27}$$

Substituting Eqs. (7.17) and (7.18) into (7.26) and (7.27) yields

$$\begin{aligned} x &= \frac{1}{1+\mathcal{M}}\Big[2(\alpha_1 x+\alpha_2 x^2+\ldots)(a_0+a_1 x+\ldots)+2^{-\nu+1}(\alpha_1 x+\ldots)^2(a_0+\ldots)^2 \\ &\quad +\ldots+\alpha_1 x+\alpha_2 x^2+\ldots+2^{-\nu}(\alpha_1 x+\alpha_2 x^2\ldots)^2+\ldots\Big], \end{aligned} \tag{7.28}$$

and

$$\begin{aligned} (a_0+a_1 x+\ldots)^2\, x &= \frac{1}{1-\mathcal{M}}\Big[(\alpha_1 x+\alpha_2 x^2+\ldots)(a_0+a_1 x+\ldots)^2 \\ &\quad +2^{-\nu}(\alpha_1 x+\ldots)^2(a_0+\ldots)^2+\ldots+2(\alpha_1 x+\alpha_2 x^2+\ldots) \\ &\quad \times(a_0+a_1 x+\ldots)+2^{-\nu+1}(\alpha_1 x+\alpha_2 x^2+\ldots)^2+\ldots\Big]. \end{aligned} \tag{7.29}$$

By comparing the respective coefficients of different powers of x in Eqs. (7.28) and (7.29), we can calculate successively the coefficients $\alpha_1, \alpha_2, \ldots$ and $a_1, a_2, \ldots$.

7.3.1 First Order

Comparing the coefficients of the power x^1 in Eqs. (7.28) and (7.29) yields the following set of equations

$$1 = (1+\mathcal{M})^{-1}\left(2\alpha_1 a_0+\alpha_1\right), \tag{7.30}$$

$$a_0^2 = (1-\mathcal{M})^{-1}\left(\alpha_1 a_0^2+2\alpha_1 a_0\right). \tag{7.31}$$

In order to calculate α_1, one of these equations is sufficient as we have already determined a_0 in Eq. (7.22). Substituting Eq. (7.25) in (7.30) or (7.31), respectively, leads to

$$\alpha_1 = \left(a_0+1+a_0^{-1}\right)^{-1}. \tag{7.32}$$

Using Eq. (7.22) the latter can be rewritten as

$$\alpha_1 = \frac{1}{3}\sqrt{4-3\,\mathcal{M}^2}-\frac{1}{3}\,. \tag{7.33}$$

To calculate α_2 and a_1 we have to compare the coefficients of the next order in x.

7.3.2 Second Order

Comparing the coefficients of x^2 in (7.28) and (7.29) and using Eqs. (7.25) and (7.32) leads to the following matrix equation

$$\mathbf{M}\begin{pmatrix} a_1 \\ \alpha_2 \end{pmatrix} = 2^{-\nu}\alpha_1^2\begin{pmatrix} -2a_0^2-1 \\ a_0^2+2 \end{pmatrix}, \tag{7.34}$$

with the matrix

$$\mathbf{M} = \begin{pmatrix} 2\alpha_1 & 2a_0+1 \\ 2\alpha_1 & -a_0(a_0+2) \end{pmatrix}. \tag{7.35}$$

The inverse of $\mathbf{M}$ is easily calculated as

$$\mathbf{M}^{-1} = \frac{1}{\det \mathbf{M}} \begin{pmatrix} -a_0(a_0+2) & -(2a_0+1) \\ -2\alpha_1 & 2\alpha_1 \end{pmatrix}. \tag{7.36}$$

Inverting (7.34) with the help of (7.36) by using Eqs. (7.25), (7.32) leads to

$$a_1 = -2^{-\nu} a_0 \frac{a_0^2-1}{a_0^2+4a_0+1}, \tag{7.37}$$

$$\alpha_2 = -\frac{2^{-\nu}\, 3\, \alpha_1^2 (a_0^2+1)}{a_0^2+4a_0+1}. \tag{7.38}$$

The coefficients of higher order in x can be calculated in the same manner. In Figure 7.2 the numerical results of the fugacity and the magnetic fugacity is compared with the analytical result just obtained for the magnetization $\mathcal{M} = 0.25$. As can clear be seen, taking the first two contributions terms of the analytical result already yields a good agreement with the exact numerical result for $\mathcal{T} \gg 1$.

7.4 Particles in Ferro- and Antiferromagnetic Phase

In this section we discuss the particle occupation number of the different Zeeman states for the ferro- and antiferromagnetic phase. We will see that the spinor gas exhibits a quite interesting behavior in these two phases.

We start with the ensemble being in the ferromagnetic phase. Substituting the solutions of the algebraic Gross-Pitaevskii equations for the ferromagnetic phase, which are summarized in Figure 5.2, in Eqs. (7.12) and (7.13) yields

$$\mathcal{N} = \mathcal{N}_1^{\mathrm{C}} + \frac{\mathcal{T}^\nu}{\zeta(\nu)} \left\{ \zeta(\nu) + \zeta_\nu(z) + \zeta_\nu(z^2) + \frac{3}{2} \frac{\delta_{3\nu}}{\mathcal{T}} \frac{\bar{\omega}}{\tilde{\omega}} \left[\frac{\zeta(3)}{N} \right]^{1/3} \Big[\zeta(2) + \zeta_2(z) + \zeta_2(z^2) \Big] \right\}, \tag{7.39}$$

$$\mathcal{M} = \mathcal{N}_1^{\mathrm{C}} + \frac{\mathcal{T}^\nu}{\zeta(\nu)} \left\{ \zeta(\nu) - \zeta_\nu(z^2) + \frac{3}{2} \frac{\delta_{3\nu}}{\mathcal{T}} \frac{\bar{\omega}}{\tilde{\omega}} \left[\frac{\zeta(3)}{N} \right]^{1/3} \Big[\zeta(2) - \zeta_2(z^2) \Big] \right\}. \tag{7.40}$$

In contrast to Eqs. (7.1) and (7.2), where we used the fugacity z and magnetic fugacity z_η to adjust the total number of particles and the total magnetization of the system, we have to use now as an adjusting parameter the particle number of the condensed fraction in the first Zeeman state $\mathcal{N}_1^{\mathrm{C}}$ and the fugacity z. The numerical result for the homogeneous and the harmonically trapped spinor gas is plotted in Figure 7.3. Before we discuss Figure 7.3,

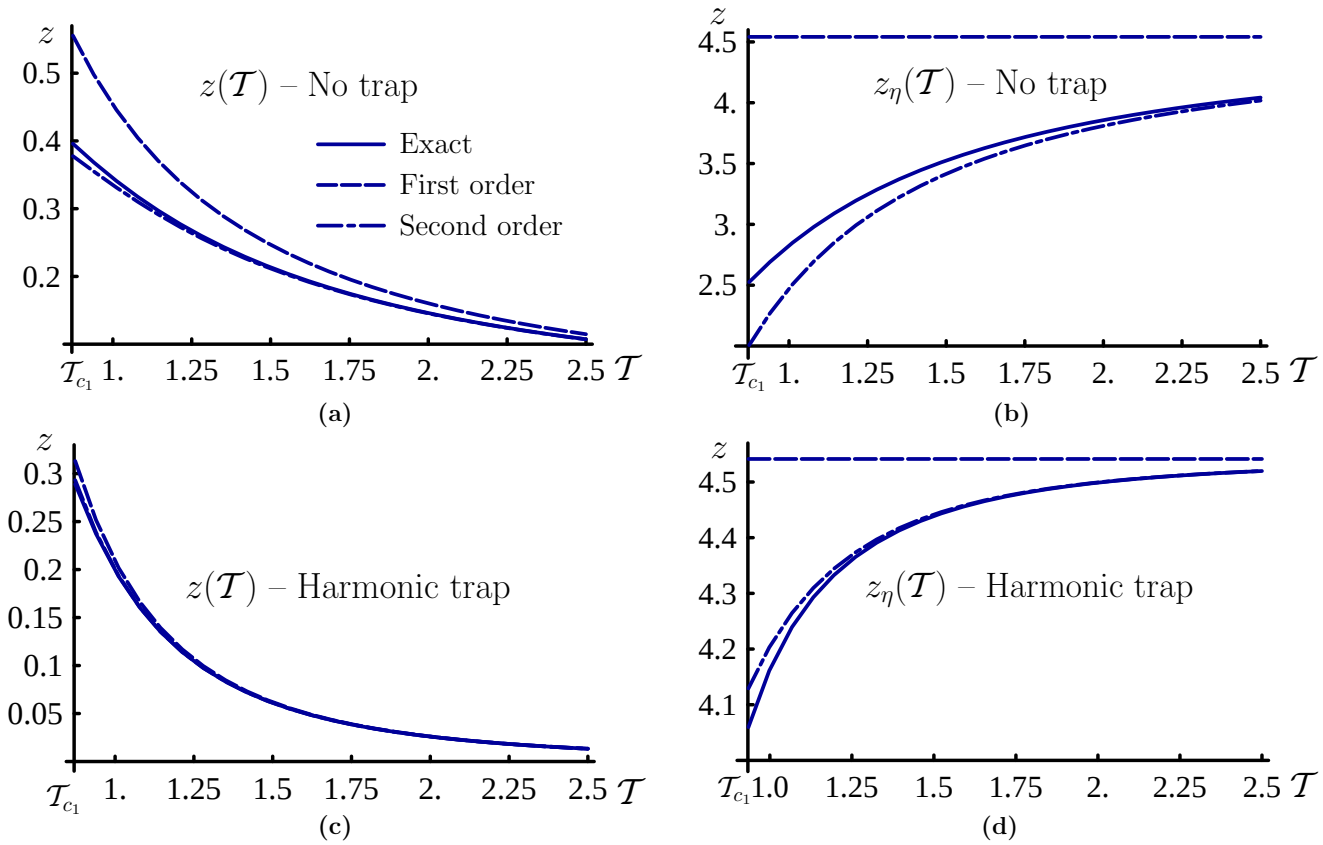

Figure 7.2: Exact versus approximative solutions of fugacity z and magnetic fugacity z_η in the high-temperature limit. In **(a), (b)** homogeneous and in **(c), (d)** harmonically trapped spinor gas with magnetization $\mathcal{M} = 0.25$.

we also treat the antiferromagnetic case. Again, taking the solutions of the Gross-Pitaevskii equations for the antiferromagnetic spinor gas from Figure 5.2 and substituting them into Eqs. (7.12) and (7.13) yields

$$1 = \mathcal{N}_1^{\mathrm{C}} + \mathcal{N}_0^{\mathrm{C}} + \mathcal{N}_{-1}^{\mathrm{C}} + 3\,\mathcal{T}^{\nu}\left\{1 + \frac{3}{2}\,\frac{\delta_{3\nu}}{\mathcal{T}}\,\frac{\bar{\omega}}{\tilde{\omega}}\,\frac{\zeta(2)}{\zeta(3)}\left[\frac{\zeta(3)}{N}\right]^{1/3}\right\}, \tag{7.41}$$

$$\mathcal{M} = \mathcal{N}_1^{\mathrm{C}} - \mathcal{N}_{-1}^{\mathrm{C}}. \tag{7.42}$$

In contrast to Eqs. (7.1), (7.2) and Eqs. (7.39), (7.40), where we had two adjusting parameter, we have in Eqs. (7.41), (7.42) three parameters, namely, the occupation numbers of each Zeeman state in the condensed fraction. Therefore, in order to fix the value of the additional adjusting parameter we need another condition. To find this extra condition we remember the discussion in Section 5.3. There, we emphasized that a double condensation of the states $|a = 0\rangle$ and $|a = -1\rangle$ occurs at the second critical temperature. As none of both states is preferred for $\mathcal{T} \leq \mathcal{T}_{c_2}$, we assume the condition $\mathcal{N}_1^{\mathrm{C}} = \mathcal{N}_0^{\mathrm{C}}$ [56]. From Eqs. (7.41) and (7.42)

we then deduce

$$\mathcal{N}_1^{\mathrm{C}} - \mathcal{M} = \mathcal{N}_0^{\mathrm{C}} = \mathcal{N}_{-1}^{\mathrm{C}} = \frac{1-\mathcal{M}}{3} - \mathcal{T}^{\nu}\left\{1 + \frac{3}{2}\frac{\delta_{3\nu}}{\mathcal{T}}\frac{\bar{\omega}}{\tilde{\omega}}\frac{\zeta(2)}{\zeta(3)}\left[\frac{\zeta(3)}{N}\right]^{1/3}\right\}. \tag{7.43}$$

We thus have for temperatures below $\mathcal{T}_{c_2}$ an analytical result for the occupation numbers.

We finish this chapter with a discussion of Figure 7.3. We first treat the homogeneous case. As discussed in Section 7.2, coming from temperatures far above the first critical temperature, the occupation numbers of each Zeeman state is altered only weakly by changing the temperature. This is what one would expect from an ideal classical spinor gas. As long as the temperatures are far above the first critical temperatures the average distances between the particle are large compared to the average spatial extension of a single particle. Therefore, quantum effects can be neglected. Reaching temperatures near to $\mathcal{T}_{c_1}$ the extension of a single particle is close to the average distance between neighboring particles. Thus the bosonic quantum mechanical nature of the particles can no longer be neglected. Depending on the total magnetization of the system this manifests itself in a deviation of the occupation number from the high-temperature behavior in the gas phase, as can be seen in Figure 7.3 for the magnetization $\mathcal{M} = 0.25$.

Reaching the first critical temperature, the $|a = 1\rangle$ state of the system starts to Bose-Einstein condense. In Figure 7.3 the condensed part of the spinor gas is denoted by the dashed line. It can be seen quite clearly that the particles in the condensed fraction are fully polarized. Furthermore, the thermal occupation numbers of the different Zeeman states change drastically. We see that the occupation number of the thermal particles in the first Zeeman level $\mathcal{N}_1^{\mathrm{T}}$ reduces drastically with decreasing temperature. Reaching $\mathcal{T}_{c_2}$, the system shows a remarkable property. Here, the occupation number of each thermal Zeeman state is equal, i.e., the magnetization of the thermal cloud is zero which correspond to an antiferromagnetic behavior. It is worthwhile noticing that for the special case of a magnetization of $\mathcal{M} = 0.25$, the occupation number of each thermal Zeeman component and the occupation number of the condensed first Zeeman state coincide. From an experimental point of view this is an interesting observation, because it is much easier to measure and compare identical occupation numbers of different Zeeman states than to compare different ones.

Going below the second critical temperature, the behavior of the occupation numbers can be described analytically, see Eq. (7.43). It is remarkable that the second phase transition shows a double condensation [56], i.e., particles being in the Zeeman state $|a = 0\rangle$ and $|a = -1\rangle$ start to Bose-Einstein condense at the same critical temperature. Furthermore, we have the characteristic property of the antiferromagnetic phase that the particle numbers of the excited are the same in every Zeeman state, i.e., the magnetization of the thermal cloud remains zero for $\mathcal{T} \leq \mathcal{T}_{c_2}$. At zero temperature all excited particles Bose-Einstein condense, so in complete analogy to a scalar Bose-Einstein condensate the ideal spinor condensate shows no depletion of the ground-state at zero temperature. As it can be seen from Eq. (7.43), the number of particles being in the Bose-Einstein condensed state are the same for Zeeman

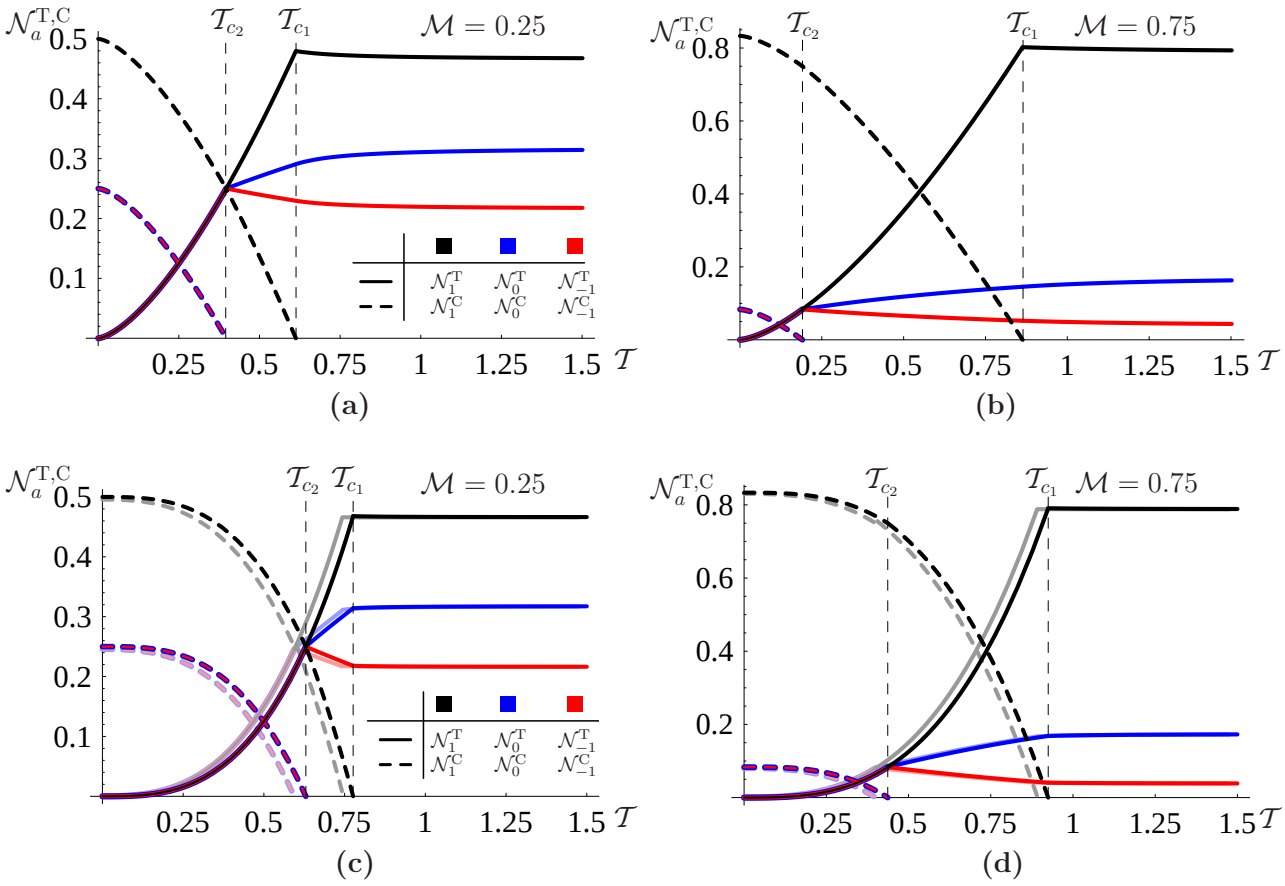

Figure 7.3: Particle occupation of Zeeman state a for the thermal and condensed fraction in case of **(a)**, **(b)** homogeneous and **(c)**, **(d)** harmonically trapped spinor gas with magnetizations $\mathcal{M} = 0.25$ and 0.75. For **(c)** and **(d)** the case of an infinite number of particles $N \to \infty$ (dark color) and of a finite number of $N = 10.000$ particles (bright color) is plotted.

state $|a = 0, -1\rangle$, whereas the number of particles being in the condensed $|a = 1\rangle$ state differs at a given magnetization by a constant which remains the same for $\mathcal{T} \leq \mathcal{T}_{c_2}$. Note that the discussion of harmonically trapped spinor gas can be given in complete analogy to the homogeneous spinor gas. They just differ qualitatively. This can be seen from Figure 7.3.

Chapter 8

Heat Capacity

In this chapter the heat capacity of a homogeneous and a harmonically trapped $F = 1$ spinor gas is discussed. Like in the chapters before we emphasize how the temperature dependence of the heat capacity changes with the total magnetization of the system. We will see that the phase transitions discussed above also show up in a characteristic way in the heat capacity. In the following we will neglect the finite size scaling.

8.1 General Procedure

The heat capacity is defined as

$$C_V = \left.\frac{\partial U}{\partial T}\right|_{N,M,V}, \tag{8.1}$$

where U is the internal energy given by

$$U = \mathcal{F} + TS + \mu N + \eta M. \tag{8.2}$$

For convenience, we calculate instead of Eq. (8.1) the heat capacity per particle

$$\frac{C_V}{Nk_B} = \left.\frac{1}{Nk_BT_0}\frac{\partial U}{\partial \mathcal{T}}\right|_{\mathcal{N},\mathcal{M},V}, \tag{8.3}$$

where we also performed a change of variables using Eq. (6.8). In Eq. (8.2), S denotes the entropy

$$S = -\left.\frac{1}{T_0}\frac{\partial \mathcal{F}}{\partial \mathcal{T}}\right|_{V,\mu,\eta}. \tag{8.4}$$

and $\mathcal{F}$ is the grand-canonical free energy of the system. Using the property that the effective action $\Gamma[\Psi^*, \Psi]$ reduces at extremized Background fields to the grand-canonical free energy and (4.36), (5.10), (6.5) we obtain approximation

$$\frac{\mathcal{F}}{Nk_B} = -\frac{\mathcal{T}^{\nu+1}}{\zeta(\nu)}\Big[\zeta_{\nu+1}(zz_\eta) + \zeta_{\nu+1}(z) + \zeta_{\nu+1}(z/z_\eta)\Big]. \tag{8.5}$$

Note that the tree-level action $\mathcal{A}[\Psi^*, \Psi]$ in Eq. (4.36) does not contribute to the grand-canonical free energy in (8.5) if we consider the Gross-Pitaevskii equations (5.10) to be fulfilled. This means that the condensed particles do not contribute to the thermal properties of the gas, which is due the Gross-Pitaevskii equations (5.11)–(5.13). To calculate the total number of particles and the total magnetization of the system, we cannot start directly from Eq. (8.5), but have to proceed according to Chapter 5. Using Eqs. (5.15), (5.16), (6.5), (8.2), (8.4), and (8.5) yields for the internal energy

$$U = \nu \frac{\mathcal{T}^{\nu+1}}{\zeta(\nu)} \Big[\zeta_{\nu+1}(z z_\eta) + \zeta_{\nu+1}(z) + \zeta_{\nu+1}(z/z_\eta) \Big]. \tag{8.6}$$

The latter equation is the starting point for calculating the heat capacity (8.3) for *all* phases.

8.2 Gas Phase

In this section we calculate the heat capacity of a $F = 1$ spinor gas in the gas phase. Furthermore, we will show that for $\mathcal{T} \to \infty$ the heat capacity follows the Dulong-Petit law. In addition, we calculate the heat capacity in the limit $\mathcal{T} \searrow \mathcal{T}_{c_1}$.

8.2.1 Derivation

The internal energy of the system being in the gas phase is simply given by the general expression (8.6). Using Eq. (8.3) we get after a straight-forward calculation for the heat capacity

$$\begin{aligned} \frac{C_V}{N k_B} = \nu \frac{\mathcal{T}^\nu}{\zeta(\nu)} \Bigg\{ & (\nu+1) \Big[\zeta_{\nu+1}(z z_\eta) + \zeta_{\nu+1}(z) + \zeta_{\nu+1}(z/z_\eta) \Big] \\ & + \zeta_\nu(z z_\eta)\, \mathcal{T} \frac{\partial}{\partial \mathcal{T}} \log z z_\eta + \zeta_\nu(z)\, \mathcal{T} \frac{\partial}{\partial \mathcal{T}} \log z + \zeta_\nu(z/z_\eta)\, \mathcal{T} \frac{\partial}{\partial \mathcal{T}} \log z/z_\eta \Bigg\}. \end{aligned} \tag{8.7}$$

To get rid of the partial derivatives in Eq. (8.7) we make use of the condition that the total number of particles and the total magnetization are not altered by changing temperature, i.e.,

$$\left. \frac{\partial \mathcal{N}}{\partial \mathcal{T}} \right|_{\mathcal{N},\mathcal{M},V} = 0, \qquad \left. \frac{\partial \mathcal{M}}{\partial \mathcal{T}} \right|_{\mathcal{N},\mathcal{M},V} = 0. \tag{8.8}$$

With (5.19), (5.20) the latter yields a coupled set of equations, which can be written as a matrix equation

$$\mathbf{M} \frac{\mathcal{T}^{\nu+1}}{\zeta(\nu)} \frac{\partial}{\partial \mathcal{T}} \begin{pmatrix} \log z \\ \log z_\eta \end{pmatrix} = -\nu \begin{pmatrix} \mathcal{N} \\ \mathcal{M} \end{pmatrix}, \tag{8.9}$$

$$\mathbf{M} = \begin{pmatrix} \zeta_{\nu-1}(z z_\eta) + \zeta_{\nu-1}(z) + \zeta_{\nu-1}(z/z_\eta) & \zeta_{\nu-1}(z z_\eta) - \zeta_{\nu-1}(z/z_\eta) \\ \zeta_{\nu-1}(z z_\eta) - \zeta_{\nu-1}(z/z_\eta) & \zeta_{\nu-1}(z z_\eta) + \zeta_{\nu-1}(z/z_\eta) \end{pmatrix}, \tag{8.10}$$

In order to solve Eq. (8.9) for $\partial_T z$ and $\partial_T z_\eta$, we have to invert $\mathbf{M}$, which is simply

$$\mathbf{M}^{-1} = \frac{1}{\det \mathbf{M}} \begin{pmatrix} \zeta_{\nu-1}(zz_\eta) + \zeta_{\nu-1}(z/z_\eta) & -\zeta_{\nu-1}(zz_\eta) + \zeta_{\nu-1}(z/z_\eta) \\ -\zeta_{\nu-1}(zz_\eta) + \zeta_{\nu-1}(z/z_\eta) & \zeta_{\nu-1}(zz_\eta) + \zeta_{\nu-1}(z) + \zeta_{\nu-1}(z/z_\eta) \end{pmatrix}, \tag{8.11}$$

with the determinant

$$\det \mathbf{M} = 4\zeta_{\nu-1}\left(zz_\eta\right)\zeta_{\nu-1}\left(z/z_\eta\right) + \zeta_{\nu-1}\left(z\right)\Big[\zeta_{\nu-1}\left(zz_\eta\right) + \zeta_{\nu-1}\left(z/z_\eta\right)\Big]. \tag{8.12}$$

Multiplying (8.9) from the left side with (8.11) yields

$$\frac{\mathcal{T}^{\nu+1}}{\zeta(\nu)}\frac{\partial}{\partial \mathcal{T}} \begin{pmatrix} \log z \\ \log z_\eta \end{pmatrix} = \mathbf{a}, \tag{8.13}$$

with the vector

$$\mathbf{a} = -\frac{\nu}{\det \mathbf{M}^{(0)}} \begin{pmatrix} \mathcal{N}\left[\zeta_{\nu-1}\left(zz_\eta\right) + \zeta_{\nu-1}\left(z/z_\eta\right)\right] - \mathcal{M}\left[\zeta_{\nu-1}\left(zz_\eta\right) - \zeta_{\nu-1}\left(z/z_\eta\right)\right] \\ -\mathcal{N}\left[\zeta_{\nu-1}\left(zz_\eta\right) - \zeta_{\nu-1}\left(z/z_\eta\right)\right] + \mathcal{M}\left[\zeta_{\nu-1}\left(zz_\eta\right) + \zeta_{\nu-1}\left(z\right) + \zeta_{\nu-1}\left(z/z_\eta\right)\right] \end{pmatrix}. \tag{8.14}$$

Substituting Eqs. (8.13), (8.14) into (8.7) yields for the heat capacity in the gas phase

$$\begin{aligned} \frac{C_V}{Nk_B} &= \nu(\nu+1)\frac{\zeta_{\nu+1}\left(zz_\eta\right) + \zeta_{\nu+1}\left(z\right) + \zeta_{\nu+1}\left(z/z_\eta\right)}{\zeta_{\nu}\left(zz_\eta\right) + \zeta_{\nu}\left(z\right) + \zeta_{\nu}\left(z/z_\eta\right)} - \nu^2\Big\{\zeta_{\nu-1}\left(zz_\eta\right) + \zeta_{\nu-1}\left(z/z_\eta\right) - \\ &\quad - 2\,\mathcal{M}\Big[\zeta_{\nu-1}\left(zz_\eta\right) - \zeta_{\nu-1}\left(z/z_\eta\right)\Big] + \mathcal{M}^2\Big[\zeta_{\nu-1}\left(zz_\eta\right) + \zeta_{\nu-1}\left(z\right) + \zeta_{\nu-1}\left(z/z_\eta\right)\Big]\Big\} \\ &\quad \times \frac{\zeta_{\nu}\left(zz_\eta\right) + \zeta_{\nu}\left(z\right) + \zeta_{\nu}\left(z/z_\eta\right)}{4\,\zeta_{\nu-1}\left(zz_\eta\right)\zeta_{\nu-1}\left(z/z_\eta\right) + \zeta_{\nu-1}\left(z\right)\left[\zeta_{\nu-1}\left(zz_\eta\right) + \zeta_{\nu-1}\left(z/z_\eta\right)\right]} \end{aligned} \tag{8.15}$$

In Figure 8.1, which at the end of this chapter, the heat capacity is plotted versus the temperature for the typical magnetizations $\mathcal{M} = 0.25$ and 0.75.

8.2.2 High-Temperature Limit

In Figure 8.1, we see that the heat capacity of both the homogeneous and harmonically trapped spinor gas tends for high temperatures to a constant value. To quantify this, we use the definition of the polylogarithmic function (4.21) and Eqs. (7.3)–(7.6), so that we get for (8.15) the following expression

$$\begin{aligned} \lim_{T\to\infty}\frac{C_V}{Nk_B} &= \nu(\nu+1) - \nu^2\Big\{zz_\eta + zz_\eta^{-1} - 2\frac{z_\eta - z_\eta^{-1}}{z_\eta + 1 + z_\eta^{-1}}\left(zz_\eta - zz_\eta^{-1}\right) \\ &\quad + \left(\frac{z_\eta - z_\eta^{-1}}{z_\eta + 1 + z_\eta^{-1}}\right)^2\left(zz_\eta + z + zz_\eta^{-1}\right)\Big\}\frac{zz_\eta + z + zz_\eta^{-1}}{4z^2 + z(zz_\eta + zz_\eta^{-1})}. \end{aligned} \tag{8.16}$$

It turns out that the all z, z_η cancel each other, so that we obtain

$$\lim_{\mathcal{T}\to\infty} \frac{C_V}{Nk_B} = \nu. \tag{8.17}$$

In other words, the homogeneous and the harmonically trapped spinor gas fulfill the *Dulong-Petit law* [45]

$$\lim_{\mathcal{T}\to\infty} C_V = \nu N k_B, \tag{8.18}$$

which states that every degree of freedom contributes with $k_B/2$ to the heat capacity. This is an important result, as it confirms our result for the heat capacity in the high-temperature limit.

8.2.3 First Critical Temperature

We investigate now the other interesting limit of the heat capacity where we reach the first critical temperature from above. According to Figure 5.2 we have at T_{c_1} the conditions $N_a^{\mathrm{C}} = 0$ and $E_{\mathbf{0}} - \mu - \eta = 0$. With the definition of z and z_η in Eqs. (4.22) and (4.23), this corresponds to

$$\lim_{T\searrow T_{c_1}} z z_\eta \to 1. \tag{8.19}$$

Therefore, we can make use of the replacement

$$\lim_{T\searrow T_{c_1}} \to \lim_{z z_\eta \to 1}. \tag{8.20}$$

For the limit $z z_\eta \to 1$ we have to treat the case of a homogeneous and harmonically trapped spinor condensate separately. The reason is that in Eq. (8.15) terms of the kind $\zeta_{\nu-1}(z z_\eta)$ occur, which diverge in the homogeneous case $\nu = 3/2$ for $z z_\eta \to 1$. They remain finite for the harmonically trapped case $\nu = 3$. Therefore, using

$$\lim_{z z_\eta \to 1} \zeta_{\nu-1}(z z_\eta)\Big|_{\nu=3/2} \to \infty \tag{8.21}$$

we get for the heat capacity in case of a homogeneous spinor gas

$$\lim_{z z_\eta \to 1} \frac{C_V}{Nk_B} = \frac{15}{4}\frac{\zeta\left(5/2\right) + \zeta_{5/2}\left(z\right) + \zeta_{5/2}(z^2)}{\zeta\left(3/2\right) + \zeta_{3/2}\left(z\right) + \zeta_{3/2}(z^2)} - \frac{9}{4}\frac{\zeta\left(3/2\right) + \zeta_{3/2}\left(z\right) + \zeta_{3/2}(z^2)}{\zeta_{1/2}(z) + 4\zeta_{1/2}(z^2)}(1-\mathcal{M})^2. \tag{8.22}$$

The corresponding limit of the harmonically trapped spinor gas reads

$$\begin{aligned}\lim_{z z_\eta \to 1} \frac{C_V}{Nk_B} &= 12\frac{\zeta(4) + \zeta_4\left(z\right) + \zeta_4\left(z^2\right)}{\zeta(3) + \zeta_3\left(z\right) + \zeta_3\left(z^2\right)} - 9\Big\{\zeta(2) + \zeta_2\left(z^2\right) - 2\,\mathcal{M}\Big[\zeta(2) - \zeta_2\left(z^2\right)\Big] \\ &+ \mathcal{M}^2\Big[\zeta(2) + \zeta_2\left(z\right) + \zeta_2\left(z^2\right)\Big]\Big\}\frac{\zeta(3) + \zeta_3\left(z\right) + \zeta_3\left(z^2\right)}{4\,\zeta(2)\,\zeta_2\left(z^2\right) + \zeta_2\left(z\right)\left[\zeta(2) + \zeta_2\left(z^2\right)\right]}.\end{aligned} \tag{8.23}$$

Comparing Eq. (8.22) with (8.23), we see that the divergent term occurring in the homogeneous case causes a cancelation of a number of terms, which do not cancel out in the harmonic case (8.23).

8.3 Ferromagnetic Phase

In the last section we have derived the heat capacity of a $F = 1$ spinor gas for a temperature above $\mathcal{T}_{c_1}$. We study now the heat capacity of a spinor system which is in the ferromagnetic phase, i.e., we cover the temperature range $\mathcal{T}_{c_2} \leq \mathcal{T} \leq \mathcal{T}_{c_1}$. The derivation of the heat capacity in the ferromagnetic phase is analogous to the one given in the last section. Substituting the conditions for the ferromagnetic phase (5.23), (5.24) in Eq. (8.6) yields for the internal energy of the system in the ferromagnetic phase

$$\frac{U}{Nk_B} = \nu \frac{\mathcal{T}^{\nu+1}}{\zeta(\nu)} \Big[\zeta(\nu+1) + \zeta_{\nu+1}(z) + \zeta_{\nu+1}(z^2)\Big]. \tag{8.24}$$

The calculation of the heat capacity is now straight-forward. With Eqs. (8.3) and (8.24) we get

$$\frac{C_V}{Nk_B} = \nu \frac{\mathcal{T}^{\nu}}{\zeta(\nu)} \left\{(\nu+1)\Big[\zeta(\nu+1)+\zeta_{\nu+1}(z)+\zeta_{\nu+1}(z^2)\Big] + \Big[\zeta_\nu(z)+2\zeta_\nu(z^2)\Big]\mathcal{T}\frac{\partial}{\partial \mathcal{T}}\log z\right\} \tag{8.25}$$

We remove the partial derivatives with respect to T by using the conservation of the total number of particles (7.39) and of the magnetization (7.40). Note that, in the ferromagnetic phase, we have a contribution to the total number of particles and to the magnetization which is due to the condensed fraction. We eliminate this contribution by subtracting $\mathcal{M}$ in (7.40) from $\mathcal{N}$ in (7.39). Performing the partial derivative with respect to $\mathcal{T}$ yields

$$\mathcal{T}\frac{\partial}{\partial \mathcal{T}}(\mathcal{N}-\mathcal{M}) = \nu\frac{\mathcal{T}^{\nu}}{\zeta(\nu)}\Big[\zeta_\nu(z)+2\zeta_\nu(z^2)\Big] + \frac{\mathcal{T}^{\nu}}{\zeta(\nu)}\Big[\zeta_{\nu-1}(z)+4\zeta_{\nu-1}(z^2)\Big]\mathcal{T}\frac{\partial}{\partial \mathcal{T}}\log z = 0. \tag{8.26}$$

Thus, we obtain

$$\frac{\mathcal{T}}{\zeta(\nu)}\frac{\partial}{\partial \mathcal{T}}\log z = -\frac{\nu}{\zeta(\nu)}\frac{\zeta_\nu(z)+2\zeta_\nu(z^2)}{\zeta_{\nu-1}(z)+4\zeta_{\nu-1}(z^2)}. \tag{8.27}$$

Substituting (8.27) in (8.25) yields for the heat capacity in the ferromagnetic phase

$$\frac{C_V}{Nk_B} = \nu\frac{\mathcal{T}^{\nu}}{\zeta(\nu)}\left\{\nu(\nu+1)\Big[\zeta(\nu+1)+\zeta_{\nu+1}(z)+\zeta_{\nu+1}(z^2)\Big] \; - \; \nu\frac{\left[\zeta_\nu(z)+2\zeta_\nu(z^2)\right]^2}{\zeta_{\nu-1}(z)+4\zeta_{\nu-1}(z^2)}\right\}. \tag{8.28}$$

We study the two limiting cases where the temperature reaches $\mathcal{T}_{c_1}$ and $\mathcal{T}_{c_2}$, respectively. Substituting the zeroth-order contribution of Eq. (6.13) in (8.28) yields for the T_{c_1}–limit of the heat capacity

$$\begin{aligned}\lim_{\mathcal{T}\nearrow\mathcal{T}_{c_1}}\frac{C_V}{Nk_B} &= \nu(\nu+1)\frac{\zeta(\nu+1)+\zeta_{\nu+1}(z)+\zeta_{\nu+1}(z^2)}{\zeta(\nu)+\zeta_\nu(z)+\zeta_\nu(z^2)} \\ &\quad -\nu^2\frac{\left[\zeta_\nu(z)+2\zeta_\nu(z^2)\right]^2}{[\zeta(\nu)+\zeta_\nu(z)+\zeta_\nu(z^2)][\zeta_{\nu-1}(z)+4\zeta_{\nu-1}(z^2)]}.\end{aligned} \tag{8.29}$$

We note, that the fugacity z is continuous for all temperatures, i.e., at the same total number of particles and total magnetization we have

$$\lim_{\mathcal{T}\searrow\mathcal{T}_{c_i}} z = \lim_{\mathcal{T}\nearrow\mathcal{T}_{c_i}} z, \qquad i = 1, 2. \tag{8.30}$$

This is an important remark, because it allows us to compare the limits of the heat capacity coming from above and below $\mathcal{T}_i$. Comparing Eqs. (8.22), (8.23), (8.29) and that the heat capacity is continuous at $\mathcal{T}_{c_1}$ yields for the homogeneous spinor gas

$$\lim_{\mathcal{T}\searrow\mathcal{T}_{c_1}} \frac{C_V}{Nk_B} - \lim_{\mathcal{T}\nearrow\mathcal{T}_{c_1}} \frac{C_V}{Nk_B} = 0, \qquad \nu = 3/2, \tag{8.31}$$

whereas the harmonically trapped spinor gas leads to the jump

$$\begin{aligned}\lim_{\mathcal{T}\searrow\mathcal{T}_{c_1}} \frac{C_V}{Nk_B} - \lim_{\mathcal{T}\nearrow\mathcal{T}_{c_1}} \frac{C_V}{Nk_B} = &- 9\,\frac{\zeta(3)+\zeta_3(z)+\zeta_3(z^2)}{4\,\zeta(2)\,\zeta_2(z^2)+\zeta_2(z)\,[\zeta(2)+\zeta_2(z^2)]} \\ &\times\left\{\zeta(2)+\zeta_2\left(z^2\right)-2\,\mathcal{M}\left[\zeta(2)-\zeta_2\left(z^2\right)\right]+\mathcal{M}^2\left[\zeta(2)+\zeta_2(z)+\zeta_2\left(z^2\right)\right]\right\} \\ &+ 9\,\frac{\zeta(3)+\zeta_3(z)+\zeta_3(z^2)}{\zeta_2(z)+4\zeta_2(z^2)}\,(1-\mathcal{M})^2, \qquad \nu = 3. \end{aligned} \tag{8.32}$$

From Eq. (8.31) and (8.32) we see that the heat capacity of a homogeneous and harmonically trapped spinor gas are fundamentally different.

We are also interested in the limit $\mathcal{T} \to \mathcal{T}_{c_2}$. According to Figure 5.2 we have the following condition for the fugacity

$$\lim_{\mathcal{T}\to\mathcal{T}_{c_2}} z = 1. \tag{8.33}$$

Furthermore, using Eq. (6.18) for the second critical temperature leads for the $\mathcal{T}_{c_2}$ limit of the heat capacity of the homogeneous spinor gas to

$$\lim_{\mathcal{T}\searrow\mathcal{T}_{c_2}} \frac{C_V}{Nk_B} = \frac{15}{4}\frac{\zeta(5/2)}{\zeta(3/2)}\,(1-\mathcal{M}) \tag{8.34}$$

and for the harmonically trapped spinor gas

$$\lim_{\mathcal{T}\searrow\mathcal{T}_{c_2}} \frac{C_V}{Nk_B} = \left\{12\,\frac{\zeta(4)}{\zeta(3)} - \frac{27}{5}\frac{\zeta(3)}{\zeta(2)}\right\}(1-\mathcal{M}). \tag{8.35}$$

8.4 Antiferromagnetic Phase

We turn now to the calculation of the heat capacity in the antiferromagnetic phase. In complete analogy to the case of a spinor gas in the gas and the ferromagnetic phase we obtain for the internal energy of a spinor gas in the antiferromagnetic phase

$$\frac{U}{Nk_B} = 3\nu\frac{\mathcal{T}^{\nu+1}}{\zeta(\nu)}\zeta(\nu+1). \tag{8.36}$$

The heat capacity then reads

$$\frac{C_V}{Nk_B} = 3\nu(\nu+1)\frac{\zeta(\nu+1)}{\zeta(\nu)}\,\mathcal{T}^{\nu}. \tag{8.37}$$

We also calculate the limits of the heat capacity for the limit $\mathcal{T} \to 0$ and $\mathcal{T} \to \mathcal{T}_{c_2}$.

The $\mathcal{T} \to 0$ limit is trivial

$$\lim_{\mathcal{T}\to 0} \frac{C_V}{Nk_B} = 0. \tag{8.38}$$

This is exactly the result which is predicted by the third law of thermodynamics.

We turn to the limit $\mathcal{T} \to \mathcal{T}_{c_2}$. Substituting Eq. (6.18) in Eq. (8.37) leads to the following result

$$\lim_{\mathcal{T}\nearrow\mathcal{T}_{c_2}} \frac{C_V}{Nk_B} = \nu(\nu+1)\frac{\zeta(\nu+1)}{\zeta(\nu)}\,(1-\mathcal{M}). \tag{8.39}$$

With Eqs. (8.34), (8.35), and (8.39) we get for the jump of the heat capacity in the homogeneous case

$$\lim_{\mathcal{T}\searrow\mathcal{T}_{c_2}} \frac{C_V}{Nk_B} - \lim_{\mathcal{T}\nearrow\mathcal{T}_{c_2}} \frac{C_V}{Nk_B} = 0, \qquad \nu = 3/2, \tag{8.40}$$

and for the harmonically trapped case

$$\lim_{\mathcal{T}\searrow\mathcal{T}_{c_2}} \frac{C_V}{Nk_B} - \lim_{\mathcal{T}\nearrow\mathcal{T}_{c_2}} \frac{C_V}{Nk_B} = -\frac{27}{5}\frac{\zeta(3)}{\zeta(2)}(1-\mathcal{M}), \qquad \nu = 3. \tag{8.41}$$

In analogy to the first phase transition discussed above, we see that a homogeneous spinor gas has a continuous heat capacity, whereas the harmonically trapped spinor gas shows a jump which is described by Eq. (8.41). In Figure 8.2 we have plotted the jump of the heat capacity for both the first and the second phase transition. There are two remarkable details. First, we see that the jump depends on the total magnetization of the system. Furthermore, there exists a special value for the magnetization, where the size of the first and the second jump become equal. Another remarkable property is, that the second jump vanishes for a fully polarized spinor condensate. This is not a surprising result, because the antiferromagnetic phase vanishes for a full polarized $F = 1$ spinor gas.

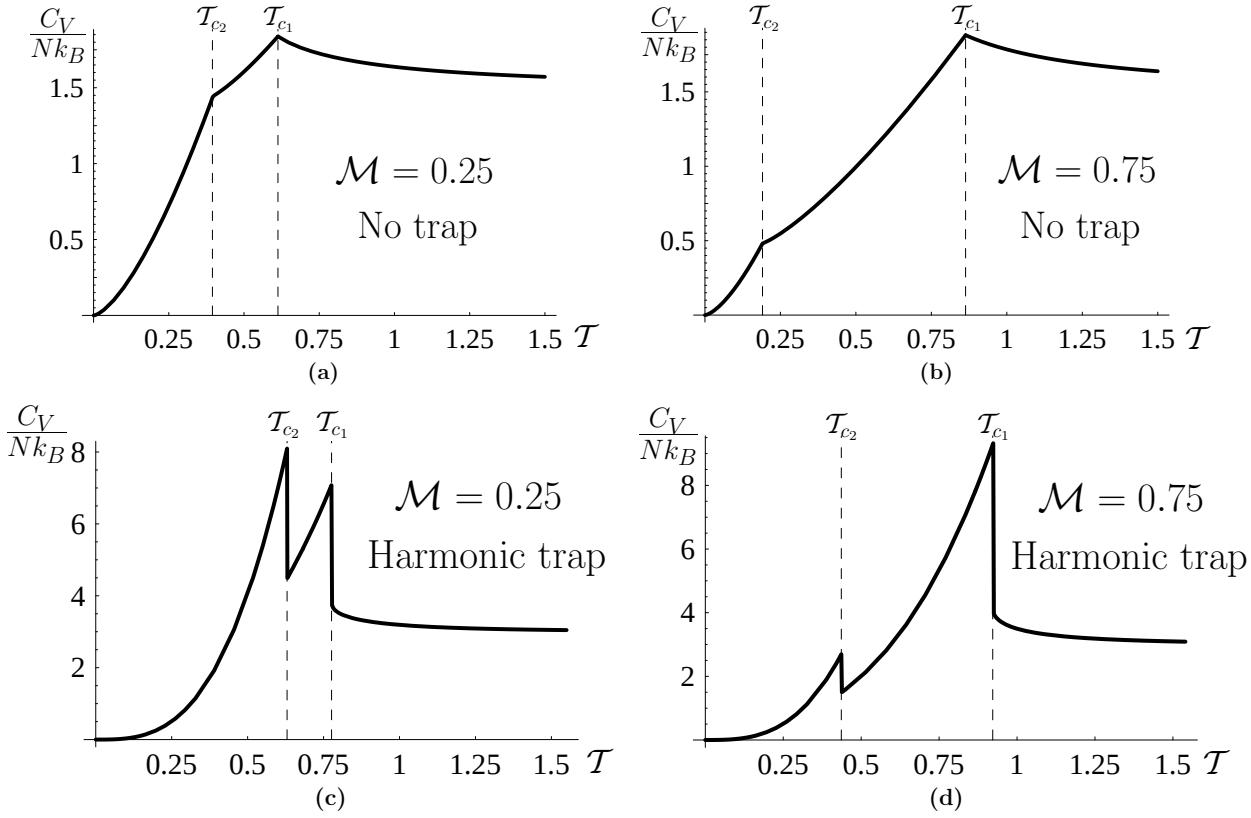

Figure 8.1: Heat capacity of **(a)**, **(b)** homogeneous and **(c)**, **(d)** harmonically trapped spinor gas for magnetizations $\mathcal{M} = 0.25$ and 0.75.

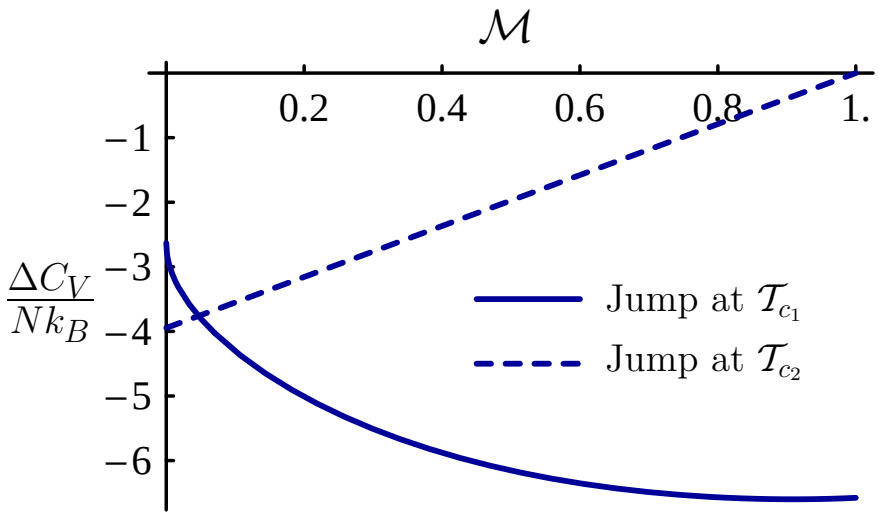

Figure 8.2: Discontinuity-jump of heat capacity for harmonically trapped spinor gas at $\mathcal{T}_{c_1}$ and $\mathcal{T}_{c_2}$.

Part III

Weakly Interacting Spinor Gas

Chapter 9

Interaction Potential

This chapter provides an appropriate description of the interaction between particles of a dilute spinor gas in the low-temperature regime. We will see that in such a system it is sufficient to consider only a two-particle interaction between particles. Furthermore, we will show that in this regime the interaction of the $F = 1$ spinor gas is adequately described by only two scalars.

9.1 Experimental Environment

In order to study BECs theoretically, we can use several simplifications, which are mainly due to the experimental environment. In the following we mention some typical physical values of a spinor Bose-Einstein condensate experiment, which are taken from Ref. [25]. There, the total number of particles in the system are around $5 - 10 \times 10^5$. The particle density ranges from $10^{14} - 10^{15}\,\mathrm{cm}^{-3}$. By contrast, the density of particles in air under standard conditions is around $10^{19}\,\mathrm{cm}^{-3}$, therefore, the spinor gas can be considered as very dilute. The critical temperature in case of sodium is experimentally measured to be of the order $1-2\,\mu$K, i.e., the particles are considerably slow. Due to the dilute environment, the most probable interaction between particles will be the two-particle interaction. However, three-particle collisions also occur in the system. Two particles being involved in such a three-body collision may form a molecule, whereas the third carries away the released momentum and energy. Due to the trapping configuration, which is very sensitive to the properties of the particles, the particles will leave the trap after the three-body collision. Therefore, they do not directly contribute to effects being seen in spinor Bose-Einstein experiments, but cause a considerable trap loss. We will neglect such trap losses and consider only two-particle interactions.

9.2 Pseudopotential

In general, the appropriate choice of the two-particle interaction potential plays an important role in explaining the physics of a collisional process. We first consider spinless particles. The exact atom-atom interaction potential can only be calculated numerically. However, for

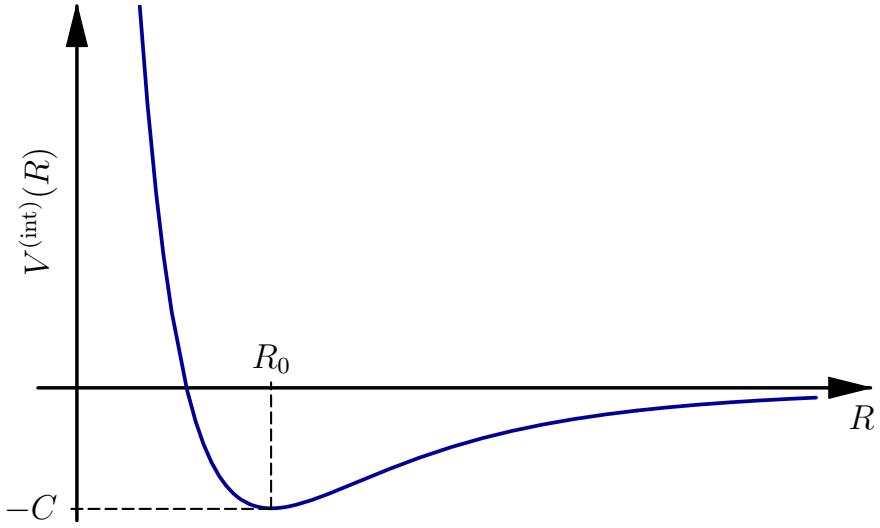

Figure 9.1: Lennard-Jones potential (9.1) shows the typical behavior of an atom-atom interaction potential.

many cases it is sufficient to approximate this interaction potential by the Lennard-Jones potential [72]

$$V^{(\mathrm{int})}\left(\mathbf{x}_1 - \mathbf{x}_2\right) = 2C\left[\frac{1}{2}\left(\frac{R_0}{R}\right)^{12} - \left(\frac{R_0}{R}\right)^{6}\right], \qquad R \equiv |\mathbf{x}_1 - \mathbf{x}_2|, \tag{9.1}$$

where R_0 denotes the position of the potential minimum and C its depth. Both R_0 and C are empirical constants. We have shown such a potential in Figure 9.1.

Equation (9.1) already imposes that the particles interact via central forces. This is not true for particles with a non-vanishing magnetic dipole moment [66]. For low temperatures it turns out, that we can replace Eq. (9.1) by a *pseudopotential* [45, 73]

$$V^{(\mathrm{int})}\left(\mathbf{x}_1 - \mathbf{x}_2\right) = g\,\delta\left(\mathbf{x}_1 - \mathbf{x}_2\right), \tag{9.2}$$

where the interaction strength is summarized by one single parameter g. Furthermore, we introduce the s-wave scattering length a, which is defined through the interaction strength by [67]

$$g = \frac{4\pi\hbar^2}{M}\,a \tag{9.3}$$

with the single-particle mass M. Note that the interaction potential (9.2) cannot reproduce for example bounding states of two colliding particles. However, it provides a good description of the physics for particle distances $R \gg |a|$, which is important for studying thermodynamic properties of a system. We note that the s-wave scattering length a may take positive or negative values. The former correspond to a repulsive and the latter to an

attractive interaction potential. With the help of Feshbach resonances it has been demonstrated [5] that Bose-Einstein condensates with an attractive interaction could be unstable so that they collapses.

The generalization of the pseudopotential (9.2) to a system of two atoms with spin $F = 1$ is given by [22, 23]

$$V^{(\mathrm{int})}(\mathbf{x}_1 - \mathbf{x}_2) = \delta(\mathbf{x}_1 - \mathbf{x}_2) \sum_{f=0}^{2} g_f \mathcal{P}_f. \tag{9.4}$$

Here, $\mathcal{P}_f$ denotes the projection operator, which projects the pair wave function of atom 1 and atom 2 into the total hyperfine spin state f. The constants g_0, g_1, and g_2 are the respective interaction strengths defined in analogy to Eq. (9.3) as

$$g_f = \frac{2\pi\hbar^2}{\mu} a_f, \qquad \mu = \frac{M_1 M_2}{M_1 + M_2}, \tag{9.5}$$

where μ is the reduced mass of the colliding atoms.

The physical description of the two-particle interaction potential (9.4) is the following. Consider two $F = 1$ particles, which are at distances where they do not interact with each other. Each of them is completely described by a single particle wave function. However, if the particles start to interact with each other, they have to be described by a two-particle wave function. Using the rules for adding two angular momenta, the two-particle system can have a total angular momentum of $f = 0,\ 1$, and 2. The crucial point is now, that the strength of the particle-particle interaction is not necessarily the same for each f. This is taken into account by introducing different interaction strength g_f as done in Eq. (9.4).

In case of a system with identical bosonic particles, we have to take the bosonic symmetrization condition into account. It follows, that the odd f contribution in (9.4) vanishes (see App. D), i.e., the pseudopotential reduces to

$$V^{(\mathrm{int})}(\mathbf{x}_1 - \mathbf{x}_2) = \delta(\mathbf{x}_1 - \mathbf{x}_2) \Big(g_0 \mathcal{P}_0 + g_2 \mathcal{P}_2 \Big). \tag{9.6}$$

In Figure 9.2 we have schematically drawn the collision of two particle via a delta potential. For practical purposes, we rewrite 9.6 as shown in Appendix D as

$$\boxed{V^{(\mathrm{int})}(\mathbf{x}_1 - \mathbf{x}_2) = \delta(\mathbf{x}_1 - \mathbf{x}_2)(c_0 \mathbb{1}_1 \mathbb{1}_2 + c_2 \hat{\mathbf{F}}_1 \cdot \hat{\mathbf{F}}_2)} \tag{9.7}$$

with the operator of angular momentum $\hat{\mathbf{F}}_i$ acting on the i^{th} atom, the unit operator $\mathbb{1}_i$, and the newly introduced interaction strengths

$$c_0 = (g_0 + 2g_2)/3 \quad \text{and} \quad c_2 = (g_2 - g_0)/3. \tag{9.8}$$

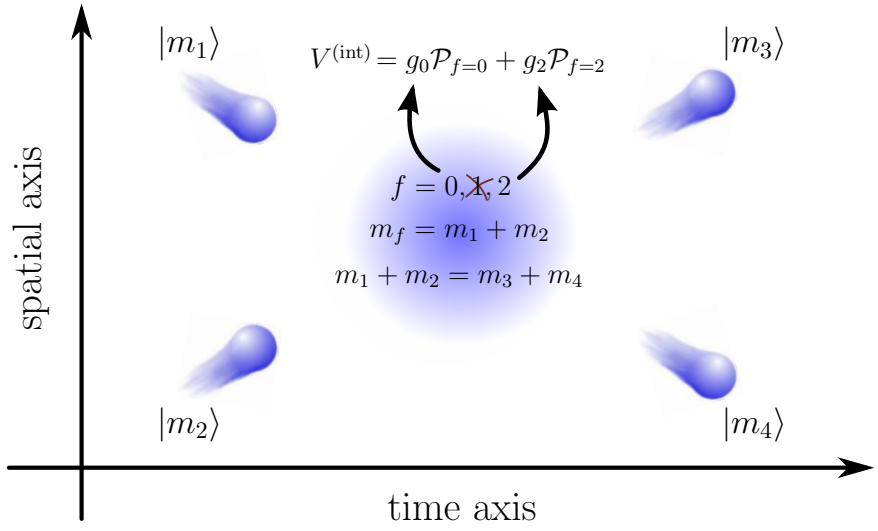

Figure 9.2: Collision of two particles with delta interaction. Two particles being initially in the *one*-particle states $|m_1\rangle$ and $|m_2\rangle$ couple in the interaction zone with each other to a *two*-particle state. The two-particle state can take the angular momentum f=0 or f=2, whereas f=1 is forbidden due to the principal bosonic symmetrization condition. Depending on the total angular momentum of the two-particle state, the interaction potential differs in its strength, which is accounted for with different interaction strength g_0, g_2. The angular momentum is conserved after the collision.

In analogy to Eq. (9.8) we define newly s-wave scattering lengths

$$\tilde{a}_0 = (a_0 + 2a_2)/3, \qquad \tilde{a}_2 = (a_2 - a_0)/3. \tag{9.9}$$

In matrix representation Eq. (9.7) reads

$$\boxed{V^{(\mathrm{int})}_{aba'b'}(\mathbf{x}_1 - \mathbf{x}_2) = \delta(\mathbf{x}_1 - \mathbf{x}_2)\left(c_0\delta_{ab}\delta_{a'b'} + c_2 F^j_{ab}F^j_{a'b'}\right)} \quad , \tag{9.10}$$

where the operators of angular momentum are replaced by the respective spin-1 matrices given in Eq. (2.17).

Chapter 10

Gross-Pitaevskii Equations

In Chapter 5 we studied the Gross-Pitaevskii equations and their solutions for a non-interacting $F = 1$ spinor gas. It turned out that it is possible to solve the Gross-Pitaevskii equations analytically for the case of a homogeneous and a harmonically trapped system. In this chapter, we study the Gross-Pitaevskii equations for the case of a weakly interacting spinor gas. We will see, that their solutions cannot be given analytically, so that we have to employ several approximations. We start this chapter with deriving the Gross-Pitaevskii equations of the interacting $F = 1$ system, which provides the basis for studying all possible phases. We will then work out their solutions and discuss them. At the end, we show that in case of a non-magnetization conserving system, the solutions of the Gross-Pitaevskii equations can be summarized in a compact form, which provides a deeper insight about spinor condensates with non-vanishing particle interaction.

10.1 Action of Interacting Spinor Gas

The starting point for the calculation of the Gross-Pitaevskii equations is the action of the system:

$$\mathcal{A}[\psi^*, \psi] = \mathcal{A}^{(0)}[\psi^*, \psi] + \mathcal{A}^{(\mathrm{int})}[\psi^*, \psi]. \tag{10.1}$$

The first contribution is equal to the action of the non-interacting spinor gas (2.47), whereas the second contribution, given in (2.48), is due to the interaction of the particles.

As discussed in the last chapter, for low temperatures it is possible to approximate the potential of the two-particle interaction by an appropriate pseudopotential (9.10). Substituting the latter into (2.48) yields for the interaction contribution of the action [22, 23]

$$\mathcal{A}^{(\mathrm{int})}[\psi^*, \psi] = \frac{1}{2}\int_0^{\hbar\beta} d\tau \int d^3x \left\{ c_0 \Big[\psi_a^*(\mathbf{x},\tau)\psi_a(\mathbf{x},\tau)\Big]^2 + c_2 \sum_{j=x,y,z} \Big[\psi_a^*(\mathbf{x},\tau)F_{ab}^j\psi_b(\mathbf{x},\tau)\Big]^2 \right\}. \tag{10.2}$$

Splitting the spinor-fields ψ into a background field Ψ and a fluctuation field $\delta\psi$, leads with (3.9)

$$\mathcal{A}[\Psi^* + \delta\psi^*, \Psi + \delta\psi] = \mathcal{A}[\Psi^*, \Psi] + \mathcal{A}^{(2)}[\delta\psi^*, \delta\psi] + \mathcal{A}^{(\mathrm{cor})}[\delta\psi^*, \delta\psi]. \tag{10.3}$$

Here, the tree-level action $\mathcal{A}[\Psi^*,\Psi]$ is simply the action (10.1) evaluated at the background fields. Using Eqs. (3.7) and (9.10), the fluctuating part of the action is given by

$$\begin{aligned}\mathcal{A}^{(2)} &= \int_0^{\hbar\beta} d\tau \int d^3x\, \delta\psi_a^* \Bigg\{ \left[\left(\hbar\frac{\partial}{\partial\tau} - \frac{\hbar^2}{2M}\Delta + V(\mathbf{x}) - \mu \right) \delta_{ab} - \eta F^z_{ab} \right] \delta\psi_b \\ &+ \frac{c_0}{2}\Big[(\Psi_a^*\delta\psi_a)^2 + (\Psi_a\delta\psi_a^*)^2 + 2\Psi_a^*\Psi_a\delta\psi_b^*\delta\psi_b + 2\Psi_a^*\delta\psi_a\delta\psi_b^*\Psi_b \Big] \\ &+ \frac{c_2}{2}\sum_{j=x,y,z}\Big[(\Psi_a^* F^j_{ab}\delta\psi_b)^2 + (\delta\psi_a^* F^j_{ab}\Psi_b)^2 + 2\Psi_a^* F^j_{ab}\Psi_b\delta\psi_c^* F^j_{cd}\,\delta\psi_d + 2\delta\psi_a^* F^j_{ab}\Psi_b\Psi_c^* F^j_{cd}\,\delta\psi_d \Big] \Bigg\}\end{aligned} \tag{10.4}$$

and with Eq. (3.8) we obtain the correlation action

$$\begin{aligned}\mathcal{A}^{(\mathrm{cor})} &= \int_0^{\hbar\beta} d\tau \int d^3x \left\{ \frac{c_0}{2}\Big[2\Psi_a^*\delta\psi_a\delta\psi_b^*\delta\psi_b + 2\delta\psi_a^*\Psi_a\delta\psi_b^*\delta\psi_b + (\delta\psi_a^*\delta\psi_a)^2 \Big] \right. \\ &+ \left. \frac{c_2}{2}\sum_{j=x,y,z}\Big[2\delta\psi_a^* F^j_{ab}\Psi_b\,\delta\psi_c^*\,F^j_{cd}\,\delta\psi_d + 2\Psi_a^* F^j_{ab}\,\delta\psi_b\delta\psi_c^* F^j_{cd}\,\delta\psi_d + (\delta\psi_a^* F^j_{ab}\delta\psi_b)^2 \Big] \right\}.\end{aligned} \tag{10.5}$$

For convenience we omitted writing the dependence of the fields on the respective space-time points.

10.2 Derivation of Gross-Pitaevskii Equations

According to (3.15), the leading order of the effective action is determined by the Euclidean action (10.1) evaluated at the background fields. The background fields in turn, are calculated by extremizing the Euclidean action with respect to the background fields. The resulting set of equations are the Gross-Pitaevskii equations. For a general two-particle interaction potential they are given by (3.19), (3.20). For our particular interaction potential 9.10 they read

$$\begin{aligned}0 &= \left\{ \left[\hbar\frac{\partial}{\partial\tau} - \frac{\hbar^2}{2M}\Delta + V(\mathbf{x}) - \mu \right] \delta_{ab} - \eta F^z_{ab} \right\} \Psi_b + c_0 \Psi^*_{a'}\Psi_{a'}\Psi_a \\ &+ c_2 F^j_{ab}\Psi_b\Psi^*_{a'}F^j_{a'b'}\Psi_{b'}, \qquad a = 1,0,-1.\end{aligned} \tag{10.6}$$

Using the explicit form of the spin matrices (2.17) yields the identities

$$\Psi_a^* F^x_{ab}\Psi_b = \frac{1}{\sqrt{2}}\Big(\Psi_1^*\Psi_0 + \Psi_0^*\Psi_1 + \Psi_0^*\Psi_{-1} + \Psi_{-1}^*\Psi_0 \Big), \tag{10.7}$$

$$\Psi_a^* F^y_{ab}\Psi_b = \frac{i}{\sqrt{2}}\Big(-\Psi_1^*\Psi_0 + \Psi_0^*\Psi_1 - \Psi_0^*\Psi_{-1} + \Psi_{-1}^*\Psi_0 \Big), \tag{10.8}$$

$$\Psi_a^* F^z_{ab}\Psi_b = \Psi_1^*\Psi_1 - \Psi_{-1}^*\Psi_{-1}\ , \tag{10.9}$$

which are used to rewrite (10.6) more conveniently

$$
\begin{aligned}
-\hbar\frac{\partial}{\partial\tau}\Psi_1 &= \Big[-\frac{\hbar^2}{2M}\Delta + (c_0+c_2)\Big(|\Psi_1|^2+|\Psi_0|^2\Big) \\
&\quad + (c_0-c_2)|\Psi_{-1}|^2 + V(\mathbf{x}) - (\mu+\eta)\Big]\Psi_1 + c_2\Psi_{-1}^*\Psi_0^2, \qquad (10.10)\\
-\hbar\frac{\partial}{\partial\tau}\Psi_0 &= \Big[-\frac{\hbar^2}{2M}\Delta + (c_0+c_2)\Big(|\Psi_1|^2+|\Psi_{-1}|^2\Big) \\
&\quad + c_0|\Psi_0|^2 + V(\mathbf{x}) - \mu\Big]\Psi_0 + 2c_2\Psi_0^*\Psi_1\Psi_{-1}, \qquad (10.11)\\
-\hbar\frac{\partial}{\partial\tau}\Psi_{-1} &= \Big[-\frac{\hbar^2}{2M}\Delta + (c_0+c_2)\Big(|\Psi_{-1}|^2+|\Psi_0|^2\Big) \\
&\quad + (c_0-c_2)|\Psi_1|^2 + V(\mathbf{x}) - (\mu-\eta)\Big]\Psi_{-1} + c_2\Psi_1^*\Psi_0^2. \qquad (10.12)
\end{aligned}
$$

The latter Gross-Pitaevskii equations represent a coupled set of differential equations. In contrast to the algebraic Gross-Pitaevskii equations of an ideal spinor gas (5.10), they cannot be solved analytically without further simplifications.

10.3 Solution of Gross-Pitaevskii Equations

We show in this section, how the two-particle interaction changes the system properties. In order to properly solve the Gross-Pitaevskii equations, we adopt the Thomas-Fermi approximation, which consists in neglecting the kinetic part in (10.10)–(10.12), i.e., we perform the replacement

$$-\frac{\hbar^2}{2M}\Delta \to 0. \qquad (10.13)$$

In Ref. [67] it is shown for low temperatures that the Thomas-Fermi solution of the condensates wave function is in excellent agreement with the exact solution for the bulk of the condensate, whereas at the condensate surface its solution deviates from the exact one. However, for our purposes it is a quite good approximation. Moreover, we assume the background fields to be independent of imaginary time. This corresponds to the case of a stationary spinor Bose-Einstein condensate.

Thus, we start by rewriting the background fields as

$$\Psi_a(\mathbf{x}) = \sqrt{n_a(\mathbf{x})}e^{i\varphi_a(\mathbf{x})}, \qquad n_a(\mathbf{x}), \varphi_a(\mathbf{x}) \in \mathbb{R}, \qquad a = 1, 0, -1, \qquad (10.14)$$

where $n_a(\mathbf{x}) = |\Psi_a(\mathbf{x})|^2$ is the condensates particle density in the a^{th} Zeeman state. Using the latter, we obtain for the Gross-Pitaevskii equations (10.10)–(10.12):

$$0 = \Big[c_0\, n + c_2(m + n_0) + V(\mathbf{x}) - \mu - \eta\Big]\sqrt{n_1}e^{i\varphi_1} + c_2 n_0\sqrt{n_{-1}}e^{i\left(2\varphi_0 - \varphi_{-1}\right)}, \tag{10.15}$$

$$0 = \Big\{\Big[c_0\, n + c_2(n - n_0) + V(\mathbf{x}) - \mu\Big]e^{i\varphi_0} + 2c_2\sqrt{n_1 n_{-1}}e^{i\left(-\varphi_0 + \varphi_1 + \varphi_{-1}\right)}\Big\}\sqrt{n_0}, \tag{10.16}$$

$$0 = \Big[c_0\, n + c_2(-m + n_0) + V(\mathbf{x}) - \mu + \eta\Big]\sqrt{n_{-1}}e^{i\varphi_{-1}} + c_2 n_0\sqrt{n_1}e^{i\left(2\varphi_0 - \varphi_1\right)} \tag{10.17}$$

with the total condensates particle density

$$n(\mathbf{x}) = n_1(\mathbf{x}) + n_0(\mathbf{x}) + n_{-1}(\mathbf{x}) \tag{10.18}$$

and the total condensates magnetization density

$$m(\mathbf{x}) = n_1(\mathbf{x}) - n_{-1}(\mathbf{x}). \tag{10.19}$$

10.3.1 Investigation of Different Cases

In order to find the most general solution of Eqs. (10.15)–(10.17), we discuss the Gross-Pitaevskii equations for every possible particle occupation number of the Zeeman states, which are given by

$$\begin{array}{lll} 1.)\ n_1 = n_0 = n_{-1} = 0, & 4.)\ n_0 \neq 0, n_1 = n_{-1} = 0, & 7.)\ n_1, n_{-1} \neq 0, n_0 = 0, \\ 2.)\ n_1 \neq 0, n_0 = n_{-1} = 0, & 5.)\ n_1, n_0 \neq 0, n_{-1} = 0, & 8.)\ n_1, n_{-1}, n_0 \neq 0. \\ 3.)\ n_{-1} \neq 0, n_0 = n_1 = 0, & 6.)\ n_{-1}, n_0, \neq 0, n_1 = 0. & \end{array} \tag{10.20}$$

We substitute each of the possibilities (10.20) in the Gross-Pitaevskii equations (10.15)–(10.17) and discuss them in tabular form:

1.) The first case solves all Gross-Pitaevskii equations identically. It represents the physical situation that no particles are in the condensed fraction.

2.) Equations (10.16) and (10.17) are solved identically. From Eq. (10.15) we deduce with help of (10.18), (10.19) the relation

$$(c_0 + c_2)n(\mathbf{x}) + V(\mathbf{x}) - \mu - \eta = 0. \tag{10.21}$$

3.) In complete analogy to 2.), Eqs. (10.15) and (10.16) are solved directly and we deduce from (10.17)

$$(c_0 + c_2)n(\mathbf{x}) + V(\mathbf{x}) - \mu + \eta = 0. \tag{10.22}$$

4.) Equations (10.15) and (10.17) are identically fulfilled. From Eq. (10.16) we get the condition

$$c_0\, n(\mathbf{x}) + V(\mathbf{x}) - \mu = 0 \tag{10.23}$$

5.) Equation (10.17) leads to the equation $c_2 n_1(\mathbf{x}) n_0(\mathbf{x}) = 0$. For $c_2 \neq 0$ this contradicts against the assumptions, hence, there is no solution for this case.

6.) No solution, see 5.).

7.) From Eqs. (10.15) and (10.17) one obtains the following set equations

$$c_0\, n(\mathbf{x}) + c_2\, m(\mathbf{x}) + V(\mathbf{x}) - \mu - \eta = 0, \tag{10.24}$$

$$c_0\, n(\mathbf{x}) - c_2\, m(\mathbf{x}) + V(\mathbf{x}) - \mu + \eta = 0, \tag{10.25}$$

which are rewritten as

$$c_2\, m(\mathbf{x}) - \eta = 0, \tag{10.26}$$

$$c_0\, n(\mathbf{x}) + V(\mathbf{x}) - \mu = 0. \tag{10.27}$$

8.) The Gross-Pitaevskii equations have to be fulfilled separately for both real and imaginary part. According to (10.14), the imaginary contributions are due to the complex exponential functions. Therefore, we deduce from Eqs. (10.15)–(10.17)

$$2\varphi_0(\mathbf{x}) = \varphi_1(\mathbf{x}) + \varphi_{-1}(\mathbf{x}) + p\,\pi, \quad p \in \mathbb{Z}. \tag{10.28}$$

Note that the latter is also fulfilled by a global change phase, i.e.,

$$\varphi_a(\mathbf{x}) \to \varphi_a(\mathbf{x}) + \theta(\mathbf{x}), \quad a = 1, 0 - 1,\ \theta(\mathbf{x}) \in \mathbb{R}. \tag{10.29}$$

Substituting (10.28) in Eqs. (10.15)–(10.17) yields

$$0 = \Big\{ c_0\, n + c_2(m + n_0) + V(\mathbf{x}) - \mu - \eta \Big\} \sqrt{n_1} \pm c_2 n_0 \sqrt{n_{-1}}, \tag{10.30}$$

$$0 = c_0\, n + c_2(n - n_0) + V(\mathbf{x}) - \mu \pm 2c_2 \sqrt{n_1 n_{-1}}, \tag{10.31}$$

$$0 = \Big\{ c_0\, n + c_2(-m + n_0) + V(\mathbf{x}) - \mu + \eta \Big\} \sqrt{n_{-1}} \pm c_2 n_0 \sqrt{n_1}. \tag{10.32}$$

In the latter equations the upper sign represents the case where p in Eq. (10.28) is an even number, whereas the lower sign holds for p being an odd number.

By adding and subtracting Eqs. (10.30) and (10.32) from each other and using (10.18), (10.19) we get

$$0 = c_2\, n_0 \left(\sqrt{n_1 n_{-1}} \mp \frac{n_0}{2} \right) + n \left(c_0 \sqrt{n_1 n_{-1}} \pm c_2 \frac{n_0}{2} \right) + [V(\mathbf{x}) - \mu] \sqrt{n_1 n_{-1}}, \tag{10.33}$$

$$0 = c_2\, m \left(\sqrt{n_1 n_{-1}} \mp \frac{n_0}{2} \right) - \eta \sqrt{n_1 n_{-1}}. \tag{10.34}$$

Furthermore, we deduce from Eqs. (10.31) and (10.33) the relation

$$0 \;=\; \sqrt{n_1 n_{-1}}(n-2n_0) \mp \frac{1}{2}\Big[n_0(n-n_0) - 4n_1 n_{-1}\Big] \tag{10.35}$$

We discuss the latter equations for both p even and p odd:

a) p **even**:

For p being an even number, the upper sign holds in (10.33)–(10.35). We have to discuss two cases:

Case 1: $m(\mathbf{x}) = 0 \iff n_1(\mathbf{x}) = n_{-1}(\mathbf{x}) \neq 0$

From Eq. (10.34) we deduce

$$\eta\sqrt{n_1 n_{-1}} = 0 \quad \Rightarrow \quad \eta = 0. \tag{10.36}$$

Substituting the assumption $n_1(\mathbf{x}) = n_{-1}(\mathbf{x})$ in (10.35) yields $n_0(\mathbf{x}) = 2n_1(\mathbf{x})$. With Eq. (10.18) we then obtain

$$n_1(\mathbf{x}) = n_{-1}(\mathbf{x}) = n(\mathbf{x})/4, \qquad n_0(\mathbf{x}) = n(\mathbf{x})/2. \tag{10.37}$$

Finally, inserting the latter in (10.33) gives the following relation for the condensate density

$$\Big(c_0 + c_2\Big)n(\mathbf{x}) + V(\mathbf{x}) - \mu = 0. \tag{10.38}$$

Case 2: $m(\mathbf{x}) \neq 0$

We directly obtain from Eq. (10.34)

$$n_0(\mathbf{x}) = 2\left[1 - \frac{\eta}{c_2\, m(\mathbf{x})}\right]\sqrt{n_1(\mathbf{x})n_{-1}(\mathbf{x})}. \tag{10.39}$$

Substituting the latter in (10.35) yields the condition

$$n(\mathbf{x}) = n_0(\mathbf{x})\left[1 + \frac{c_2 m(\mathbf{x})}{c_2 m(\mathbf{x}) - \eta}\right]. \tag{10.40}$$

We substitute this into Eq. (10.33) leading to

$$n(\mathbf{x})\left[c_0 + 2c_2\frac{c_2 m(\mathbf{x})}{2c_2 m(\mathbf{x}) - \eta}\right] + \frac{c_2 m(\mathbf{x})}{c_2 m(\mathbf{x}) - \eta}\Big[V(\mathbf{x}) - \mu\Big] = 0. \tag{10.41}$$

We note that the latter reduces for $\eta = 0$ to (10.38).

b) p **odd**:

Now, the lower sign in Eqs. (10.33)–(10.35) is considered.

Case 1: $m(\mathbf{x}) = 0 \iff n_1(\mathbf{x}) = n_{-1}(\mathbf{x}) \neq 0$

In this case Eq. (10.35) is directly fulfilled. Note that this is not the case for 1a). There, for vanishing magnetization density, the particle densities must obey the more strict condition (10.37). With Eq. (10.34) we get $\eta = 0$. Substituting $n_1(\mathbf{x}) = n_{-1}(\mathbf{x})$ in Eq. (10.33) yields the relation

$$c_0 n(\mathbf{x}) + V(\mathbf{x}) - \mu = 0. \tag{10.42}$$

Case 2: $m(\mathbf{x}) \neq 0$

We obtain from Eq. (10.34)

$$n_0(\mathbf{x}) = 2\left[\frac{\eta}{c_2\, m(\mathbf{x})} - 1\right]\sqrt{n_1(\mathbf{x}) n_{-1}(\mathbf{x})}. \tag{10.43}$$

We substitute this into (10.35) yielding the condition

$$n(\mathbf{x}) = n_0(\mathbf{x})\left[1 - \frac{c_2 m(\mathbf{x})}{c_2 m(\mathbf{x}) - \eta}\right]. \tag{10.44}$$

With Eq. (10.33) this leads to

$$n(\mathbf{x})\left[c_0 - 2c_2 m(\mathbf{x})/\eta\right] + \frac{c_2 m(\mathbf{x})}{c_2 m(\mathbf{x}) - \eta}\Big[V(\mathbf{x}) - \mu\Big] = 0. \tag{10.45}$$

10.3.2 Discussion of Solutions

We discuss the latter solutions. The first one, is the most trivial one, because it indicates that no particles are in the condensate fraction, which corresponds to a system being in the gas phase.

The solutions 2.) and 3.) are essentially the same. They correspond to magnetizations with opposite direction, where η simply changes its sign. These solutions correspond to the ferromagnetic solution obtained for a ideal spinor gas in Chapter 5, where the BEC fraction was fully polarized.

Before we turn to 4.), we discuss the solutions 5.), 6.). We first note that both describe essentially the same physical system, where we use the same arguments as used in 1.), 2.). With the assumption of 5.) and 6.), it is not possible to solve the Gross-Pitaeskii equations. We also had the same situation for the ideal $F = 1$ spinor system as discussed in Chapter 5. Therefore, it is not possible to have a condensate where only the Zeeman states $|1\rangle$ and $|0\rangle$ are Bose-Einstein condensed.

We discuss now the solutions 4.) and 7.). Stating that for vanishing magnetization solution 7.) is equivalent to 4.), we can restrict our discussion to 7.). This solution of the Gross-Pitaevskii equation is quite interesting, because it states that we may have *magnetized* spinor condensate, where only two Zeeman components are condensed at the same

time. This is in contrast to the ideal $F = 1$ spinor system, where such a solution was not possible. There, the second phase was characterized by a double condensation.

The solution 8.) represents a spinor Bose-Einstein condensate, where all three Zeeman states of the BEC fraction are occupied. Here, we have two different kind of solutions, which essentially depend on the magnetization of the system. In the first solution, a vanishing magnetization occurs only for one particular particle configuration, which is given by (10.37). Note that this is not the case for 8b.).

10.3.3 System without Conservation of Magnetization

We finish this chapter by considering the special case of a system where the conservation of magnetization is *not* fulfilled. This is for example the case for particles, whose magnetic dipole moment cannot neglected anymore. As discussed in Chapter 2, neglecting the conservation of the magnetization correspond to setting $\eta = 0$. By doing so, we observe that the solution derived above, can be divided into two different:

Solution A: 4.), 7.), 8b.)

$$\varphi_1 + \varphi_{-1} + (2p+1)\pi = 2\varphi_0, \qquad p \in \mathbb{Z}, \tag{10.46}$$

$$n_1(\mathbf{x}) - n_{-1}(\mathbf{x}) = 0, \tag{10.47}$$

$$c_0\, n(\mathbf{x}) + V(\mathbf{x}) - \mu = 0. \tag{10.48}$$

Solution B: 2.), 3.), 8a.)

$$\varphi_1 + \varphi_{-1} + 2p\,\pi = 2\varphi_0, \qquad p \in \mathbb{Z}, \tag{10.49}$$

$$n_0(\mathbf{x}) - 2\sqrt{n_1(\mathbf{x}) n_{-1}(\mathbf{x})} = 0, \tag{10.50}$$

$$(c_0 + c_2) n(\mathbf{x}) + V(\mathbf{x}) - \mu = 0. \tag{10.51}$$

We read from Solution A, that the magnetization in z-direction is always zero. Note, that this is also the case in 8b.), otherwise we would have a divergency in (10.45). Therefore, we refer to this solution to be *antiferromagnetic*. For reasons which will soon become clear we refer to the second solution to be *ferromagnetic*. Note that the ferromagnetic and the antiferromagnetic solution must not be mixed up with the ferromagnetic and antiferromagnetic phase of Chapter 5. We derive now the most general expression of the order parameter $\Psi_a(\mathbf{x})$ for both the antiferromagnetic and the ferromagnetic state.

Antiferromagnetic State:

Using Eqs. (10.18) and (10.47) we may introduce the convenient notation

$$\sqrt{n_1(\mathbf{x})} = \sqrt{n_{-1}(\mathbf{x})} = \sqrt{\frac{n(\mathbf{x})}{2}} \sin\tilde{\beta}, \qquad 0 \leq \tilde{\beta} \leq \frac{\pi}{2} \tag{10.52}$$

$$\sqrt{n_0(\mathbf{x})} = \sqrt{n(\mathbf{x})} \cos\tilde{\beta}. \tag{10.53}$$

According to Eq. (10.14) the vector order parameter $\mathbf{\Psi}(\mathbf{x}) = \Big(\Psi_1(\mathbf{x}), \Psi_0(\mathbf{x}), \Psi_{-1}(\mathbf{x})\Big)^T$ then reads

$$\mathbf{\Psi}(\mathbf{x}) = \sqrt{n(\mathbf{x})}\, e^{i\tilde{\theta}} \begin{pmatrix} \frac{1}{\sqrt{2}} \sin\tilde{\beta}\, e^{i\varphi_1} \\ \cos\tilde{\beta}\, e^{i\varphi_0} \\ \frac{1}{\sqrt{2}} \sin\tilde{\beta}\, e^{i\varphi_{-1}} \end{pmatrix}, \qquad 0 \leq \tilde{\beta} \leq \frac{\pi}{2}. \tag{10.54}$$

In order to maintain the complete generality of the order parameter we have multiplied a global phase factor $e^{i\tilde{\theta}}$ to the latter [see also Eq. (10.29)].

Substituting Eq. (10.46) in (10.54) leads to

$$\mathbf{\Psi}(\mathbf{x}) = \sqrt{n(\mathbf{x})}\, e^{i\left[\tilde{\theta}+\frac{\pi}{2}+(\varphi_1+\varphi_{-1})/2\right]} \begin{pmatrix} \frac{1}{\sqrt{2}} \sin\tilde{\beta}\, e^{-i\left(\varphi_{-1}-\varphi_1\right)/2-i\frac{\pi}{2}} \\ \cos\tilde{\beta}\, e^{ip\,\pi} \\ \frac{1}{\sqrt{2}} \sin\tilde{\beta}\, e^{i\left(\varphi_{-1}-\varphi_1\right)/2-i\frac{\pi}{2}} \end{pmatrix}, \quad 0 \leq \tilde{\beta} \leq \frac{\pi}{2},\ p \in \mathbb{Z}. \tag{10.55}$$

We continue simplifying the order parameter by introducing of the new variables

$$\theta \equiv \tilde{\theta} + (\pi + \varphi_1 + \varphi_{-1})/2, \tag{10.56}$$

$$\tau \equiv -\frac{1}{2}(\varphi_1 + \varphi_{-1}), \tag{10.57}$$

$$\alpha \equiv \frac{1}{2}(\varphi_{-1} - \varphi_1 - \pi), \tag{10.58}$$

$$\beta \equiv \tilde{\beta} + p\pi, \tag{10.59}$$

and finally obtain the most general solution for the Gross-Pitaevskii equations of the antiferromagnetic state

$$\boxed{\mathbf{\Psi}(\mathbf{x}) = \sqrt{n(\mathbf{x})}\, e^{i\theta} \begin{pmatrix} -\frac{1}{\sqrt{2}} \sin\beta\, e^{-i\alpha} \\ \cos\beta \\ \frac{1}{\sqrt{2}} \sin\beta\, e^{i\alpha} \end{pmatrix}, \qquad \alpha, \beta, \theta \in \mathbb{R}.} \tag{10.60}$$

The special solutions 1.), 4.), 7.), and 8b.) of the last subsection are easily verified to be particular solutions of Eq. (10.60). The total particle density is determined by the condition

$$c_0\, n(\mathbf{x}) + V(\mathbf{x}) - \mu = 0. \tag{10.61}$$

It is also possible to write Eq. (10.60) with the help of the unitary spin rotation matrix

$$\mathcal{U}(\alpha, \beta, \gamma) = e^{-iF^z\alpha} e^{-iF^y\beta} e^{-iF^z\gamma}, \tag{10.62}$$

where $\alpha,\ \beta,\ \gamma$ are Euler angles. Applying this to (10.60) yields [22]

$$\mathbf{\Psi}(\mathbf{x}) = \sqrt{n(\mathbf{x})}\, e^{i\theta}\, \mathcal{U}(\alpha, \beta, \gamma) \begin{pmatrix} 0 \\ 1 \\ 0 \end{pmatrix}. \tag{10.63}$$

Note that the order parameter does not depend on the Euler angle γ. The latter solution clearly reflects the invariance of the action (2.47), (10.1), (10.2) to a change of the global phase of the condensates wave function and to a rotation in spin-space. Therefore, we could have obtained the latter solution by simply guessing one particular solution and then using the symmetries of the action as done in Ref. [22]. Using the general result that the scalar product of two vectors is not altered by multiplying both vectors with an unitary matrix [42], we easily find that the expectation value of angular momentum vanishes, i.e.,

$$\langle \mathbf{F} \rangle \equiv \int d^3x \, \mathbf{\Psi}^\dagger(\mathbf{x}) \, \mathbf{F} \, \mathbf{\Psi}(\mathbf{x}) = \mathbf{0}, \tag{10.64}$$

where we used the definition $\mathbf{F} = \left(F^x, F^y, F^z\right)^T$ with the spin matrices F^x, F^y, F^z defined in (2.17). This again confirms that the state corresponds to an antiferromagnetic state.

Ferromagnetic State:

To determine the most general solution for the order parameter for the ferromagnetic state, we proceed analogous to the antiferromagnetic case. Using Eqs. (10.18) and (10.50) we may introduce the following convenient parametrization

$$\sqrt{n_1(\mathbf{x})} \equiv \sqrt{n(\mathbf{x})} \cos^2 \frac{\tilde{\beta}}{2}, \tag{10.65}$$

$$\sqrt{n_{-1}(\mathbf{x})} \equiv \sqrt{n(\mathbf{x})} \sin^2 \frac{\tilde{\beta}}{2}, \tag{10.66}$$

$$\sqrt{n_0(\mathbf{x})} = \sqrt{2n(\mathbf{x})} \cos \frac{\tilde{\beta}}{2} \sin \frac{\tilde{\beta}}{2}, \qquad 0 \leq \tilde{\beta} \leq \pi. \tag{10.67}$$

Substituting the latter in Eq. (10.14) yields for the order parameter of the ferromagnetic state

$$\mathbf{\Psi}(\mathbf{x}) = \sqrt{n(\mathbf{x})} \, e^{i\tilde{\theta}} \begin{pmatrix} \cos^2 \frac{\tilde{\beta}}{2} \, e^{i\varphi_1} \\ \sqrt{2} \sin \frac{\tilde{\beta}}{2} \cos \frac{\tilde{\beta}}{2} \, e^{i\varphi_0} \\ \sin^2 \frac{\tilde{\beta}}{2} \, e^{i\varphi_{-1}} \end{pmatrix}, \qquad 0 \leq \tilde{\beta} \leq \pi. \tag{10.68}$$

We continue in complete analogy to the last subsection by introducing the abbreviations

$$\alpha = \frac{\varphi_{-1} - \varphi_1}{2}, \tag{10.69}$$

$$\tau = -\frac{\varphi_1 - \varphi_{-1}}{2}, \tag{10.70}$$

$$\theta = \tilde{\theta} - \tau, \tag{10.71}$$

$$\beta \equiv \tilde{\beta} + p\pi. \tag{10.72}$$

Thus, Eq. (10.68) reads

$$\boxed{\boldsymbol{\Psi}(\mathbf{x}) = \sqrt{n(\mathbf{x})}\, e^{i\theta} \begin{pmatrix} \cos^2\frac{\beta}{2}\, e^{-i\alpha} \\ \sqrt{2}\sin\frac{\beta}{2}\cos\frac{\beta}{2} \\ \sin^2\frac{\beta}{2}\, e^{i\alpha} \end{pmatrix}, \qquad \alpha, \beta, \theta \in \mathbb{R},} \tag{10.73}$$

where $n(\mathbf{x})$ obeys the relation

$$(c_0 + c_2)\, n(\mathbf{x}) + V(\mathbf{x}) - \mu = 0. \tag{10.74}$$

We also rewrite Eq. (10.73) with the help of the spin rotation matrix (10.62), which finally yields

$$\boldsymbol{\Psi}(\mathbf{x}) = \sqrt{n(\mathbf{x})}\, \mathcal{U}(\alpha, \beta, \gamma) \begin{pmatrix} 1 \\ 0 \\ 0 \end{pmatrix}, \tag{10.75}$$

where we have set $\gamma \equiv -\theta$. Note that in (10.75) the global phase factor $e^{i\theta}$ was absorbed in the spin rotation matrix, whereas in the antiferrmagnetic case Eq. (10.63) this was not possible. This has also physical consequences. If one calculates the superfluid velocity $\mathbf{v}_s \propto \boldsymbol{\Psi}^\dagger \nabla \boldsymbol{\Psi}$ of the system, it turns out that it depends on the gradient of the global phase factor. Therefore, in case of the ferromagnetic solution, the superfluid velocity is directly coupled with the spin rotation, which is not the case for the antiferromagnetic solution (see discussion in Ref. [22]). We also calculate the expectation value of the angular momentum. From Eq. (10.75) we deduce

$$|\, \langle \mathbf{F} \rangle \,| = \int d^3x\, n(\mathbf{x}) \equiv N, \qquad (\hbar \equiv 1). \tag{10.76}$$

Hence, all particles are polarized in the same direction, which justifies to call this phase ferromagnetic.

Occurrence of Phases

To the end of this chapter we derive the conditions for the occurrence of the antiferromagnetic and ferromagnetic state. As discussed above, the two phases extremize the Euclidian action (10.1). However, we do not know if the phases maximize or minimize it. Therefore, we take the interacting part of the Euclidian action (10.2). Using the vectorial notation for the background fields and omitting the imaginary time dependency it reads

$$\mathcal{A}^{(\mathrm{int})}[\Psi^*, \Psi] = \frac{1}{2}\int_0^{\hbar\beta} d\tau \int d^3x \left\{ c_0 \Big[\boldsymbol{\Psi}^\dagger(\mathbf{x})\boldsymbol{\Psi}(\mathbf{x})\Big]^2 + c_2 \sum_{j=x,y,z} \Big[\boldsymbol{\Psi}^\dagger(\mathbf{x})\mathbf{F}^j\boldsymbol{\Psi}(\mathbf{x})\Big]^2 \right\}. \tag{10.77}$$

The first term on the right-hand side is simply an invariant, whereas the second term depends on the spin configuration of the system. For positive c_2 it is seen from the latter equation that

the Euclidian action is minimized by minimization of the sum of the second term. This is exactly the case in the antiferromagnetic phase, i.e., the background field (10.64) minimizes the Euclidean action for $c_2 > 0$ [22, 23]. In contrast, for $c_2 < 0$, the Euclidean action is minimized by the ferromagnetic solution (10.76). Therefore, the behavior of the atoms are essentially determined by the sign of c_2. A example for a ferromagnetic atom is ^{87}Rb and for an antiferromagnetic ^{23}Na.

Chapter 11

First Critical Temperature in Perturbation Theory

In the last chapter we have shown for a particular case that a two-particle interaction leads to a noticeable change of the physical properties of the system. In this chapter we study the influence of such an interaction to the first critical temperature for a harmonically trapped $F = 1$ spinor gas. To this end we will adopt perturbation theory, which is a widely used and a well-known analytical approximation method [43]. It is applied to systems, which are exactly solvable for a vanishing coupling parameter. Then, it is possible to expand the physical quantities of the system into a power expansion with respect to the coupling parameter. One prominent example for a weak-coupling parameter is the fine-structure constant $\alpha \approx 1/137$ of quantum electrodynamics (QED). Due to its smallness, physical quantities in QED are perturbatively treated with a high accuracy. On the other hand, it is also possible to calculate series expansions for systems with a strong-coupling parameter. One method is based on a variational approach given in Ref. [57] and is called variational perturbation theory [47, 48, Chapter 5]. In our system we have the former case, namely a weak-coupling parameters, which we identify with the interaction strengths c_0, c_2. For vanishing interaction strengths c_0, c_2 the system reduces to the ideal case, which we have extensively treated in Part II.

11.1 Grand-Canonical Partition Function

We start with deriving a perturbative expression for the grand-canonical partition function

$$\mathcal{Z} = \left[\prod_{a=-1}^{1} \oint \mathcal{D}\psi_a^* \oint \mathcal{D}\psi_a\right] e^{-\mathcal{A}[\psi^*,\psi]/\hbar}, \tag{11.1}$$

where the action is given as a sum of a non-interacting action functional $\mathcal{A}^{(0)}[\psi^*, \psi]$ in (2.47) and an interacting functional $\mathcal{A}^{(\mathrm{int})}[\psi^*, \psi]$ given in (2.48). Considering only a weak two-particle interaction, we may assume $\mathcal{A}^{(\mathrm{int})}$ as a small correction to $\mathcal{A}^{(0)}$. Therefore, we

expand the Boltzmann factor $e^{-(\mathcal{A}^{(0)}+\mathcal{A}^{(\mathrm{int})})/\hbar}$ in Eq. (11.1) in a Taylor series around the non-interacting action $\mathcal{A}^{(0)}$, which yields with (2.48) the grand-canonical partition function in a perturbative expansion

$$\begin{aligned}\mathcal{Z} &= \mathcal{Z}^{(0)}\Bigg\{1-\frac{1}{2\hbar}\int_0^{\hbar\beta}d\tau\int d^3x\int d^3x'\,V^{(\mathrm{int})}_{aba'b'}(\mathbf{x},\mathbf{x}') \\ &\quad\times\left\langle\psi^*_a(\mathbf{x},\tau)\psi_b(\mathbf{x},\tau)\psi^*_{a'}(\mathbf{x}',\tau)\psi_{b'}(\mathbf{x}',\tau)\right\rangle^{(0)}+\ldots\Bigg\}. \qquad (11.2)\end{aligned}$$

Here $\mathcal{Z}^{(0)}$ denotes the partition function of the non-interacting system (2.73) and $\langle\bullet\rangle^{(0)}$ is the expectation value of the quantity $\bullet$ in the non-interacting system. The general definition of this expectation value is given in (2.33), whereas within the functional integral approach it reads

$$\left\langle\bullet\right\rangle^{(0)}=\frac{1}{\mathcal{Z}^{(0)}}\left[\prod_{a=-1}^{1}\oint\mathcal{D}\psi^*_a\oint\mathcal{D}\psi_a\right]\bullet\; e^{-\mathcal{A}^{(0)}[\psi^*,\psi]/\hbar}. \qquad (11.3)$$

In order to calculate the expectation value of the fields, we use the generating grand-canonical partition function (2.52), which was introduced in Section 2.5. Using (2.72), it allows us to write the *two-point correlation function* as

$$\begin{aligned}\left\langle\psi_a(\mathbf{x},\tau)\psi^*_b(\mathbf{x}',\tau')\right\rangle^{(0)} &= \frac{\hbar^2}{\mathcal{Z}^{(0)}}\frac{\delta}{\delta j_b(\mathbf{x}',\tau')}\frac{\delta}{\delta j^*_a(\mathbf{x},\tau)}\mathcal{Z}^{(0)}[j^*,j]\Big|_{j^*=0}^{j=0} \\ &= G^{(0)}_{ab}(\mathbf{x},\tau;\mathbf{x}',\tau'), \qquad (11.4)\end{aligned}$$

where the Green's function is given in Eq. (2.74). Moreover, we have used the property that the functional derivatives with respect to the current fields $j_a(\mathbf{x},\tau)$, $j^*_a(\mathbf{x},\tau)$ interchange with the functional integrals with respect to the fields $\psi_a(\mathbf{x},\tau)$, $\psi^*_a(\mathbf{x},\tau)$.

Analogously, the four-point correlation function in (11.2) reads

$$\begin{aligned}&\left\langle\psi^*_a(\mathbf{x},\tau)\psi_b(\mathbf{x},\tau)\psi^*_{a'}(\mathbf{x}',\tau)\psi_{b'}(\mathbf{x}',\tau)\right\rangle^{(0)} \\ &\quad=\frac{\hbar^4}{\mathcal{Z}^{(0)}[j^*,j]}\frac{\delta}{\delta j_a(\mathbf{x},\tau)}\frac{\delta}{\delta j^*_b(\mathbf{x},\tau)}\frac{\delta}{\delta j_{a'}(\mathbf{x}',\tau)}\frac{\delta}{\delta j^*_{b'}(\mathbf{x}',\tau)}\mathcal{Z}^{(0)}[j^*,j]\Big|_{j=0}^{j^*=0}. \qquad (11.5)\end{aligned}$$

Thus, the latter expectation value is completely determined by the generating grand-canonical partition function $\mathcal{Z}^{(0)}[j^*,j]$. This is also true for expectation values of higher orders in the fields. Explicit calculation of (11.5) with the help of the generating partition function (2.72) yields the following relation between the four-point correlation function and the Green's function

$$\left\langle \psi_a^*(\mathbf{x},\tau)\psi_b(\mathbf{x},\tau)\psi_{a'}^*(\mathbf{x}',\tau)\psi_{b'}(\mathbf{x}',\tau)\right\rangle^{(0)} = G_{ba}^{(0)}(\mathbf{x},\tau;\mathbf{x},\tau)G_{b'a'}^{(0)}(\mathbf{x}',\tau;\mathbf{x}',\tau) + G_{ba'}^{(0)}(\mathbf{x},\tau;\mathbf{x}',\tau)G_{b'a}^{(0)}(\mathbf{x}',\tau;\mathbf{x},\tau). \tag{11.6}$$

Using the identity (11.4), one identifies (11.6) as the famous *Wick's theorem* [58]. Furthermore, according to (11.2) and (11.6), the perturbative calculation of the grand-canonical partition function reduces to the evaluation of integrals over products of Green's functions.

We now turn our attention to the physical meaning of the Green's function. Therefore, we start to derive a relation between the Green's function and the particle density of the system. In Chapter 2 we have derived for the total number of particles the following quantum statistical identity

$$\begin{aligned} N &= \frac{1}{\beta}\frac{\partial}{\partial\mu}\log\mathcal{Z}^{(0)} \\ &= \sum_{a=-1}^{1}\int d^3x\, n_a^{(0)}(\mathbf{x}) \end{aligned} \tag{11.7}$$

and, correspondingly, for the total magnetization

$$\begin{aligned} M &= \frac{1}{\beta}\frac{\partial}{\partial\eta}\log\mathcal{Z}^{(0)} \\ &= \int d^3x \left[n_1^{(0)}(\mathbf{x}) - n_{-1}^{(0)}(\mathbf{x})\right], \end{aligned} \tag{11.8}$$

where $n_a^{(0)}(\mathbf{x})$ denotes the particle density of the Zeeman state $|a\rangle$ in case of a non-interacting system. On the other hand, using Eqs. (2.73), (2.74) and the orthonormality condition (2.2), it is straightforward to verify

$$\frac{1}{\beta}\frac{\partial}{\partial\mu}\log\mathcal{Z}^{(0)} = \sum_{a=-1}^{1}\int d^3x\, G_{aa}^{(0)}(\mathbf{x},\tau;\mathbf{x},\tau) \tag{11.9}$$

and

$$\frac{1}{\beta}\frac{\partial}{\partial\eta}\log\mathcal{Z}^{(0)} = \int d^3x \left[G_{11}^{(0)}(\mathbf{x},\tau;\mathbf{x},\tau) - G_{-1-1}^{(0)}(\mathbf{x},\tau;\mathbf{x},\tau)\right]. \tag{11.10}$$

We emphasize that $G_{ab}^{(0)}(\mathbf{x},\tau;\mathbf{x},\tau)$ in the latter equations are evaluated for *equal* space-time points. Comparing Eqs. (11.7) and (11.9) with each other we get the relation

$$n_a^{(0)}(\mathbf{x}) = G_{aa}^{(0)}(\mathbf{x},\tau;\mathbf{x},\tau), \qquad a = +1, 0, -1. \tag{11.11}$$

Therefore, the diagonal elements of the Green's function correspond for equal space-time points to the particle densities of the respective Zeeman state. Using Eqs. (11.4) and (11.11) yields

$$n_a^{(0)}(\mathbf{x}) = \left\langle \psi_a(\mathbf{x},\tau)\psi_a^*(\mathbf{x},\tau)\right\rangle^{(0)}, \qquad a = +1, 0, -1. \tag{11.12}$$

Therefore, we define the total particle density of the non-interacting system as

$$n^{(0)}(\mathbf{x}) \equiv \sum_{a=-1}^{1} n_a^{(0)}(\mathbf{x}) = \sum_{a=-1}^{1} G_{aa}^{(0)}(\mathbf{x},\tau;\mathbf{x},\tau) \tag{11.13}$$

and the corresponding total magnetization density as

$$m^{(0)}(\mathbf{x}) \equiv n_1^{(0)}(\mathbf{x}) - n_{-1}^{(0)}(\mathbf{x}) = G_{11}^{(0)}(\mathbf{x},\tau;\mathbf{x},\tau) - G_{-1-1}^{(0)}(\mathbf{x},\tau;\mathbf{x},\tau). \tag{11.14}$$

11.2 Grand-Canonical Free Energy

In the last subsection we have derived a general perturbative expression for the grand-canonical partition function of an interacting $F = 1$ spinor gas. We now explicitly calculate the corresponding grand-canonical free energy (2.34) for the case of a harmonically trapped spinor gas, where we restrict ourself to the semiclassical approximation.

11.2.1 General Interaction Potential

Substituting (11.2) in the grand-canonical free energy (2.34) yields in first-order perturbation theory

$$\mathcal{F} = \mathcal{F}^{(0)} + \mathcal{F}^{(D)} + \mathcal{F}^{(E)}. \tag{11.15}$$

The first contribution is the grand-canonical free energy of the non-interacting spinor system

$$\mathcal{F}^{(0)} = -\frac{1}{\beta}\log \mathcal{Z}^{(0)}. \tag{11.16}$$

For the system being in the gas phase, the latter expression has already been evaluated in Eq. (4.36), yielding

$$\mathcal{F}^{(0)} = -\frac{1}{\beta(\beta\hbar\tilde{\omega})^3}\left[\zeta_4(e^{\beta(\mu+\eta)}) + \zeta_4(e^{\beta\mu}) + \zeta_4(e^{\beta(\mu-\eta)})\right] \tag{11.17}$$

The second contribution is the so-called direct term

$$\mathcal{F}^{(\mathrm{D})} = \frac{1}{2\beta\hbar}\int_0^{\hbar\beta} d\tau \int d^3x \int d^3x'\, V_{aba'b'}^{(\mathrm{int})}(\mathbf{x},\mathbf{x}') G_{ba}^{(0)}(\mathbf{x},\tau;\mathbf{x},\tau) G_{b'a'}^{(0)}(\mathbf{x}',\tau;\mathbf{x}',\tau), \tag{11.18}$$

and the last term is called the exchange term

$$\mathcal{F}^{(\mathrm{E})} = \frac{1}{2\beta\hbar}\int_0^{\hbar\beta} d\tau \int d^3x \int d^3x'\, V_{aba'b'}^{(\mathrm{int})}(\mathbf{x},\mathbf{x}') G_{ba'}^{(0)}(\mathbf{x},\tau;\mathbf{x}',\tau) G_{b'a}^{(0)}(\mathbf{x}',\tau;\mathbf{x},\tau). \tag{11.19}$$

The grand-canonical free energy is conveniently represented in a graphical way, namely, with the help of Feynman diagrams [43]. In order to interpret the Feynman diagrams correctly, we have to introduce the corresponding Feynman rules of our systems.

11.2.2 Feynman Rules

The diagrammatical representation of the non-interacting Green's function (2.74) is given by a straight line with an arrow

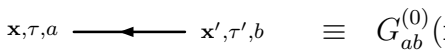

$$\equiv \quad G^{(0)}_{ab}(\mathbf{x},\tau;\mathbf{x}',\tau'). \tag{11.20}$$

Furthermore, two vertices connected by a dashed line denote the interaction potential

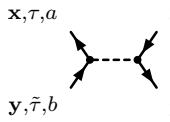

$$\equiv \quad -\frac{1}{\hbar}U_{aba'b'}(\mathbf{x},\tau;\mathbf{y},\tilde{\tau};\mathbf{x}',\tau';\mathbf{y}',\tilde{\tau}'), \tag{11.21}$$

where we have defined

$$U_{aba'b'}(\mathbf{x},\tau;\mathbf{y},\tilde{\tau};\mathbf{x}',\tau';\mathbf{y}',\tilde{\tau}') \equiv \delta(\tau-\tau')\delta(\tau-\tilde{\tau})\delta(\tau'-\tilde{\tau}')\delta(\mathbf{x}-\mathbf{y})\delta(\mathbf{x}'-\mathbf{y}')V_{aba'b'}(\mathbf{x},\mathbf{x}'). \tag{11.22}$$

This rather formal way of writing the interaction potential is necessary to define properly the graphical connection of the Green's function and the interaction potential, which has to be performed according to the rule

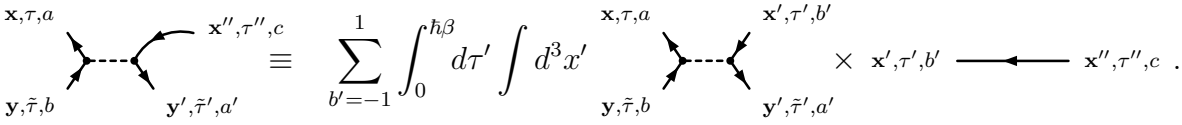

$$\equiv \quad \sum_{b'=-1}^{1}\int_0^{\hbar\beta} d\tau' \int d^3x' \quad \times \quad . \tag{11.23}$$

Note that according to the latter rule we connect the ends with the same sets of indices. After performing the integrations and the summation, the respective indices vanish from the diagrams.

Applying the latter rules to (11.18) and (11.19), we obtain for the direct term

$$\mathcal{F}^{(\mathrm{D})} = -\frac{1}{2\beta} \tag{11.24}$$

and for the exchange term

$$\mathcal{F}^{(\mathrm{E})} = -\frac{1}{2\beta} \quad . \tag{11.25}$$

We just state that the grand-canonical free energy reads in second order perturbation theory

$$\mathcal{F}^{(2)} = \frac{1}{4} + + \frac{1}{2} + \frac{1}{4} + \frac{1}{2} . \tag{11.26}$$

Most conveniently, higher order contributions to the grand-canonical free energy can be obtained by adopting a graphical recursion formula presented in Ref. [59].

11.2.3 Delta Interaction Potential

So far, we have not specified the two-particle interaction $V_{aba'b'}(\mathbf{x},\mathbf{x}')$ in (11.22). Using the two-particle interaction (9.10) and the diagonal form of the Green's function (2.74) gives for the direct contribution of the grand-canonical free energy (11.18)

$$\mathcal{F}^{(\mathrm{D})} = \frac{1}{2\beta\hbar}\int_0^{\hbar\beta} d\tau \int d^3x \left[c_0 \left(\sum_{a=-1}^{1} G_0^{(a)} \right)^2 + c_2 \left(G_0^{(1)} - G_0^{(-1)} \right)^2 \right] \tag{11.27}$$

and for the exchange contribution (11.19)

$$\mathcal{F}^{(\mathrm{E})} = \frac{1}{2\beta\hbar}\int_0^{\hbar\beta} d\tau \int d^3x \left\{ c_0 \sum_{a=-1}^{1} {G_0^{(a)}}^2 + c_2 \left[\left(\sum_{a=-1}^{1} G_0^{(a)} \right)^2 - {G_0^{(0)}}^2 - 2G_0^{(1)}G_0^{(-1)} \right] \right\}, \tag{11.28}$$

where we used the abbreviation

$$G_0^{(a)} \equiv G_0^{(a)}(\mathbf{x},\tau;\mathbf{x},\tau). \tag{11.29}$$

As it can be seen from (2.74), the Green's function does not depend on the imaginary time anymore for $\tau = \tau'$. Therefore, the time integrals in Eqs. (11.27) and (11.28) are trivially be integrated out. Using (11.13) and (11.14) we get for the direct term

$$\mathcal{F}^{(\mathrm{D})} = \frac{1}{2}\int d^3x \left[c_0 n^{(0)}(\mathbf{x})^2 + c_2 m^{(0)}(\mathbf{x})^2 \right] \tag{11.30}$$

and correspondingly for the exchange contribution

$$\mathcal{F}^{(\mathrm{E})} = \frac{1}{2}\int d^3x \left\{ c_0 \sum_{a=-1}^{1} n_a^{(0)}(\mathbf{x})^2 + c_2 \left[n^{(0)}(\mathbf{x})^2 - n_0^{(0)}(\mathbf{x})^2 - 2n_1^{(0)}(\mathbf{x}) n_{-1}^{(0)}(\mathbf{x}) \right] \right\}. \tag{11.31}$$

As seen from (11.30) and (11.31), the direct contribution depends only on the total particle density and the total magnetization, whereas the exchange contribution is also sensitive to the particle density in a single Zeeman state. Furthermore, we observe that, if the system occupies only one Zeeman state, then $\mathcal{F}^{(\mathrm{D})}$ coincides with $\mathcal{F}^{(\mathrm{E})}$.

In order to calculate analytically the spatial integrals in (11.30) and (11.31), we use the semiclassical expression of the Green's function (see Appendix C.2). For $\tau = \tau'$ and $\mathbf{x} = \mathbf{x}'$ it is given by

$$G_0^{(a)}(\mathbf{x},\tau;\mathbf{x},\tau) = \frac{1}{\lambda^3}\,\zeta_{3/2}\left(e^{-\beta[V(\mathbf{x})-\mu-a'\eta]} \right), \qquad a = 1, 0, -1. \tag{11.32}$$

The integrals in (11.30) and (11.31) are then analytically solvable. The explicit calculation is shown in Appendix C.3. Using (11.27), (11.28), (11.32), (C.25), and (C.28) yields the

direct free energy

$$\begin{aligned}\mathcal{F}^{(\mathrm{D})} &= \frac{1}{2}\frac{1}{(\lambda\beta\hbar\tilde{\omega})^3}\Big\{c_0\Big[\zeta_{\frac{3}{2},\frac{3}{2},\frac{3}{2}}\left(e^{\beta(\mu+\eta)}\right)+\zeta_{\frac{3}{2},\frac{3}{2},\frac{3}{2}}\left(e^{\beta\mu}\right)+\zeta_{\frac{3}{2},\frac{3}{2},\frac{3}{2}}\left(e^{\beta(\mu-\eta)}\right)\\ &\quad+2\zeta_{\frac{3}{2},\frac{3}{2},\frac{3}{2}}\left(e^{\beta(\mu+\eta)},e^{\beta(\mu-\eta)}\right)+2\zeta_{\frac{3}{2},\frac{3}{2},\frac{3}{2}}\left(e^{\beta(\mu+\eta)},e^{\beta\mu}\right)+2\zeta_{\frac{3}{2},\frac{3}{2},\frac{3}{2}}\left(e^{\beta(\mu-\eta)},e^{\beta\mu}\right)\Big]\\ &\quad+c_2\Big[\zeta_{\frac{3}{2},\frac{3}{2},\frac{3}{2}}\left(e^{\beta(\mu+\eta)}\right)+\zeta_{\frac{3}{2},\frac{3}{2},\frac{3}{2}}\left(e^{\beta(\mu-\eta)}\right)-2\zeta_{\frac{3}{2},\frac{3}{2},\frac{3}{2}}\left(e^{\beta(\mu+\eta)},e^{\beta(\mu-\eta)}\right)\Big]\Big\} \qquad (11.33)\end{aligned}$$

and the exchange term of the free energy

$$\begin{aligned}\mathcal{F}^{(\mathrm{E})} &= \frac{1}{2}\frac{1}{(\lambda\beta\hbar\tilde{\omega})^3}\Big\{c_0\Big[\zeta_{\frac{3}{2},\frac{3}{2},\frac{3}{2}}\left(e^{\beta(\mu+\eta)}\right)+\zeta_{\frac{3}{2},\frac{3}{2},\frac{3}{2}}\left(e^{\beta\mu}\right)+\zeta_{\frac{3}{2},\frac{3}{2},\frac{3}{2}}\left(e^{\beta(\mu-\eta)}\right)\Big] \qquad (11.34)\\ &\quad+c_2\Big[\zeta_{\frac{3}{2},\frac{3}{2},\frac{3}{2}}\left(e^{\beta(\mu+\eta)}\right)+\zeta_{\frac{3}{2},\frac{3}{2},\frac{3}{2}}\left(e^{\beta(\mu-\eta)}\right)+2\zeta_{\frac{3}{2},\frac{3}{2},\frac{3}{2}}\left(e^{\beta(\mu+\eta)},e^{\beta\mu}\right)+2\zeta_{\frac{3}{2},\frac{3}{2},\frac{3}{2}}\left(e^{\beta(\mu-\eta)},e^{\beta\mu}\right)\Big]\Big\},\end{aligned}$$

where we have introduced the generalized polylogarithmic function

$$\begin{aligned}\zeta_{a,b,c}\left(z_1,z_2\right) &\equiv \sum_{n=1}^{\infty}\sum_{n'=1}^{\infty}\frac{z_1^n\,z_2^{n'}}{n^a\,n'^b(n+n')^c},\\ \zeta_{a,b,c}\left(z\right) &\equiv \zeta_{a,b,c}\left(z,z\right). \qquad (11.35)\end{aligned}$$

Moreover, we define the total first-order contribution to the grand-canonical free energy as

$$\mathcal{F}^{(\mathrm{D+E})} = \mathcal{F}^{(\mathrm{D})} + \mathcal{F}^{(\mathrm{E})}. \qquad (11.36)$$

This provides us the basis for studying the interacting system up to the first order in perturbation theory.

11.3 Particle Number / Magnetization

In this subsection we calculate the dependence of the fugacity and the magnetic fugacity on the total number of particles and the total magnetization. This is important, because μ and η have to be chosen in such a way that the total number of particles and the total magnetization are conserved. We start with the normalized number of particles which is given by

$$\mathcal{N} = -\frac{1}{N}\frac{\partial\mathcal{F}}{\partial\mu}. \qquad (11.37)$$

In analogy to the treatment of the ideal spinor gas we set

$$N \equiv \frac{\zeta(3)}{(\hbar\beta_0\tilde{\omega})^3}\ . \qquad (11.38)$$

Here the zero in the subscript indicates that β is computed at the critical temperature T_0, which is defined in Eq. (6.7) as the critical temperature of a full-polarized ideal spinor gas without finite-size scaling. Using (11.15)–(11.17), (11.33), (11.34), and the differentiation rules (C.32), (C.33) we obtain for the normalized total number of particles

$$\mathcal{N} = \mathcal{N}^{(0)}(\mu,\eta,\mathcal{T}) + \mathcal{N}^{(\mathrm{D+E})}(\mu,\eta,\mathcal{T}), \tag{11.39}$$

with the zeroth order contribution

$$\mathcal{N}^{(0)}(\mu,\eta,\mathcal{T}) = \frac{\mathcal{T}^3}{\zeta(3)}\left[\zeta_3\left(e^{\beta(\mu+\eta)}\right) + \zeta_3\left(e^{\beta\mu}\right) + \zeta_3\left(e^{\beta(\mu-\eta)}\right)\right] \tag{11.40}$$

and with contribution due to the particle interaction

$$\begin{aligned}\mathcal{N}^{(\mathrm{D+E})}(\mu,\eta,\mathcal{T}) = -2\,\frac{\mathcal{T}^{7/2}}{\zeta(3)\lambda_0}\Bigg\{&(\tilde{a}_0+\tilde{a}_2)\Big[\zeta_{\frac{3}{2},\frac{3}{2},\frac{1}{2}}\left(e^{\beta(\mu+\eta)}\right) + \zeta_{\frac{3}{2},\frac{3}{2},\frac{1}{2}}\left(e^{\beta(\mu-\eta)}\right)\\ &+ \zeta_{\frac{3}{2},\frac{3}{2},\frac{1}{2}}\left(e^{\beta(\mu+\eta)},e^{\beta\mu}\right) + \zeta_{\frac{3}{2},\frac{3}{2},\frac{1}{2}}\left(e^{\beta(\mu-\eta)},e^{\beta\mu}\right)\Big] + \tilde{a}_0\,\zeta_{\frac{3}{2},\frac{3}{2},\frac{1}{2}}\left(e^{\beta\mu}\right)\\ &+ (\tilde{a}_0-\tilde{a}_2)\,\zeta_{\frac{3}{2},\frac{3}{2},\frac{1}{2}}\left(e^{\beta(\mu+\eta)},e^{\beta(\mu-\eta)}\right)\Bigg\},\end{aligned} \tag{11.41}$$

where the s-wave scattering lengths $\tilde{a}_j$ are defined in (9.9). Note that according to the definition of the normalized quantities (2.37) we have $\mathcal{N}=1$. However, for the time being we continue to use the notation $\mathcal{N}$, as it indicates that this term corresponds to the total number of particles. Analogously we get for the normalized magnetization

$$\mathcal{M} = \mathcal{M}^{(0)}(\mu,\eta,\mathcal{T}) + \mathcal{M}^{(\mathrm{D+E})}(\mu,\eta,\mathcal{T}), \tag{11.42}$$

with the zeroth order contribution

$$\mathcal{M}^{(0)}(\mu,\eta,\mathcal{T}) = \frac{\mathcal{T}^3}{\zeta(3)}\left\{\zeta_3\left(e^{\beta(\mu+\eta)}\right) - \zeta_3\left(e^{\beta(\mu-\eta)}\right)\right\} \tag{11.43}$$

and with the contribution due to the particle interaction

$$\begin{aligned}\mathcal{M}^{(\mathrm{D+E})}(\mu,\eta,\mathcal{T}) = -2\,\frac{\mathcal{T}^{7/2}}{\zeta(3)\lambda_0}\Bigg\{&(\tilde{a}_0+\tilde{a}_2)\Big[\zeta_{\frac{3}{2},\frac{3}{2},\frac{1}{2}}\left(e^{\beta(\mu+\eta)}\right) - \zeta_{\frac{3}{2},\frac{3}{2},\frac{1}{2}}\left(e^{\beta(\mu-\eta)}\right)\\ &+ \zeta_{\frac{1}{2},\frac{3}{2},\frac{3}{2}}\left(e^{\beta(\mu+\eta)},e^{\beta\mu}\right) - \zeta_{\frac{1}{2},\frac{3}{2},\frac{3}{2}}\left(e^{\beta(\mu-\eta)},e^{\beta\mu}\right)\Big]\\ &+ (\tilde{a}_0-\tilde{a}_2)\Big[\zeta_{\frac{1}{2},\frac{3}{2},\frac{3}{2}}\left(e^{\beta(\mu+\eta)},e^{\beta(\mu-\eta)}\right) - \zeta_{\frac{1}{2},\frac{3}{2},\frac{3}{2}}\left(e^{\beta(\mu-\eta)},e^{\beta(\mu+\eta)}\right)\Big]\Bigg\}.\end{aligned} \tag{11.44}$$

As can be seen from the latter equations, both the fugacity and the magnetic fugacity have to be determined as a function of temperature. In principle, Eqs. (11.39)–(11.44) could be solved numerically for any temperature above the first critical temperature. However, here

we are only interested in calculating the first critical temperature $\mathcal{T}_{c_1}$. Assuming that μ_{c_1}, η_{c_1} and $\mathcal{T}_{c_1}$ depend only weakly on the interaction we may write

$$\mu_{c_1} \approx \mu_{c_1}^{(0)} + \mu_{c_1}^{(1)}, \qquad \mu_{c_1}^{(1)} \ll \mu_{c_1}^{(0)}, \tag{11.45}$$

$$\eta_{c_1} \approx \eta_{c_1}^{(0)} + \eta_{c_1}^{(1)}, \qquad \eta_{c_1}^{(1)} \ll \eta_{c_1}^{(0)}, \tag{11.46}$$

$$\mathcal{T}_{c_1} \approx \mathcal{T}_{c_1}^{(0)} + \mathcal{T}_{c_1}^{(1)}, \qquad \mathcal{T}_{c_1}^{(1)} \ll \mathcal{T}_{c_1}^{(0)}, \tag{11.47}$$

where $\mu_{c_1}^{(0)}$, $\eta_{c_1}^{(0)}$, $\mathcal{T}_{c_1}^{(0)}$ are the respective solutions for the ideal spinor gas and $\mu_{c_1}^{(1)}$, $\eta_{c_1}^{(1)}$, $\mathcal{T}_{c_1}^{(1)}$ the respective first-order corrections. The subscript c_1 indicates that the quantities are computed at the first critical temperature $\mathcal{T} = \mathcal{T}_{c_1}$. Substituting Eqs. (11.45)–(11.47) in Eqs. (11.39)–(11.44) and neglecting terms of the order $\tilde{a}_i\tilde{a}_j$ or higher orders yields at the critical point

$$\begin{aligned}\mathcal{N} = &\left[1 + 3\frac{\mathcal{T}_{c_1}^{(1)}}{\mathcal{T}_{c_1}^{(0)}}\right]\mathcal{N}^{(0)}\left(\mu_{c_1}^{(0)}, \eta_{c_1}^{(0)}, \mathcal{T}_{c_1}^{(0)}\right) + \mathcal{N}^{(\mathrm{D+E})}\left(\mu_{c_1}^{(0)}, \eta_{c_1}^{(0)}, \mathcal{T}_{c_1}^{(0)}\right) \\ &- \frac{{\mathcal{T}_{c_1}^{(0)}}^3}{\zeta(3)}\frac{\mathcal{T}_{c_1}^{(1)}}{\mathcal{T}_{c_1}^{(0)}}\beta_{c_1}^{(0)}\Big[\left(\mu_{c_1}^{(0)} + \eta_{c_1}^{(0)}\right)\zeta_2(zz_\eta) + \mu_{c_1}^{(0)}\zeta_2(z) + \left(\mu_{c_1}^{(0)} - \eta_{c_1}^{(0)}\right)\zeta_2(z/z_\eta)\Big] \\ &+ \frac{{\mathcal{T}_{c_1}^{(0)}}^3}{\zeta(3)}\beta_{c_1}^{(0)}\left(\mu_{c_1}^{(1)} + \eta_{c_1}^{(1)}\right)\Big[\zeta_2(zz_\eta) + \zeta_2(z) + \zeta_2(z/z_\eta)\Big] - \frac{{\mathcal{T}_{c_1}^{(0)}}^3\beta_{c_1}^{(0)}\eta_{c_1}^{(1)}}{\zeta(3)}\Big[\zeta_2(z) + 2\,\zeta_2(z/z_\eta)\Big]\end{aligned} \tag{11.48}$$

and for the total magnetization

$$\begin{aligned}\mathcal{M} = &\left[1 + 3\frac{\mathcal{T}_{c_1}^{(1)}}{\mathcal{T}_{c_1}^{(0)}}\right]\mathcal{M}^{(0)}\left(\mu_{c_1}^{(0)}, \eta_{c_1}^{(0)}, \mathcal{T}_{c_1}^{(0)}\right) + \mathcal{M}^{(\mathrm{D+E})}\left(\mu_{c_1}^{(0)}, \eta_{c_1}^{(0)}, \mathcal{T}_{c_1}^{(0)}\right) \\ &- \frac{{\mathcal{T}_{c_1}^{(0)}}^3}{\zeta(3)}\frac{\mathcal{T}_{c_1}^{(1)}}{\mathcal{T}_{c_1}^{(0)}}\beta_{c_1}^{(0)}\Big[\left(\mu_{c_1}^{(0)} + \eta_{c_1}^{(0)}\right)\zeta_2(zz_\eta) - \left(\mu_{c_1}^{(0)} - \eta_{c_1}^{(0)}\right)\zeta_2(z/z_\eta)\Big] \\ &+ \frac{{\mathcal{T}_{c_1}^{(0)}}^3}{\zeta(3)}\beta_{c_1}^{(0)}\left(\mu_{c_1}^{(1)} + \eta_{c_1}^{(1)}\right)\Big[\zeta_2(zz_\eta) - \zeta_2(z/z_\eta)\Big] + 2\,\frac{{\mathcal{T}_{c_1}^{(0)}}^3\beta_{c_1}^{(0)}\eta_{c_1}^{(1)}}{\zeta(3)}\,\zeta_2(z/z_\eta),\end{aligned} \tag{11.49}$$

where we have introduced the abbreviations

$$\beta_{c_1}^{(0)} = 1/(k_B T_{c_1}^{(0)}), \qquad z = e^{\beta_{c_1}^{(0)}\mu_{c_1}^{(0)}}, \qquad z_\eta = e^{\beta_{c_1}^{(0)}\eta_{c_1}^{(0)}}. \tag{11.50}$$

To eliminate the last term in (11.48) we use (11.49) and solve for $\mathcal{T}_{c_1}^{(1)}$ leading to

$$\begin{aligned}\frac{\mathcal{T}_{c_1}^{(1)}}{\mathcal{T}_{c_1}^{(0)}} &= \left\{\Delta\mathcal{N}+\Delta\mathcal{M}\left(1+\frac{\zeta_2(z)}{2\zeta_2(z/z_\eta)}\right)-\frac{{\mathcal{T}_{c_1}^{(0)}}^3}{2\zeta(3)}\beta_{c_1}^{(0)}\left(\mu_{c_1}^{(1)}+\eta_{c_1}^{(1)}\right)\right.\\ &\quad\left.\times\left[4\zeta_2(zz_\eta)+\zeta_2(z/z_\eta)+\frac{\zeta_2(zz_\eta)\zeta_2(z)}{\zeta_2(z/z_\eta)}\right]\right\}\Big/\left\{3\left[\mathcal{N}^{(0)}\left(\mu_{c_1}^{(0)},\eta_{c_1}^{(0)},\mathcal{T}_{c_1}^{(0)}\right)\right.\right.\\ &\quad\left.+\mathcal{M}^{(0)}\left(\mu_{c_1}^{(0)},\eta_{c_1}^{(0)},\mathcal{T}_{c_1}^{(0)}\right)\left(1+\frac{\zeta_2(z)}{2\zeta_2(z/z_\eta)}\right)\right]-\frac{{\mathcal{T}_{c_1}^{(0)}}^3}{2\zeta(3)}\beta_{c_1}^{(0)}\\ &\quad\left.\times\left(\mu_{c_1}^{(0)}+\eta_{c_1}^{(0)}\right)\left(4\zeta_2(zz_\eta)+\zeta_2(z)+\frac{\zeta_2(z)\zeta_2(zz_\eta)}{\zeta_2(z/z_\eta)}\right)\right\},\end{aligned}\tag{11.51}$$

where we have defined

$$\Delta\mathcal{N} \equiv \mathcal{N}-\mathcal{N}^{(0)}\left(\mu_{c_1}^{(0)},\eta_{c_1}^{(0)},\mathcal{T}_{c_1}^{(0)}\right)-\mathcal{N}^{(\mathrm{D+E})}\left(\mu_{c_1}^{(0)},\eta_{c_1}^{(0)},\mathcal{T}_{c_1}^{(0)}\right),\tag{11.52}$$

$$\Delta\mathcal{M} \equiv \mathcal{M}-\mathcal{M}^{(0)}\left(\mu_{c_1}^{(0)},\eta_{c_1}^{(0)},\mathcal{T}_{c_1}^{(0)}\right)-\mathcal{M}^{(\mathrm{D+E})}\left(\mu_{c_1}^{(0)},\eta_{c_1}^{(0)},\mathcal{T}_{c_1}^{(0)}\right).\tag{11.53}$$

For vanishing two-particle interaction the quantities $\Delta\mathcal{N}$, $\Delta\mathcal{M}$, $\mu_{c_1}^{(1)}+\eta_{c_1}^{(1)}$ become equally zero and therefore also the critical temperature shift $\mathcal{T}_{c_1}^{(1)}$ vanishes. To explicitly calculate (11.51), we have to know the quantities $\mathcal{T}_{c_1}^{(0)}$, $\mu_{c_1}^{(0)}$, $\eta_{c_1}^{(0)}$ and $\mu_{c_1}^{(1)}+\eta_{c_1}^{(1)}$. In principle, the first three quantities could be taken from Part II of this thesis, where we have treated the ideal spinor gas. The last quantity, which is due to the interaction, could also be obtained by solving the Gross-Pitaevksii equation in first order for the interacting spinor gas. However, this would be inconsistent with the present perturbative treatment of the problem. For example, the Gross-Pitaevskii equations are, in principle, only valid in the zero-temperature limit, where nearly all particles are Bose-Einstein condensed. In contrast, the perturbative approach is only valid for temperatures above the first phase transition. Thus, it would be delicate to mix those two different approaches. Therefore, we calculate $\mathcal{T}_{c_1}^{(0)}$, $\mu_{c_1}^{(0)}$, $\eta_{c_1}^{(0)}$ and $\mu_{c_1}^{(1)}+\eta_{c_1}^{(1)}$ consistently within perturbation theory.

11.4 Criterion for Phase Transition

We have to find a criterion where the phase transition occurs. Two major characteristics of Bose-Einstein condensates are that particles macroscopically occupy the ground state and that the correlation between the particles start to diverge. This is because they share the same wave-function with the same phase. Therefore, we introduce the criterion that one of the correlation functions

$$G_{ab}(\mathbf{x},\tau;\mathbf{x}',\tau')=\frac{1}{\mathcal{Z}}\left[\prod_{a'=-1}^{1}\oint\mathcal{D}\psi_{a'}^*\oint\mathcal{D}\psi_{a'}\right]\psi_a(\mathbf{x},\tau)\psi_b^*(\mathbf{x}',\tau')e^{-\mathcal{A}[\psi^*,\psi]/\hbar}\tag{11.54}$$

diverges at the first critical temperature. Note that (11.54) defines the Green's function of the *interacting* system, where the Feynman diagrammatical representation is given in analogy to the non-interacting Green's function (11.20) by

$$\equiv \quad G_{ab}(\mathbf{x},\tau;\mathbf{x}',\tau'). \tag{11.55}$$

Thus, the divergence of $G_{ab}(\mathbf{x},\tau;\mathbf{x}',\tau')$ implies that its functional inverse $G^{-1}_{ab}(\mathbf{x},\tau;\mathbf{x}',\tau')$, defined as

$$\int_0^{\hbar\beta} d\tau'' \int d^3x''\, G^{-1}_{ac}(\mathbf{x},\tau;\mathbf{x}'',\tau'')G_{cb}(\mathbf{x}'',\tau'';\mathbf{x}',\tau') = \delta_{ab}\delta(\mathbf{x}-\mathbf{x}')\delta(\tau-\tau'), \tag{11.56}$$

vanishes. Both the Green's function of the interacting system G_{ab} and its functional inverse cannot be calculated analytically. Therefore, we write the functional inverse as the sum of the functional inverse of the ideal spinor gas and an additional term, called the self-energy:

$$G^{-1}_{ab}(\mathbf{x},\tau;\mathbf{x}',\tau') = G^{(0)\,-1}_{ab}(\mathbf{x},\tau;\mathbf{x}',\tau') - \Sigma_{ab}(\mathbf{x},\tau;\mathbf{x}',\tau'). \tag{11.57}$$

We introduce the Feynman diagrammatical symbol for the self-energy as

$$\equiv \quad \Sigma_{ab}(\mathbf{x},\tau;\mathbf{x}',\tau'). \tag{11.58}$$

Note that in the latter definition the small arrows on the left and right side of the circle, belong to the definition of the self-energy and must not be mixed up with the symbol of the Green's function (11.20).

In (11.57), the functional inverse of the non-interacting Green's function is given by

$$G^{(0)\,-1}_{ab}(\mathbf{x},\tau;\mathbf{x}',\tau') = \frac{1}{\hbar}\delta(\mathbf{x}-\mathbf{x}')\delta(\tau-\tau')\left\{\left[\hbar\frac{\partial}{\partial\tau} - \frac{\hbar^2}{2M}\Delta + V(\mathbf{x}) - \mu\right]\delta_{ab} - \eta F^z_{ab}\right\}, \tag{11.59}$$

which comes from the fact, that the Green's function fulfills the differential equation (2.75). In order to get rid of the derivatives in Eqs. (11.57), (11.59), we perform a Fourier-Matsubara decomposition of the Green's function

$$G^{-1}_{ab}(\mathbf{x},\tau;\mathbf{x}',\tau') = \frac{1}{\hbar\beta}\sum_{m=-\infty}^{\infty} e^{-i\omega_m(\tau-\tau')}\int\frac{d^3k}{(2\pi)^3}e^{i\mathbf{k}(\mathbf{x}-\mathbf{x}')}G^{-1}_{ab}\left(\mathbf{k},\omega_m;\frac{\mathbf{x}+\mathbf{x}'}{2}\right). \tag{11.60}$$

Note that we imposed $G^{-1}_{ab}(\mathbf{x},\tau;\mathbf{x}',\tau')$ to be $\hbar\beta$ periodic and therefore we were able to perform a Matsubara decomposition, where $\omega_m = 2\pi m/(\hbar\beta)$ denote the Matsubara frequencies.

Comparing (11.57), (11.59) with (11.60) leads to the identification

$$G_{ab}^{-1}(\mathbf{k},\omega_m;\mathbf{x}) = \frac{1}{\hbar}\left\{\left[-i\hbar\omega_m + \frac{\hbar^2\mathbf{k}^2}{2M} + V(\mathbf{x}) - \mu\right]\delta_{ab} - \eta F_{ab}^z\right\} - \Sigma_{ab}(\mathbf{k},\omega_m;\mathbf{x}) \tag{11.61}$$

with the Fourier-Matsubara transformed of the self-energy

$$\Sigma_{ab}(\mathbf{k},\omega_m;\mathbf{x}) = \int_0^{\hbar\beta} d\tau\, e^{i\omega_m\tau}\int d^3x' e^{-i\mathbf{k}\cdot\mathbf{x}'}\Sigma_{ab}(\mathbf{x}+\mathbf{x}'/2,\tau;\mathbf{x}-\mathbf{x}'/2,0). \tag{11.62}$$

In (11.60), we have decomposed the inverse of the correlation function in its Fourier components. Physically, we know that the correlation function only diverges for particles starting to Bose-Einstein condense. Such particles are in the ground-state and therefore the corresponding contribution to the Green's function is the one describing particles with $\mathbf{k} = \mathbf{0}$. Furthermore, these particles do not depend on imaginary time. Therefore, only the $\mathbf{k} = \mathbf{0}$, $\omega_m = 0$ contribution to the Green's function can diverge. Correspondingly, only $G_{ab}^{-1}(\mathbf{0},0;\mathbf{x})$ can become zero at the first phase transition. By defining an effective potential

$$V_{ab}^{(\mathrm{eff})}(\mathbf{x},\mu,\eta) \equiv \hbar\, G_{ab}^{-1}(\mathbf{0},0;\mathbf{x}) \tag{11.63}$$

the problem reduces to the determination of the point, where the minimum of $V_{ab}^{(\mathrm{eff})}(\mathbf{x},\mu,\eta)$ becomes zero with respect to $\mathbf{x}$, μ and η, i.e., we have the condition

$$\boxed{\min_{\mathbf{x}} V_{ab}^{(\mathrm{eff})}(\mathbf{x},\mu_{c_1},\eta_{c_1}) = 0.} \tag{11.64}$$

Using (11.61) we can equally write for (11.63)

$$V_{ab}^{(\mathrm{eff})}(\mathbf{x},\mu,\eta) = \Big[V(\mathbf{x}) - \mu\Big]\delta_{ab} - \eta F_{ab}^z - \hbar\,\Sigma_{ab}(\mathbf{0},0;\mathbf{x}). \tag{11.65}$$

Before explicitly calculating the self-energy, we consider an ideal spinor gas. In this particular case we have the identity $G_{ab}^{-1} = G_{ab}^{(0)-1}$. From (11.57) we then deduce that the self-energy vanishes identically and therefore the effective potential reduces to

$$V_{ab}^{(\mathrm{eff},0)}(\mathbf{x},\mu,\eta) = \Big[V(\mathbf{x}) - \mu^{(0)}\Big]\delta_{ab} - \eta^{(0)} F_{ab}^z. \tag{11.66}$$

The superscript denotes that we are in the ideal spinor system. Considering a positive magnetizated spinor gas we get with (11.64), (11.66) the condition

$$\min_{\mathbf{x}} V_{11}^{(\mathrm{eff},0)}(\mathbf{x},\mu,\eta) = -(\mu_{c_1}^{(0)} + \eta_{c_1}^{(0)}) = 0. \tag{11.67}$$

The quantity $V_{11}^{(\mathrm{eff})}$ is related to $G_{11}^{(0)}$ through Eq. (11.63) and the fact that the Green's function is diagonal in our system. Furthermore, we know from (11.11) that for equal space-time points $G_{11}^{(0)}$ coincides with the particle density of the first Zeeman state. We therefore deduce, that particles in the first Zeeman state first Bose-Einstein condense. We turn back to the case of an weakly-interacting spinor gas and calculate the self-energy of the system.

11.5 Self-Energy

In order to calculate the self-energy we start with the Schwinger-Dyson equation [43]

$$G_{ab}(\mathbf{x},\tau;\mathbf{x}',\tau') = G^{(0)}_{ab}(\mathbf{x},\tau;\mathbf{x}',\tau') \tag{11.68}$$
$$+\int_0^{\hbar\beta} d\tau'' \int d^3x'' \int_0^{\hbar\beta} d\tau''' \int d^3x''' \, G^{(0)}_{ac}(\mathbf{x},\tau;\mathbf{x}'',\tau'')\Sigma_{cd}(\mathbf{x}'',\tau'';\mathbf{x}''',\tau''')G_{db}(\mathbf{x}''',\tau''';\mathbf{x}',\tau').$$

In terms of Feynman diagrams, it reads with (11.20), (11.55), and (11.58)

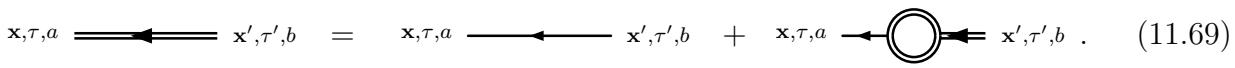

(11.69)

To prove the Schwinger-Dyson equation we simply insert the definition of the self-energy (11.57) in (11.68), use (11.56) and the corresponding equation for the non-interacting Green's function. Note that the Schwinger-Dyson equation is still an exact expression. Furthermore, we have the relation

$$\frac{1}{\mathcal{Z}_0}\left[\prod_{a=-1}^{1}\oint \mathcal{D}\psi^*_a \oint \mathcal{D}\psi_a\right] \psi_a(\mathbf{x},\tau)\psi^*_b(\mathbf{x}',\tau')\, e^{-\mathcal{A}[\psi^*,\psi]/\hbar} \tag{11.70}$$
$$= G^{(0)}_{ab}(\mathbf{x},\tau;\mathbf{x}',\tau') - \frac{1}{2\hbar}\int_0^{\hbar\beta} d\tau'' \int d^3x'' \int_0^{\hbar\beta} d\tau''' \int d^3x''' \, \delta(\tau''-\tau''')V^{(\mathrm{int})}_{cdc'd'}(\mathbf{x}'',\mathbf{x}''')$$
$$\times\left\langle \psi_a(\mathbf{x},\tau)\psi^*_b(\mathbf{x}',\tau')\psi^*_c(\mathbf{x}'',\tau'')\psi_d(\mathbf{x}'',\tau'')\psi^*_{c'}(\mathbf{x}''',\tau''')\psi_{d'}(\mathbf{x}''',\tau''')\right\rangle^{(0)},$$

which is derived in analogy to Section 11.1 by expanding the exponential function into a Taylor series around $\mathcal{A}^{(0)}$ and using the first-order result of the partition function (11.2) in (11.54). Thus, using the Wick rule and the symmetry properties of the interaction potential (2.5), the Green's function in first-order perturbation theory reads

$$G_{ab}(\mathbf{x},\tau;\mathbf{x}',\tau') = G^{(0)}_{ab}(\mathbf{x},\tau;\mathbf{x}',\tau') - \frac{1}{\hbar}\int_0^{\hbar\beta} d\tau'' \int d^3x'' \int_0^{\hbar\beta} d\tau''' \int d^3x''' \, \delta(\tau''-\tau''')V^{(\mathrm{int})}_{cdc'd'}(\mathbf{x}'',\mathbf{x}''')$$
$$\times\Big\{ G^{(0)}_{ac}(\mathbf{x},\tau;\mathbf{x}'',\tau'')G^{(0)}_{d'c'}(\mathbf{x}''',\tau''';\mathbf{x}''',\tau''')G^{(0)}_{db}(\mathbf{x}'',\tau'';\mathbf{x}',\tau')$$
$$+ G^{(0)}_{ac}(\mathbf{x},\tau;\mathbf{x}'',\tau'')G^{(0)}_{dc'}(\mathbf{x}'',\tau'';\mathbf{x}''',\tau''')G^{(0)}_{d'b}(\mathbf{x}''',\tau''';\mathbf{x}',\tau')\Big\} \tag{11.71}$$

or equivalently

$$G_{ab}(\mathbf{x},\tau;\mathbf{x}',\tau') =$$

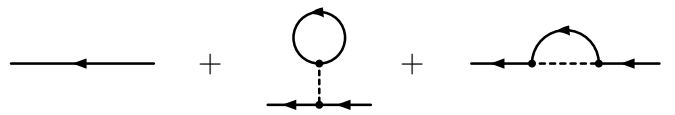
(11.72)

where we omitted for simplicity writing the respective indices. On the other hand an iteration of the Dyson equation (11.68), (11.69) leads to

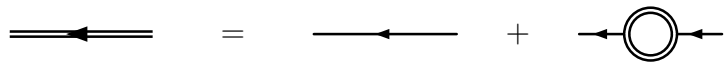

(11.73)

which corresponds to the following analytical expression

$$G_{ab}(\mathbf{x},\tau;\mathbf{x}',\tau') = G^{(0)}_{ab}(\mathbf{x},\tau;\mathbf{x}',\tau') + \int_0^{\hbar\beta} d\tau'' \int d^3x'' \int_0^{\hbar\beta} d\tau''' \int d^3x'''\, G^{(0)}_{ac}(\mathbf{x},\tau;\mathbf{x}'',\tau'')\Sigma_{cd}(\mathbf{x}'',\tau'';\mathbf{x}''',\tau''')G^{(0)}_{db}(\mathbf{x}''',\tau''';\mathbf{x}',\tau'). \tag{11.74}$$

Comparing (11.72) with (11.73) and amputating a line on the left-hand and the right-hand side of the diagrams we get the following one-particle irreducible diagrams of the self-energy

$\Sigma_{cd}(\mathbf{x}'',\tau'';\mathbf{x}''',\tau''') =$ 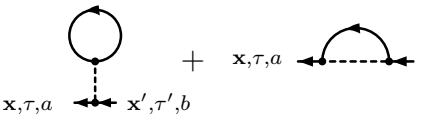

(11.75)

The first term on the right-hand side is the direct contribution to the self-energy

$$\Sigma^{(\mathrm{D})}_{cd}(\mathbf{x}'',\tau'';\mathbf{x}''',\tau''') = -\frac{1}{\hbar}\delta(\tau''-\tau''')\,\delta(\mathbf{x}''-\mathbf{x}''')\int d^3x\, V^{(\mathrm{int})}_{cdc'd'}(\mathbf{x}'',\mathbf{x})G^{(0)}_{d'c'}(\mathbf{x},\tau'';\mathbf{x},\tau''') \tag{11.76}$$

and the second one

$$\Sigma^{(\mathrm{E})}_{cd}(\mathbf{x}'',\tau'';\mathbf{x}''',\tau''') = -\frac{1}{\hbar}\delta(\tau''-\tau''')\,V^{(\mathrm{int})}_{cd'c'd}(\mathbf{x}'',\mathbf{x}''')G^{(0)}_{d'c'}(\mathbf{x}'',\tau'';\mathbf{x}''',\tau'''). \tag{11.77}$$

The dots in (11.75) denote terms of higher order, which contribute contributing to the self-energy.

The expressions of the self-energy (11.77),(11.77) are valid for an arbitrary two-particle interaction potential in first-order perturbation theory. We now substitute our particular interaction potential (9.10) in Eqs. (11.76), (11.77) and obtain for the direct diagram

$$\Sigma^{(\mathrm{D})}_{ab}(\mathbf{x},\tau;\mathbf{x}',\tau') = -\frac{1}{\hbar}\delta(\tau-\tau')\,\delta(\mathbf{x}-\mathbf{x}')\Big[c_0\, n^{(0)}(\mathbf{x})\delta_{ab} + c_2\, m^{(0)}(\mathbf{x})F^z_{ab}\Big], \tag{11.78}$$

where we also have used the relations (11.13) and (11.14). Correspondingly, the exchange contribution of the self-energy reads

$$\begin{aligned}\Sigma^{(\mathrm{E})}_{ab}(\mathbf{x},\tau;\mathbf{x}',\tau') \;=\; & -\frac{1}{\hbar}\delta(\tau-\tau')\,\delta(\mathbf{x}-\mathbf{x}')\Big[n^{(0)}_1(\mathbf{x})\,\mathrm{diag}\Big(c_0+c_2,c_2,0\Big) \\ & + n^{(0)}_0(\mathbf{x})\,\mathrm{diag}\Big(c_2,c_0,c_2\Big) + n^{(0)}_{-1}(\mathbf{x})\,\mathrm{diag}\Big(0,c_2,c_0+c_2\Big)\Big],\end{aligned} \tag{11.79}$$

where $\mathrm{diag}(a,b,c)$ denotes a 3×3 matrix with the diagonal elements a, b, c. We are now able to continue our derivation of the first critical temperature of Section 11.3.

11.6 First Critical Temperature

In order to obtain the first-order correction of the critical temperature, we have to calculate the remaining quantity $\mu_{c_1}^{(1)} + \eta_{c_1}^{(1)}$. As derived in Section 11.3, we can calculate the latter by minimizing the effective potential $V_{ab}^{(\mathrm{eff})}$. Using the semiclassical expression of the Green's function (11.32) and Eqs. (11.13), (11.14), (11.57), (11.62), (11.63), (11.75), (11.78), (11.79) yields for the diagonal components of the effective potential

$$\begin{aligned}
V_{11}^{(\mathrm{eff})}(\mathbf{x},\mu,\eta) &= V(\mathbf{x}) - \mu - \eta + \frac{1}{\lambda^3}\Big[2(c_0+c_2)\zeta_{3/2}\left(e^{-\beta[V(\mathbf{x})-\mu-\eta]}\right) \\
&\quad +(c_0+c_2)\zeta_{3/2}\left(e^{-\beta[V(\mathbf{x})-\mu]}\right) + (c_0-c_2)\zeta_{3/2}\left(e^{-\beta[V(\mathbf{x})-\mu+\eta]}\right)\Big], \\
V_{00}^{(\mathrm{eff})}(\mathbf{x},\mu,\eta) &= V(\mathbf{x}) - \mu + \frac{1}{\lambda^3}\Big[(c_0+c_2)\zeta_{3/2}\left(e^{-\beta[V(\mathbf{x})-\mu-\eta]}\right) \\
&\quad +2c_0\,\zeta_{3/2}\left(e^{-\beta[V(\mathbf{x})-\mu]}\right) + (c_0+c_2)\zeta_{3/2}\left(e^{-\beta[V(\mathbf{x})-\mu+\eta]}\right)\Big], \\
V_{-1-1}^{(\mathrm{eff})}(\mathbf{x},\mu,\eta) &= V(\mathbf{x}) - \mu + \eta + \frac{1}{\lambda^3}\Big[(c_0-c_2)\zeta_{3/2}\left(e^{-\beta[V(\mathbf{x})-\mu-\eta]}\right) \\
&\quad +(c_0+c_2)\zeta_{3/2}\left(e^{-\beta[V(\mathbf{x})-\mu]}\right) + 2(c_0+c_2)\zeta_{3/2}\left(e^{-\beta[V(\mathbf{x})-\mu+\eta]}\right)\Big]. \qquad (11.80)
\end{aligned}$$

The remaining components of the effective potential are identical zero.

In Section 11.4 we have shown that for the limiting case of a non-interacting spinor gas, the component $V_{11}^{(\mathrm{eff})}$ becomes first zero, namely, at the point $\mathbf{x} = \mathbf{0}$. Now, taking a weak interaction into account, leads to the assumption that the system deviates only weakly from the non-interacting case. Therefore, we again expect $V_{11}^{(\mathrm{eff})}$ to become first equally zero at the space-point $\mathbf{x} = \mathbf{0}$. Thus, using Eqs. (11.45), (11.46), (11.67), and (11.80) leads to the condition

$$\mu_{c_1}^{(1)} + \eta_{c_1}^{(1)} = \frac{1}{\lambda_{c_1}^3}\Big[2(c_0+c_2)\,\zeta(3/2) + (c_0+c_2)\,\zeta_{3/2}(z) + (c_0-c_2)\,\zeta_{3/2}(z^2)\Big]. \qquad (11.81)$$

This was exactly the equation, which was missing to determine the shift of the critical temperature (11.51) in first-order perturbation theory. With Eqs. (11.39)–(11.53), (11.67), and (11.81) we get for the temperature shift

$$\boxed{\frac{\mathcal{T}_{c_1}^{(1)}}{\mathcal{T}_{c_1}^{(0)}} = \alpha_0(\mathcal{M})\,\frac{a_0}{\lambda_0} + \alpha_2(\mathcal{M})\,\frac{a_2}{\lambda_0}} \qquad (11.82)$$

with the coefficient

$$\alpha_0(\mathcal{M}) = \frac{1}{9}\Bigg\{4\zeta_{\frac{1}{2},\frac{3}{2},\frac{3}{2}}(z) + 8\zeta_{\frac{1}{2},\frac{3}{2},\frac{3}{2}}\left(1,z^2\right) - 4\zeta_{3/2}(z^2)\left[2\zeta(2) + \zeta_2(z) + [\zeta(2) - \zeta_2(z^2)]\frac{\zeta_2(z)}{2\zeta_2(z^2)}\right]$$
$$+ 2\frac{\zeta_2(z)}{\zeta_2(z^2)}\left[\zeta_{\frac{1}{2},\frac{3}{2},\frac{3}{2}}\left(1,z^2\right) - \zeta_{\frac{1}{2},\frac{3}{2},\frac{3}{2}}\left(z^2,1\right)\right]\Bigg\}\sqrt{\mathcal{T}_{c_1}^{(0)}(z)}\Bigg/\Bigg\{2\zeta(3) + \zeta_3(z)$$
$$+ \frac{\zeta_2(z)}{2\,\zeta_2(z^2)}\left[\zeta(3) - \zeta_3(z^2)\right]\Bigg\} \tag{11.83}$$

and

$$\alpha_2(\mathcal{M}) = \frac{1}{9}\Bigg\{24\zeta_{\frac{1}{2},\frac{3}{2},\frac{3}{2}}(1) + 12\zeta_{\frac{1}{2},\frac{3}{2},\frac{3}{2}}(1,z) + 6\zeta_{\frac{1}{2},\frac{3}{2},\frac{3}{2}}(z,1) + 6\zeta_{\frac{1}{2},\frac{3}{2},\frac{3}{2}}\left(z,z^2\right) + 8\zeta_{\frac{1}{2},\frac{3}{2},\frac{3}{2}}(z)$$
$$+ 4\zeta_{\frac{1}{2},\frac{3}{2},\frac{3}{2}}\left(1,z^2\right) - 2\left[6\zeta(3/2) + 3\zeta_{3/2}(z) + \zeta_{3/2}(z^2)\right]\left[2\zeta(2) + \zeta_2(z)\right.$$
$$\left. + [\zeta(2) - \zeta_2(z^2)]\frac{\zeta_2(z)}{2\zeta_2(z^2)}\right] + \frac{\zeta_2(z)}{\zeta_2(z^2)}\left[6\zeta_{\frac{1}{2},\frac{3}{2},\frac{3}{2}}(1) - 6\zeta_{\frac{1}{2},\frac{3}{2},\frac{3}{2}}\left(z^2\right) + 3\zeta_{\frac{1}{2},\frac{3}{2},\frac{3}{2}}(1,z)\right.$$
$$\left. - 3\zeta_{\frac{1}{2},\frac{3}{2},\frac{3}{2}}\left(z^2,z\right) + \zeta_{\frac{1}{2},\frac{3}{2},\frac{3}{2}}\left(1,z^2\right) - \zeta_{\frac{1}{2},\frac{3}{2},\frac{3}{2}}\left(z^2,1\right)\right]\Bigg\}\sqrt{\mathcal{T}_{c_1}^{(0)}(z)}$$
$$\Bigg/\Bigg\{2\zeta(3) + \zeta_3(z) + \frac{\zeta_2(z)}{2\,\zeta_2(z^2)}\left[\zeta(3) - \zeta_3(z^2)\right]\Bigg\}. \tag{11.84}$$

Here, we have for the first critical temperature in zeroth order according to Eq. (6.13)

$$\mathcal{T}_{c_1}^{(0)}(z) = \left[\frac{\zeta(3)}{\zeta(3) + \zeta_3(z) + \zeta_3(z^2)}\right]^{1/3} \tag{11.85}$$

and, using Eq. (6.14), the respective expression for the magnetization reads

$$\mathcal{M} = \frac{\zeta(3) - \zeta_3(z^2)}{\zeta(3) + \zeta_3(z) + \zeta_3(z^2)} \quad . \tag{11.86}$$

We note that the coefficients α_0, α_2 do only depend implicitly on the magnetization, i.e., $\alpha_{0,2}(\mathcal{M}) = \alpha_{0,2}(z(\mathcal{M}))$, where z has to be determined from Eq. (11.86). In Figure 11.1, we have plotted α_0, α_2 parametrically as a function of the magnetization. We observe that the coefficients are always negative. Therefore, according to Eq. (11.82), for positive (negative) s-wave scattering lengths the critical temperature shift is always negative (positive). Positive (negative) s-wave scattering lengths correspond to repulsive (attractive) interaction during a two-particle collision, i.e., the higher (lower) the s-wave scattering lengths, the more the mean interparticle distances increase (decrease). If we take the rough criterium that Bose-Einstein condensation occurs if the de Broglie wavelengths of the particles are equal to the mean distances between the particles, then the shift of the critical temperature is directly explained.

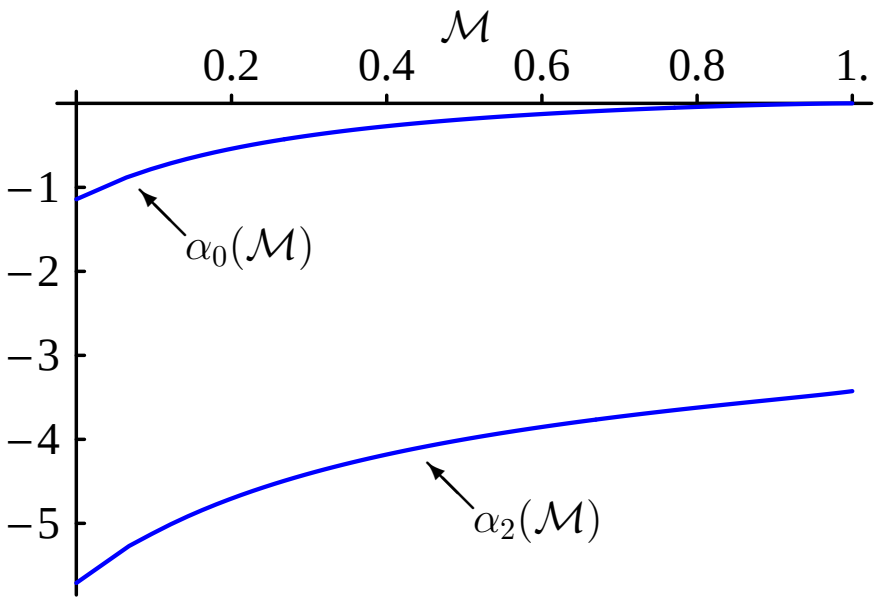

Figure 11.1: Behavior of the critical temperature shift coefficients α_0, α_2 in (11.82) as a function of magnetization. α_0 vanishes for a full polarized $F = 1$ spinor gas, which is due to that not collisions with a two-particle total angular 0 occur. For vanishing magnetization, α_2 is exactly 5 times smaller than α_0, which originates from that the two-particle state with total angular momentum 2 is five time degenerate, whereas the other one is not degenerate.

To gain more physical insight and more trust into the solution for the first critical temperature shift (11.82)–(11.84), we discuss two particular cases. At first we treat the case of a full polarized spinor gas and then the case of a non-polarized spinor gas.

11.6.1 Fully Polarized Spinor Gas

In a full polarized $F = 1$ spinor gas all particles occupy the Zeeman state $|1\rangle$. The magnetization $\mathcal{M}$ then coincides with the total number of particles $\mathcal{N} = 1$. According to Eq. (11.86) this is the case for $z \to 0$. Substituting this in Eqs. (11.83)–(11.85) and taking properly the limit $z \to 0$ yields

$$\alpha_0(\mathcal{M}{=}\mathcal{N}) = 0, \qquad \alpha_2(\mathcal{M}{=}\mathcal{N}) = \frac{4}{3\zeta(3)}\left[\zeta_{\frac{1}{2},\frac{3}{2},\frac{3}{2}}(1) - \zeta(3/2)\zeta(2)\right] \approx -3.426. \tag{11.87}$$

and consequently with (11.82), (11.85) the relative critical temperature shift reads

$$\frac{\mathcal{T}_{c_1}^{(1)}}{\mathcal{T}_{c_1}^{(0)}} = -3.426\,\frac{a_2}{\lambda_0}. \tag{11.88}$$

Therefore, for a full polarized spinor gas the contribution to the first critical temperature of the s-wave scattering length a_0 vanishes. This is because a_0 takes account to collisions, where

the two-particle state has a total angular momentum of $F = 0$ as can seen in Eqs. (9.5), (9.6). However, in a full polarized $F = 1$ spinor gas the total angular momentum of the total state of two colliding particle is necessarily always $|F = 2; a = 2\rangle$, otherwise the conservation of total angular momentum would be violated.

Our particular result (11.88) for the critical temperature shift of a *full polarized* spinor gas coincides with the one of a spinless BEC as derived in Ref. [60, 61], which recently has been approved experimentally to high accuracy [62]. This happens because, due to the conservation of the magnetization, the full polarized spinor gas behaves practically like a spinless Bose gas. Therefore, our result (11.82)–(11.84) also obtains the scalar BEC physics.

11.6.2 Non-Polarized Spinor Gas

Now, we discuss the limit of a non-polarized spinor gas. According to Eq. (11.86) a vanishing magnetization corresponds to a fugacity $z = 1$. We substitute this value in (11.83)–(11.85) and get for the coefficients

$$\alpha_0(0) = \frac{4}{3^{1/6} 9\zeta(3)} \left[\zeta_{\frac{1}{2},\frac{3}{2},\frac{3}{2}}(1) - \zeta(3/2)\zeta(2)\right] \approx -1.371, \qquad \alpha_2(0) = 5\,\alpha_0(0) \tag{11.89}$$

and according to Eqs. (11.82), (11.85) for the critical temperature shift

$$\frac{\mathcal{T}_{c_1}^{(1)}}{\mathcal{T}_{c_1}^{(0)}} = -1.371 \left(\frac{a_0}{\lambda_0} + 5\,\frac{a_2}{\lambda_0}\right). \tag{11.90}$$

This is a quite interesting result, because it states that in first-order perturbation theory the contribution of the s-wave scattering length a_2 is exactly five times higher than the one of a_0 for a vanishing total magnetization. The physical explanation is the following. In a non-polarized spinor gas all Zeeman states are completely degenerate. Therefore, during a two-particle collision, the total two-particle wave function is not restricted to only one particular state, like for the case of a fully polarized spinor gas as discussed in Sec. 11.6.1. On the contrary, the probability to form one of the two-particle states $|F = 0, a = 0\rangle$, $|F = 2, a = 2, 1, 0, -1, -2\rangle$ is the same. Therefore, due to the five times higher degeneracy of the $|F = 2\rangle$ state, the probability to form the latter state is five times higher than the one to form the state $|F = 0\rangle$. The factor five in Eq. (11.90) reflects this behavior.

11.7 Examples: Rubidium and Sodium

So far, we have discussed the coefficients α_0, α_2 in (11.82). Now, we consider two important examples, namely, a spinor condensate consisting of ^{87}Rb and ^{23}Na atoms, respectively. To this day, the only $F = 1$ spinor condensates, that have been realized experimentally, were from the latter two kinds. In Table 11.1 the s-wave scattering lengths and masses of Rubidium and Sodium are summarized. According to Table 11.1 both atoms, ^{87}Rb and ^{23}Na, have a positive s-wave scattering length. Therefore, we have a negative shift of the first

	a_0	a_2	M
^{23}Na	50.0	55.0	22.99
^{87}Rb	101.8	100.4	86.91

Table 11.1: Atomic parameters for ^{23}Na and ^{87}Rb atoms [63, 64]. a_0 and a_2 are in units of Bohr radius $a_B = 0.529 \times 10^{-10}\,\mathrm{m}$ and the atom mass M is given in units of $u = 1.66 \times 10^{-27}\,\mathrm{kg}$.

critical temperature. In Figure 11.2 we have plotted the relative (a) and absolute (b) critical temperatures for both kinds of atoms. Here, we have chosen the trap frequency $\tilde{\omega} = 2\pi\,100$ Hz and the total number of particles $N = 10^6$, as typical experimental values.

We first discuss Figure 11.2 (a). The black and the grey line denote the first and second critical temperature of an ideal $F = 1$ spinor condensate. For the ideal system these critical temperatures have been discussed extensively in Chapter 6. Note that according to (6.7), (6.13) the critical temperature of an ideal spinor condensate does not depend on the properties of the atoms, but only on the total number of particles in the system. The first-order critical temperatures of Sodium and Rubidium are denoted by a red and blue line, respectively. As it can be seen, the shift of the critical temperature of Rubidium is around four times higher than the one of Sodium. This is because of two facts. First the s-wave scattering length of Rubidium is two times higher than the corresponding of Sodium. Second, the critical temperature shift also depends according to Eq. (11.82) on the reciprocal de Broglie wave length λ_0 from Eq. (1.1), which is proportional to $1/\sqrt{M}$. Considering that the mass of Rubidium is four times higher than the mass of Sodium leads to another factor two contributing to the shift of critical temperature.

In Figure 11.2 (b) we have plotted the first critical temperature on an absolute temperature scale together with a numerical result of a Hartree-Fock-Popov approximation, which is taken from Ref. [65]. The color mapping is the same as in Fig. 11.2 (a). Our analytical result clearly predicts a larger shift of the first critical temperature than the numerical result. We point out that the analytical result has been well approved for the case of a full polarized ^{87}Rb condensate [62], which is shown in Figure 11.3. Here, the critical temperature was measured as a function of total number of particles. The dashed line denotes the critical temperature of a full polarized ^{87}Rb system with finite-size correction, which is given according to Eqs. (6.7), (6.13) by

$$T_{c1}^{(0,\mathrm{FS})} = T_{c1}^{(0)} - \frac{\hbar\bar{\omega}}{k_B}\frac{\zeta(2)}{6\zeta(3)}, \qquad T_{c1}^{(0)} = \frac{\hbar\tilde{\omega}}{k_B}\left[\frac{N}{\zeta(3)}\right]^{1/3}, \tag{11.91}$$

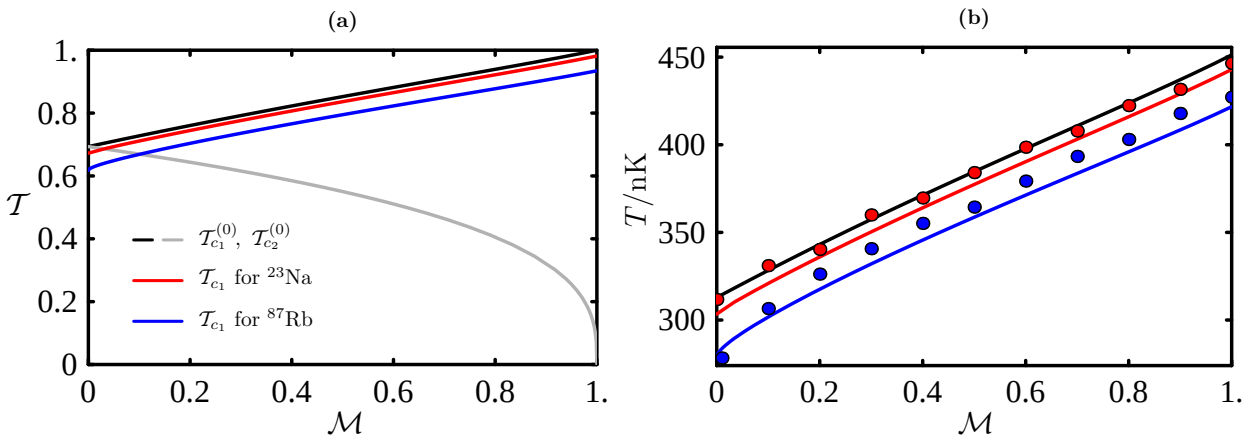

Figure 11.2: First critical temperature in first-order perturbation theory for sodium and rubidium for $N = 10^6$ and $\tilde{\omega} = 2\pi \times 100\,\mathrm{Hz}$. Due to the repulsive two-particle interaction, the critical temperature of sodium and rubidium experience a shift towards lower temperatures. In **(a)**, the critical temperatures are given on a relative temperature scale and are compared to the first and second critical temperature of a non-interacting $F = 1$ spinor gas. In **(b)**, T_{c_1} is plotted on an absolute temperature scale and compared with a numerical Hartree-Fock-Popov calculation, given in Ref. [65], where the red (sodium) and blue (rubidium) dots denote the respective numerical solutions.

whereas the solid line is the critical temperature in first-order perturbation theory, i.e., according to Eqs. (1.1), (11.88)

$$T_{c_1} = T_{c_1}^{(0,\mathrm{FS})} - 1.326\, a_2 N^{1/6} \sqrt{\frac{M\tilde{\omega}}{\hbar}}. \tag{11.92}$$

We see that the experimental observations show a good agreement with the first-order perturbative result in the limit of a full polarized spinor gas.

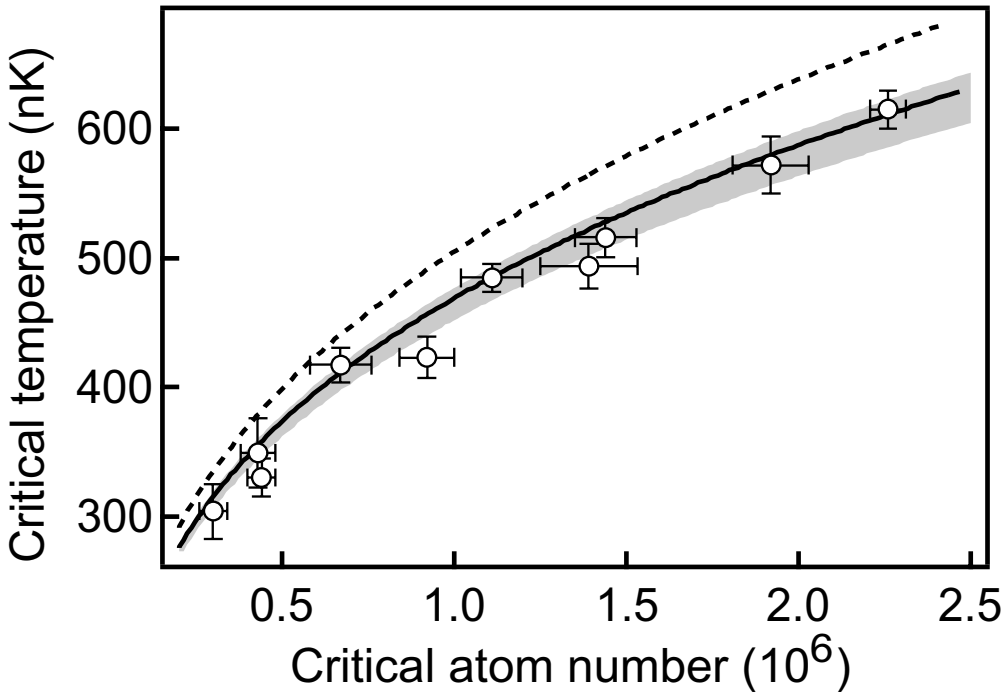

Figure 11.3: Critical temperature of a full polarized ^{87}Rb BEC as a function of atom number at T_{c_1}. The experimental points are denoted as circles. The dashed line follows the ideal gas law Eq. (11.91), whereas the solid line is the first-order perturbative result of the first critical temperature (11.92) in a full polarized system . The shaded area is the range of acceptable fits taking statistical and systematic errors into account. The figure is taken from Ref. [62].

Summary

On the basis of the quantum-field theoretical description of many-particle physics, we studied the thermodynamic properties of a $F = 1$ spinor Bose-Einstein condensate for both a non-interacting and a weakly interacting system. By doing so, we took into account the experimental constraint that the total number of particles and the total magnetization are conserved.

For the case of a non-interacting $F = 1$ spinor gas, we have shown in Chapter 5 that the additional condition of a conserving total magnetization leads to the occurrence of three phases: a gas, a ferromagnetic, and an antiferromagnetic phase [56], whose properties are depicted in Figure 5.2. In the gas phase, all particles occupy excited quantum states, whereas in the ferromagnetic phase, the spinor system consists of a full polarized Bose-Einstein condensate and a partially polarized thermal cloud. Reaching the antiferromagnetic phase, the magnetization of the BEC fraction coincides with the total magnetization of the whole system. In contrast, the magnetization of the thermal cloud vanishes completely in the antiferromagnetic phase. We then calculated in Chapter 6 the critical temperatures of those phase transitions as a function of magnetization for both a homogeneous and a harmonically trapped spinor gas, which are plotted in Figure 6.1. For the harmonically trapped spinor system, we studied its finite-size scaling where we observed a decrease of the first and the second critical temperature. In order to compare our results with future experiments, we calculated in Chapter 7 the occupation numbers of the respective Zeeman states in the thermal and the BEC fraction for different magnetizations and temperatures, which are shown in Figure 7.3. In Chapter 8 we finished the treatment of the ideal $F = 1$ spinor system by calculating the heat capacity for all three phases, which are plotted in Figure 8.1. There, we observed in case of a homogeneous spinor gas that the heat capacity is continuous for all temperatures. However, it exhibits at the first and second critical temperature a phase transition of third order. In contrast, the harmonically trapped spinor gas is continuous for all temperatures except for the first and second critical temperature, where it shows a phase transition of second order, i.e., it has a discontinuity at those temperatures. The jumps of the heat capacity at the critical points are depicted as a function of magnetization in Figure 8.2.

After having elucidated the contact interaction in a spinor Bose gas in Chapter 9, we derived in Chapter 10 the Gross-Pitaevskii equations of a weakly interacting $F = 1$ spinor gas and determined the solution within a Thomas-Fermi approximation. For the special case of a non-conserving magnetization, it turned out that the weakly interacting $F = 1$ spinor system exhibits either a ferromagnetic or an antiferromagnetic phase, depending on the sign of the interaction strength c_2 [22, 23]. The ferromagnetic phase occurs for $c_2 < 0$ and is characterized by a fully polarized BEC fraction. In contrast, for $c_2 > 0$ the BEC is not polarized at all and shows an antiferromagnetic behavior. Taking again the conservation of the magnetization into account, we continued our study in Chapter 11 with an analytical first-order perturbative calculation of the first critical temperature. For repulsive interaction strengths we predict a negative temperature shift compared to the ideal system, whereas for attractive interactions a positive shift is expected. We studied the limit of a fully polarized spinor gas, where our result coincides with the first-order result for the critical temperature of a scalar Bose gas, which was originally derived in Ref. [60] and experimentally observed in Ref. [62]. We finished this thesis by comparing our first-order result for the first critical temperature with a numerical Hartree-Fock-Popov calculation performed in Ref. [65], which was valid for arbitrary magnetizations. As shown in Figure 11.2 (b), our result predicts a larger shift towards negative temperatures.

Part IV

Appendix

Appendix A

Coherent States

In this appendix we show different properties of coherent states

$$|\psi\rangle = \exp\left\{\int d^3x\, \psi_a(\mathbf{x})\hat{\phi}_a^\dagger(\mathbf{x})\right\}|0\rangle\,, \tag{A.1}$$

which are important for deriving the functional integral picture representation of the grand-canonical partition function. In the following we consider only spinless particle, i.e., we set $\psi_a \to \psi$, $\hat{\phi}_a^\dagger \to \hat{\phi}^\dagger$. The proofs for bosons with non-vanishing spin is completely analogous.

A.1 Coherent States

In this section we explicitly show that (A.1) is a coherent state. Using Eqs. (2.2), (2.6), and (2.22) leads to following expression for the coherent state

$$|\psi\rangle = \exp\left\{\sum_{\mathbf{n}} \psi_{\mathbf{n}}\hat{\phi}_{\mathbf{n}}^\dagger\right\}|0\rangle\,, \tag{A.2}$$

where $|0\rangle$ is the vacuum state in the particle number representation. By virtue of the commutator relationship (2.11) we equally write for the latter

$$|\psi\rangle = \left[\prod_{\mathbf{n}}\sum_{N_{\mathbf{n}}=0}^{\infty}\frac{\left(\psi_{\mathbf{n}}\hat{\phi}_{\mathbf{n}}^\dagger\right)^{N_{\mathbf{n}}}}{N_{\mathbf{n}}!}\right]|0\rangle\,. \tag{A.3}$$

Applying Eq. (2.8) $N_{\mathbf{n}}$-times leads to

$$|\psi\rangle = \prod_{\mathbf{n}}\sum_{N_{\mathbf{n}}=0}^{\infty}\frac{(\psi_{\mathbf{n}})^{N_{\mathbf{n}}}}{\sqrt{N_{\mathbf{n}}!}}|N_{\mathbf{n}}\rangle\,, \tag{A.4}$$

where the state $|N_{\mathbf{n}}\rangle$ denotes that $N_{\mathbf{n}}$ particles are in the state $|\mathbf{n}\rangle$ and the total state is then given by

$$\prod_{\mathbf{n}}|N_{\mathbf{n}}\rangle = |\ldots, N_{\mathbf{n}}, \ldots\rangle\,. \tag{A.5}$$

We multiply Eq. (A.4) from the left side with the annihilation operator $\hat{\phi}_{\mathbf{n}'}$ and obtain with Eq. (2.7)

$$\hat{\phi}_{\mathbf{n}'}\,|\psi\rangle = \sum_{N_{\mathbf{n}'}=1}^{\infty} \frac{(\psi_{\mathbf{n}'})^{N_{\mathbf{n}'}}}{\sqrt{(N_{\mathbf{n}'}-1)!}}\,|N_{\mathbf{n}'}-1\rangle \prod_{\substack{\mathbf{n}\\ \mathbf{n}\neq\mathbf{n}'}} \sum_{N_{\mathbf{n}}=0}^{\infty} \frac{(\psi_{\mathbf{n}})^{N_{\mathbf{n}}}}{\sqrt{N_{\mathbf{n}}!}}\,|N_{\mathbf{n}}\rangle\,. \tag{A.6}$$

Relabeling the summation index $N_{\mathbf{n}'}$ and comparing with Eq. (A.4) directly leads to the desired result

$$\hat{\phi}_{\mathbf{n}'}\,|\psi\rangle = \psi_{\mathbf{n}'}\,|\psi\rangle\,. \tag{A.7}$$

A.2 Scalar Product

We prove that the scalar product of two coherent states is given by

$$\langle\psi|\psi'\rangle = \exp\left\{\sum_{\mathbf{n}} \psi^*_{\mathbf{n}}\psi'_{\mathbf{n}}\right\}. \tag{A.8}$$

According to Eq. (A.4) the left-hand side of (A.8) reads

$$\langle\psi|\psi'\rangle = \prod_{\mathbf{n},\mathbf{n}'} \sum_{N_{\mathbf{n}}=0}^{\infty} \sum_{N'_{\mathbf{n}'}=0}^{\infty} \frac{(\psi^*_{\mathbf{n}})^{N_{\mathbf{n}}}}{\sqrt{N_{\mathbf{n}}!}} \frac{(\psi'_{\mathbf{n}'})^{N'_{\mathbf{n}'}}}{\sqrt{N'_{\mathbf{n}'}!}}\,\langle N_{\mathbf{n}}|N_{\mathbf{n}'}\rangle\,. \tag{A.9}$$

The vectors of the occupation number representation fulfill the orthonormality condition, i.e., $\langle N_{\mathbf{n}}|N_{\mathbf{n}'}\rangle = \delta_{\mathbf{n}\mathbf{n}'}$ leading to

$$\langle\psi|\psi'\rangle = \prod_{\mathbf{n}} \sum_{N_{\mathbf{n}}=0}^{\infty} \frac{(\psi^*_{\mathbf{n}}\psi'_{\mathbf{n}})^{N_{\mathbf{n}}}}{N_{\mathbf{n}}!}, \tag{A.10}$$

which is identical to Eq. (A.8).

A.3 Closure Relationship

We show that the coherent states obey the closure relationship

$$\int \mathcal{D}\psi^* \int \mathcal{D}\psi\, e^{-(\psi|\psi)}\,|\psi\rangle\,\langle\psi| = \mathbb{1} \tag{A.11}$$

with the measure defined as

$$\int \mathcal{D}\psi^* \int \mathcal{D}\psi \equiv \left[\prod_{\mathbf{n}} \int \frac{d\psi^*_{\mathbf{n}}}{\sqrt{2\pi}} \int \frac{d\psi_{\mathbf{n}}}{\sqrt{2\pi}}\right]. \tag{A.12}$$

Using the definition $e^{(\psi|\psi)} = \langle\psi|\psi\rangle$ and substituting Eqs. (A.4), (A.8), (A.12) in (A.11) yields

$$\mathbb{1} = \left[\prod_{\mathbf{n}} \int \frac{d\psi^*_{\mathbf{n}}}{\sqrt{2\pi}} \int \frac{d\psi_{\mathbf{n}}}{\sqrt{2\pi}}\, e^{-\psi^*_{\mathbf{n}}\psi_{\mathbf{n}}}\right] \left[\prod_{\mathbf{n}'} \sum_{N_{\mathbf{n}'}=0}^{\infty} \frac{(\psi_{\mathbf{n}'})^{N_{\mathbf{n}'}}}{\sqrt{N_{\mathbf{n}'}!}} \,|N_{\mathbf{n}'}\rangle\right] \left[\prod_{\mathbf{n}''} \sum_{N'_{\mathbf{n}''}=0}^{\infty} \frac{(\psi^*_{\mathbf{n}''})^{N'_{\mathbf{n}''}}}{\sqrt{N'_{\mathbf{n}''}!}} \,\langle N'_{\mathbf{n}''}|\right] \tag{A.13}$$

To simplify the latter expression we define the product

$$\bigotimes_{\mathbf{n}} C_{\mathbf{n}} \,|N_{\mathbf{n}}\rangle \,\langle N'_{\mathbf{n}}| \equiv \left(\prod_{\mathbf{n}} C_{\mathbf{n}}\right) \left(\prod_{\mathbf{n}'} |N_{\mathbf{n}'}\rangle\right) \left(\prod_{\mathbf{n}''} \langle N'_{\mathbf{n}''}|\right), \tag{A.14}$$

where $C_{\mathbf{n}}$ may contain c-numbers, sums, and integrals. Note that

$$\bigotimes_{\mathbf{n}} |N_{\mathbf{n}}\rangle \,\langle N_{\mathbf{n}}| = |\ldots, N_{\mathbf{n}}, \ldots\rangle \,\langle \ldots, N_{\mathbf{n}}, \ldots| \neq \prod_{\mathbf{n}} |N_{\mathbf{n}}\rangle \,\langle N_{\mathbf{n}}|\,. \tag{A.15}$$

With the definition (A.14) we write (A.13) more conveniently

$$\mathbb{1} = \bigotimes_{\mathbf{n}} \int \frac{d\psi^*_{\mathbf{n}}}{\sqrt{2\pi}} \int \frac{d\psi_{\mathbf{n}}}{\sqrt{2\pi}}\, e^{-\psi^*_{\mathbf{n}}\psi_{\mathbf{n}}} \sum_{N_{\mathbf{n}}=0}^{\infty} \frac{(\psi_{\mathbf{n}})^{N_{\mathbf{n}}}}{\sqrt{N_{\mathbf{n}}!}} \,|N_{\mathbf{n}}\rangle \sum_{N'_{\mathbf{n}}=0}^{\infty} \frac{(\psi^*_{\mathbf{n}})^{N'_{\mathbf{n}}}}{\sqrt{N'_{\mathbf{n}}!}} \,\langle N'_{\mathbf{n}}|\,. \tag{A.16}$$

We perform a coordinate transformation

$$\psi_{\mathbf{n}} = r_{\mathbf{n}} e^{i\phi_{\mathbf{n}}} \qquad \Longrightarrow \qquad d\psi^*_{\mathbf{n}} d\psi_{\mathbf{n}} = 2r dr d\phi \tag{A.17}$$

and write (A.16) as

$$\mathbb{1} = \bigotimes_{\mathbf{n}} \int_0^{\infty} dr \frac{r e^{-r^2}}{\pi} \sum_{N_{\mathbf{n}}=0}^{\infty} \sum_{N'_{\mathbf{n}}=0}^{\infty} \frac{r^{N_{\mathbf{n}}+N'_{\mathbf{n}}}}{\sqrt{N_{\mathbf{n}}! N'_{\mathbf{n}}!}} \,|N_{\mathbf{n}}\rangle \,\langle N'_{\mathbf{n}}| \int_0^{2\pi} d\phi_{\mathbf{n}} e^{i\phi_{\mathbf{n}}(N_{\mathbf{n}}-N'_{\mathbf{n}})}. \tag{A.18}$$

On the right-hand side, the second integral is simply $2\pi\delta_{N_{\mathbf{n}},N'_{\mathbf{n}}}$ and therefore the latter term simplifies to

$$\mathbb{1} = \bigotimes_{\mathbf{n}} \sum_{N_{\mathbf{n}}=0}^{\infty} |N_{\mathbf{n}}\rangle \,\langle N_{\mathbf{n}}| \,\frac{2}{N_{\mathbf{n}}!} \int_0^{\infty} dr\, r^{1+2N_{\mathbf{n}}} e^{-r^2}. \tag{A.19}$$

The integral cancels the precedent factor, which leads with (A.14) to the final result

$$\mathbb{1} = \left(\sum_{N_{\mathbf{0}}=0}^{\infty} \cdots \sum_{N_{\mathbf{n}}=0}^{\infty} \cdots\right) |N_{\mathbf{0}}, \ldots, N_{\mathbf{n}}, \ldots\rangle \,\langle N_{\mathbf{0}}, \ldots, N_{\mathbf{n}}, \ldots|\,. \tag{A.20}$$

On the right-hand side we have the completeness relationship in the occupation number representation, which proves our assumption (A.11).

Appendix B

Useful Formulas

In this appendix we derive several mathematical formulas, which are used in this theses.

B.1 Poisson Summation Formula

We prove the Poisson summation formula [47]

$$\boxed{\sum_{m=-\infty}^{\infty} \delta(x-m) = \sum_{n=-\infty}^{\infty} e^{-i2\pi nx}} \quad . \tag{B.1}$$

By multiplying the latter with a function $f(x)$ and integrating over all x, we can equivalently write for Eq. (B.1)

$$\boxed{\sum_{m=-\infty}^{\infty} f(m) = \sum_{n=-\infty}^{\infty} \int_{-\infty}^{\infty} dx\, f(x) e^{-i2\pi nx}} \quad . \tag{B.2}$$

The proof is as follows. The comb function

$$s(x) \equiv \sum_{m=-\infty}^{\infty} \delta(x-m) \tag{B.3}$$

is periodic in x, i.e., we have

$$s(x+k) = s(x), \qquad k = 0, \pm 1, \pm 2, \ldots . \tag{B.4}$$

Therefore, we may expand $s(x)$ in a discrete Fourier series

$$s(x) = \sum_{n=-\infty}^{\infty} s_n e^{i2\pi xn}, \tag{B.5}$$

with the Fourier coefficients

$$s_n = \int_{-\frac{1}{2}}^{\frac{1}{2}} dx\, s(x) e^{-i2\pi xn}. \tag{B.6}$$

Substituting the definition (B.3) into Eq. (B.6) yields

$$s_n = \int_{-\frac{1}{2}}^{\frac{1}{2}} dx \sum_{m=-\infty}^{\infty} \delta(x-m) e^{-i2\pi xn} = 1. \tag{B.7}$$

Using Eqs. (B.3), (B.5) and (B.7) leads directly to the desired Poisson formula (B.1).

B.2 Schwinger Formula

Due to Schwinger [48] we have for $\alpha > 0$ the relation

$$\boxed{\frac{1}{\alpha^x} = \frac{1}{\Gamma(x)} \int_0^\infty d\tau\, \tau^{x-1} e^{-\alpha\tau},} \tag{B.8}$$

where the Gamma function is defined as

$$\Gamma(x) \equiv \int_0^\infty dt\, t^{x-1} e^{-t}. \tag{B.9}$$

The proof of the Schwinger formula (B.8) is straightforward. Performing in Eq. (B.9) a variable substitution $t = \alpha\tau$ and solving for α^{-x} yields (B.8).

A useful application of the Schwinger formula is the integral representation of the logarithmic function. We use the identity

$$\alpha^{-x} = e^{-x\log\alpha} \quad \Rightarrow \quad \frac{\partial}{\partial x}\alpha^{-x} = -\log\alpha\, e^{-x\log\alpha} \tag{B.10}$$

to write the logarithmic function as

$$\log\alpha = -\left.\frac{\partial}{\partial x}\alpha^{-x}\right|_{x=0}, \qquad \alpha > 0. \tag{B.11}$$

Using the Schwinger formula (B.8) in Eq. (B.11) yields the following integral representation of the logarithmic function

$$\boxed{\log\alpha = -\frac{\partial}{\partial x}\left\{\frac{1}{\Gamma(x)}\int_0^\infty d\tau\, \tau^{x-1} e^{-\alpha\tau}\right\}\Big|_{x=0}} \quad . \tag{B.12}$$

B.3 Sum Computation

In the following we give an application of both the Poisson summation formula and the Schwinger formula by calculating the sum

$$S \equiv \sum_{m=-\infty}^{\infty} \log\left(-i2\pi mA + B\right) \quad \text{with} \quad A, B > 0. \tag{B.13}$$

Before we evaluate the latter sum, we have to perform several manipulation. With the Poisson summation formula (B.2) we obtain

$$S = \sum_{n=-\infty}^{\infty} \int_{-\infty}^{\infty} dz \, \log\left(-i2\pi z A + B\right) e^{-i2\pi n z}. \tag{B.14}$$

With the help of the integral representation of the logarithmic function (B.12) we write the latter as

$$S = -\frac{\partial}{\partial x}\left\{ \sum_{n=-\infty}^{\infty} \frac{1}{\Gamma(x)} \int_0^{\infty} d\tau \, \tau^{x-1} e^{-\tau B} \int_{-\infty}^{\infty} dz \, e^{-i2\pi(n+A\tau)z} \right\}\Bigg|_{x=0}. \tag{B.15}$$

With the identity

$$\int_{-\infty}^{\infty} dz \, e^{i2\pi y z} = \delta(y), \tag{B.16}$$

where $\delta(y)$ is the Dirac delta function, Eq. (B.15) turns to

$$S = -\frac{\partial}{\partial x}\left\{ \sum_{n=-\infty}^{\infty} \frac{1}{\Gamma(x)} \int_0^{\infty} d\tau \, \tau^{x-1} e^{-\tau B} \, \delta(n + A\tau) \right\}\Bigg|_{x=0}. \tag{B.17}$$

Evaluating the Schwinger integral leads to

$$S = -\frac{\partial}{\partial x}\left\{ \sum_{n=1}^{\infty} \frac{1}{\Gamma(x)} \left(\frac{A}{n}\right)^{1-x} \frac{e^{-nB/A}}{A} \right\}\Bigg|_{x=0}. \tag{B.18}$$

Before we perform the differentiation with respect to x, we replace the x-dependent functions in (B.18) by their Taylor expansions

$$\tau^{1-x} = \tau + \mathcal{O}(x), \qquad \frac{1}{\Gamma(x)} = x + \mathcal{O}(x^2)\ . \tag{B.19}$$

Thus, the differentiation with respect to x yields

$$S = -\sum_{n=1}^{\infty} \frac{e^{-nB/A}}{n}\ . \tag{B.20}$$

The latter expression is the Taylor expansion of the logarithmic function, so we finally have

$$\boxed{S = \sum_{m=-\infty}^{\infty} \log\left(-i2\pi m A + B\right) = \log\left\{1 - e^{-B/A}\right\}.} \tag{B.21}$$

Appendix C

Green's Function

The Green's function of a system is a important quantity. Once it is calculated, we can derive many important physical quantities from it. For example, in Chapter 11 we have derived the connection between the Green's function and partition function, which is the basic quantity in a thermodynamic system. Therefore, we discuss in this appendix several properties of the Green's function (2.74). We start by rewriting the Green's function in a more convenient way.

C.1 Applying Poisson Summation Formula

We further simplify the Green's function given in Eq. (2.74) by performing the sum over m. The Green's function is periodic in imaginary time. Thus it is valid to apply the Poisson summation formula proved in Appendix B.1. Using (B.2) we may write for (2.74)

$$G^{(0)}_{ab}(\mathbf{x},\tau;\mathbf{x}',\tau') = \sum_{n=-\infty}^{\infty} g^{(0)}_{ab}(\mathbf{x},\mathbf{x}';\tau-\tau'+n\hbar\beta) \tag{C.1}$$

with

$$g^{(0)}_{ab}(\mathbf{x},\mathbf{x}';\tau) = -\frac{\delta_{ab}}{2\pi i}\sum_{\mathbf{n}}\varphi_{\mathbf{n}}(\mathbf{x})\varphi^*_{\mathbf{n}}(\mathbf{x}')\int_{-\infty}^{\infty}d\omega\frac{e^{-i\omega\tau}}{\omega+i(E_{\mathbf{n}}-\mu-a\eta)/\hbar}\ . \tag{C.2}$$

The ω-integral has a pole in the lower half plane, namely, at $\omega = -i(E_{\mathbf{n}p}-\mu-a\eta)/\hbar > 0$. It is easily solved with the help of the residue theorem. For $\tau > 0$, the path of integration on the real axis of the complex plane must be closed by a semicircle in the lower half plane due to convergence reasons. If the integration is performed over the whole real axis, then the contribution of the respective semicircle, which now has an infinite radius, turns out to be zero. Thus, the value of the integral is now completely determined by the residue:

$$\begin{aligned}\tau>0: \quad -\frac{1}{2\pi i}\int_{-\infty}^{\infty}d\omega\frac{e^{-i\omega\tau}}{\omega+i(E_{\mathbf{n}}-\mu-a\eta)/\hbar} &= \mathrm{Res}_{\omega}\,\frac{e^{-i\omega\tau}}{\omega+i(E_{\mathbf{n}}-\mu-a'\eta)/\hbar}\\ &= e^{-(E_{\mathbf{n}}-\mu-a\eta)\tau/\hbar}.\end{aligned} \tag{C.3}$$

The minus sign on the right hand side of the first line is due to the direction of integration.

For $\tau < 0$ we must put the semicircle in the upper half plane, otherwise the integral would diverge. There, the integrand does not have any poles, hence the integral becomes equally zero. Thus, we may summarize

$$-\frac{1}{2\pi i}\int_{-\infty}^{\infty} d\omega \frac{e^{-i\omega\tau}}{\omega + i(E_{\mathbf{n}} - \mu - a\eta)/\hbar} = \Theta(\tau) e^{-(E_{\mathbf{n}}-\mu-a\eta)\tau/\hbar}, \tag{C.4}$$

where $\Theta(\tau)$ is the step function which is defined as

$$\Theta(\tau) = \begin{cases} 1 & \text{for} \quad \tau > 0 \ , \\ 0 & \text{for} \quad \tau < 0 \ . \end{cases} \tag{C.5}$$

The function (C.2) then reads

$$g_{ab}^{(0)}(\mathbf{x}, \mathbf{x}'; \tau) = \Theta(\tau)\delta_{ab} \sum_{\mathbf{n}} \varphi_{\mathbf{n}}(\mathbf{x}) \varphi_{\mathbf{n}}^*(\mathbf{x}') e^{-(E_{\mathbf{n}}-\mu-a\eta)\tau/\hbar}. \tag{C.6}$$

We substitute the latter in Eq. (C.1) and consider two different cases. First we treat the case $\tau - \tau' \in (0, \hbar\beta)$. Performing the geometric m-sum in Eq. (C.1) then yields

$$G_{ab}^{(0)}(\mathbf{x}, \tau; \mathbf{x}', \tau') = \sum_{\mathbf{n}} \varphi_{\mathbf{n}}(\mathbf{x}) \varphi_{\mathbf{n}}^*(\mathbf{x}') \frac{e^{-(E_{\mathbf{n}}-\mu-a\eta)(\tau-\tau')/\hbar}}{1 - e^{-\beta(E_{\mathbf{n}}-\mu-a\eta)}} \, \delta_{ab}. \tag{C.7}$$

In analogy we obtain for $\tau - \tau' \in (-\hbar\beta, 0)$

$$G_{ab}^{(0)}(\mathbf{x}, \tau; \mathbf{x}', \tau') = \sum_{\mathbf{n}} \varphi_{\mathbf{n}}(\mathbf{x}) \varphi_{\mathbf{n}}^*(\mathbf{x}') \frac{e^{-(E_{\mathbf{n}}-\mu-a\eta)(\tau-\tau')/\hbar}}{e^{\beta(E_{\mathbf{n}}-\mu-a\eta)} - 1} \, \delta_{ab}. \tag{C.8}$$

Both cases can be summarized as

$$\boxed{G_{ab}^{(0)}(\mathbf{x}, \tau; \mathbf{x}', \tau') = G_0^{(a)}(\mathbf{x}, \tau; \mathbf{x}', \tau') \, \delta_{ab},} \tag{C.9}$$

where we have introduced the abbreviation

$$G_0^{(a)}(\mathbf{x}, \tau; \mathbf{x}', \tau') = \lim_{\sigma \searrow 0} \sum_{\mathbf{n}} \frac{\varphi_{\mathbf{n}}(\mathbf{x}) \varphi_{\mathbf{n}}^*(\mathbf{x}')}{2\sinh[\beta(E_{\mathbf{n}} - \mu - a\eta)/2]} \tag{C.10}$$

$$\times \left\{ \Theta(\tau - \tau') e^{-(E_{\mathbf{n}}-\mu-a\eta)(\tau-\tau'-\hbar\beta/2)/\hbar} + \Theta(\tau' - \tau) e^{-(E_{\mathbf{n}}-\mu-a\eta)(\tau-\tau'+\hbar\beta/2)/\hbar} \right\},$$

and the hyperbolic sine function $\sinh(x) \equiv -i \sin(ix)$. Note that $G_0^{(0)}(\mathbf{x}, \tau; \mathbf{x}', \tau')$ coincides with the Green's function of a non-interacting Bose gas with no spin.

The representation of the Green's function (C.10) is valid for all space-time point, except for $\tau = \tau'$. Here, due to the step functions in (C.10), we have the problem that

$$\lim_{\tau \nearrow \tau'} G_0^{(a)}(\mathbf{x}, \tau; \mathbf{x}', \tau') \neq \lim_{\tau \searrow \tau'} G_0^{(a)}(\mathbf{x}, \tau; \mathbf{x}', \tau'). \tag{C.11}$$

However, as discussed at the end of Section 2.4, we most correctly have to add an infinitesimal positive constant to τ', which was essentially due to the right time-ordering of the fields. In this case, an equal sign in (C.11) and Eq. (C.10) reduces for $\tau = \tau'$ to the important special case

$$G_0^{(a)}(\mathbf{x}, \tau; \mathbf{x}', \tau) \;=\; \sum_{\mathbf{n}} \frac{\varphi_{\mathbf{n}}(\mathbf{x}) \varphi_{\mathbf{n}}^*(\mathbf{x}')}{\exp\left[\beta(E_{\mathbf{n}} - \mu - a\eta)/2\right] - 1}. \tag{C.12}$$

C.2 Semiclassical Approximation

In spite of the simplifications of the Green's function achieved in the last section, it is still difficult to handle. This originates from the fact, that according to Eq. (C.10), we have to know all the eigenfunctions of the system. However, even if we know all the eigenfunctions, it is still very inconvenient to calculate most of the physical quantities. Therefore, we briefly introduce a semiclassical approximation of the Green's function. We start by noting that Eq. (C.6) coincides with the imaginary one-particle transition amplitude in the following way

$$g_{ab}^{(0)}(\mathbf{x}, \mathbf{x}'; \tau) = \theta(\tau) \delta_{ab}(\mathbf{x}, \tau | \mathbf{x}', 0) \Big|_{E \to E - \mu - a\eta}. \tag{C.13}$$

This is a quite important observation, because it reduces the search of an appropriate semiclassical of the Green's function (C.9) to the extensively studied time evolution amplitude (see for example [47, Chap. 4]). In leading order the semiclassical approximation of the imaginary time evolution amplitude is given by [68, Chap. 2]:

$$(\mathbf{x}, \tau | \mathbf{x}', 0) = \left(\frac{m}{2\pi\hbar\tau}\right)^{3/2} \exp\left[-\frac{m}{2\hbar\tau}(\mathbf{x} - \mathbf{x}')^2 - \frac{\tau}{\hbar} V\left(\frac{\mathbf{x} + \mathbf{x}'}{2}\right)\right]. \tag{C.14}$$

The Fourier transformed of the latter is given by

$$(\mathbf{x}, \tau | \mathbf{x}', 0) = \int \frac{d^3k}{(2\pi)^3} \exp\left\{-i\mathbf{k}(\mathbf{x} - \mathbf{x}') - \frac{\tau}{\hbar}\left[\frac{\hbar^2\mathbf{k}^2}{2m} + V\left(\frac{\mathbf{x} + \mathbf{x}'}{2}\right)\right]\right\}, \tag{C.15}$$

and therefore

$$(\mathbf{x}, \tau | \mathbf{x}', 0) \Big|_{E \to E - \mu - a\eta} = \int \frac{d^3k}{(2\pi)^3} \exp\Big[- i\mathbf{k}(\mathbf{x} - \mathbf{x}') - \tau H_a(\mathbf{x}, \mathbf{x}'; \mathbf{k})/\hbar\Big] \tag{C.16}$$

with

$$H_a(\mathbf{x}, \mathbf{x}'; \mathbf{k}) = \frac{\hbar^2\mathbf{k}^2}{2m} + V\left(\frac{\mathbf{x} + \mathbf{x}'}{2}\right) - \mu - a\eta. \tag{C.17}$$

Substituting Eqs. (C.13), (C.16), (C.17) in Eq. (C.1) and performing the same steps as done in Appendix C.1 yields for Eq. (C.10)

$$G_0^{(a)}(\mathbf{x},\tau;\mathbf{x}',\tau') = \lim_{\sigma\searrow 0}\int \frac{d^3k}{(2\pi)^3}\frac{e^{i\mathbf{k}'(\mathbf{x}-\mathbf{x}')}}{2\sinh[\beta H_a(\mathbf{x},\mathbf{x}';\mathbf{k})/2]} \tag{C.18}$$
$$\times\left\{\Theta(\tau-\tau'-\sigma)e^{-H_a(\mathbf{x},\mathbf{x}';\mathbf{k})(\tau-\tau'-\hbar\beta/2)/\hbar}+\Theta(\tau'-\tau+\sigma)e^{-H_a(\mathbf{x},\mathbf{x}';\mathbf{k})(\tau-\tau'+\hbar\beta/2)/\hbar}\right\}.$$

For equal imaginary time arguments the Green's function is given in semiclassical approximation as

$$G_0^{(a)}(\mathbf{x},\tau;\mathbf{x}',\tau) \;=\; \int\frac{d^3k}{(2\pi)^3}\,\frac{e^{i\mathbf{k}'(\mathbf{x}-\mathbf{x}')}}{\exp\left[\beta H_a(\mathbf{x},\mathbf{x}';\mathbf{k})/2\right]-1}\,. \tag{C.19}$$

This can be integrated out analytically. To do this we expand the fraction in Eq. (C.19) into a Taylor series which yields with Eq. (C.17)

$$\begin{aligned} G_0^{(a)}(\mathbf{x},\tau;\mathbf{x}',\tau) \;&=\; \sum_{n=1}^{\infty}\exp\left\{-\beta n\left[V\left(\frac{\mathbf{x}+\mathbf{x}'}{2}\right)-\mu-a\eta\right]\right\} \\ &\quad\times\int\frac{d^3k}{(2\pi)^3}\,\exp\left[i\mathbf{k}'(\mathbf{x}-\mathbf{x}')-\beta n\frac{\hbar^2\mathbf{k}^2}{2m}\right]. \end{aligned} \tag{C.20}$$

With the substitution

$$\tilde{\mathbf{k}} = \mathbf{k} - i(\mathbf{x}-\mathbf{x}')\frac{m}{\beta n\hbar^2}, \tag{C.21}$$

the latter integral becomes Gaussian and can analytically be integrated out, which leads to the result

$$G_0^{(a)}(\mathbf{x},\tau;\mathbf{x}',\tau) = \frac{1}{\lambda^3}\sum_{n=1}^{\infty}\frac{1}{n^{3/2}}\exp\left\{-n\beta\left[V\left(\frac{\mathbf{x}+\mathbf{x}'}{2}\right)-\mu-a\eta\right]\right\}e^{-\frac{m}{2\hbar^2\beta n}(\mathbf{x}-\mathbf{x}')^2}. \tag{C.22}$$

Setting $\mathbf{x}=\mathbf{x}'$ the latter can be written in the compact form

$$G_0^{(a)}(\mathbf{x},\tau;\mathbf{x},\tau) = \frac{1}{\lambda^3}\,\zeta_{3/2}\left(e^{-\beta[V(\mathbf{x})-\mu-a\eta]}\right), \tag{C.23}$$

where we used the definition of the polylogarithmic function

$$\zeta_\nu(z) = \sum_{n=1}^{\infty}\frac{z^n}{n^\nu}. \tag{C.24}$$

and the de Broglie wave length (1.1).

C.3 Integral

In this section we calculate the spatial

$$I_{aa'} \equiv \int d^3x\, G_0^{(a)}(\mathbf{x},\tau;\mathbf{x},\tau) G_0^{(a')}(\mathbf{x},\tau;\mathbf{x},\tau), \tag{C.25}$$

where the Green's function is given Eq. (C.23). Using Eq. (C.24) we can write

$$I_{aa'} = \frac{1}{\lambda^6} \sum_{n,n'=1}^{\infty} \frac{e^{n\beta(\mu+a\eta)}}{n^{3/2}} \frac{e^{n'\beta(\mu+a'\eta)}}{n'^{3/2}} \int d^3x\, e^{-\beta(n+n')V(\mathbf{x})} \tag{C.26}$$

Considering an isotropic harmonic trap

$$V(\mathbf{x}) = \frac{m}{2}\omega_j^2 x_j^2, \tag{C.27}$$

the integral (C.26) can analytically be integrated out as

$$\boxed{I_{aa'} = \frac{1}{\lambda^3} \frac{1}{(\beta\hbar\tilde{\omega})^3} \zeta_{\frac{3}{2},\frac{3}{2},\frac{3}{2}} \left(z z_\eta^a, z z_\eta^{a'} \right).} \tag{C.28}$$

Here, we have used the fugacity (4.22), the magnetic fugacity (4.23) and defined the generalized polylogarithmic function

$$\zeta_{a,b,c}(z_1,z_2) \equiv \sum_{n=1}^{\infty} \sum_{n'=1}^{\infty} \frac{z_1^n\, z_2^{n'}}{n^a\, n'^b (n+n')^c}. \tag{C.29}$$

Furthermore, we introduce for our convenience the following abbreviation

$$\zeta_{a,b,c}(z) \equiv \zeta_{a,b,c}(z,z). \tag{C.30}$$

The generalized polylogarithmic function has the following property

$$\zeta_{a,b,c}(z_1,z_2) = \zeta_{a-1,b,c+1}(z_1,z_2) + \zeta_{a,b-1,c+1}(z_1,z_2). \tag{C.31}$$

Furthermore, let z_1 and z_2 be a function of x, then taking the derivative of the generalized polylogarithmic function with respective to x yields

$$\frac{d}{dx}\zeta_{a,b,c}(z_1,z_2) = \frac{z_1'}{z_1}\zeta_{a-1,b,c}(z_1,z_2) + \frac{z_2'}{z_2}\zeta_{a,b-1,c}(z_1,z_2) \tag{C.32}$$

and

$$\frac{d}{dx}\zeta_{a,b,c}(z) = \frac{z'}{z}\zeta_{a,b,c-1}(z). \tag{C.33}$$

Appendix D

Angular Momentum

In this appendix we treat several properties of the operator of angular momentum and its consequences.

D.1 Addition of Angular Momentum

We start with briefly discussing the behavior of the total angular momentum of two particles.

D.1.1 Distinguishable Particles

Let us consider a system of two distinguishable particles with the respective one-particle wave function $|f_1 m_1\rangle$ and $|f_2 m_2\rangle$. Here, we omit other quantum number, because we are only interested in the behavior of the angular momentum. If the particles do not have a coupling among each other, for example if the inter-particle distance is large, then the latter wave functions do not change, which is due to the conservation of angular momentum. Once the particles are coupled, they have to be described by a two-particle wave function

$$|f_1 f_2; FM\rangle = \sum_{m_1 m_2} |f_1 f_2; m_1 m_2\rangle \langle f_1 f_2; m_1 m_2 | f_1 f_2; FM\rangle \,, \tag{D.1}$$

where we have multiplied the two-particle wave function from the left side with the unity operator of the spin subspace $f_1 \otimes f_2$

$$\mathbb{1}_{f_1 \otimes f_2} = \sum_{m_1, m_2} |f_1 f_2; m_1 m_2\rangle \langle f_1 f_2; m_1 m_2| \,. \tag{D.2}$$

The scalar products on the right-hand side of Eq. (D.1) are the so-called Clebsch-Gordan coefficients (see, for example, Ref. [53]). Their values are only different from zero if the equations

$$m_1 + m_2 = M \quad \text{and} \quad |f_1 - f_2| \leq F \leq f_1 + f_2 \tag{D.3}$$

are satisfied. Physically, this ensures the conservation of the total momentum. The complete total wave function of the particles is then given by the tensorial product

$$|\tilde{\Psi}\rangle = |1, 2\rangle \otimes |f_1 f_2; FM\rangle \,, \tag{D.4}$$

where $|1,2\rangle$ denotes the contributions to the wave function due to all other quantum number. Consider now two distinguishable particles, where both have an angular momentum one, i.e., $f_1 = f_2 = 1$. Then, according to Eq. (D.3), the two-particle wave function can have a total angular momentum of $F = 0, 1, 2$.

D.1.2 Identical Particles

We treat now the case of two identical particles. It can be shown that the Clebsch-Gordan coefficients obey [53]

$$\langle f_1 f_2; m_1 m_2 | FM \rangle = (-1)^{f_1+f_2-f} \langle f_2 f_1; m_2 m_1 | FM \rangle \tag{D.5}$$

and therefore

$$P_{12} \, |f_1 f_2; FM\rangle = (-1)^{f_1+f_2-F} \, |f_1 f_2; FM\rangle \, , \tag{D.6}$$

where P_{12} is the permutation operator, which interchanges particle one with particle two. The important point for a system of two identical particles is, that the physical prediction must not be altered by permuting the particles, i.e., by changing the particles indices. This is achieved by symmetrizing the two-particle wave function (D.4) with the help of the permutation operator P_{12}

$$|\Psi\rangle = |\tilde{\Psi}\rangle + P_{12}|\tilde{\Psi}\rangle. \tag{D.7}$$

On the other hand we have the properties of the Clebsch-Gordan coefficients (D.5) and (D.6), which yield with Eq. (D.4)

$$|\Psi\rangle = \begin{cases} \Big(|1,2\rangle + |2,1\rangle \Big) \otimes |f_1 f_2; FM\rangle & \text{for} \quad F - f_1 - f_2 \ \text{ even}, \\ \Big(|1,2\rangle - |2,1\rangle \Big) \otimes |f_1 f_2; FM\rangle & \text{for} \quad F - f_1 - f_2 \ \text{ odd}. \end{cases} \tag{D.8}$$

This is a important result, because it states that the parity of the two-particle wave function depends on the total angular momentum. On the other hand we know from quantum mechanics that for two particles, with each having an integer value of angular momentum, the wave-function has to be symmetric and for particles having a half-integer value antisymmetric. Therefore, Eq. (D.8) immediately leads to the result that the *two-particle* wave function of identical Bosons (integer spin) cannot have an odd quantum number of total angular momentum and Fermions (half-integer spin) cannot have an even total angular momentum. Let us consider the above case, where we had two bosons with $f_1 = f_2 = 1$. Assuming them to be equal, we get according the latter discussion, that they can form a two-particle state with total angular momentum of $F = 0, 2$, i.e., in contrast to the case of two distinguishable particles the total angular momentum state $F = 1$ has dropped out.

D.2 Operator Transformation

In this appendix we introduce a operator transformation of the projection operator

$$\mathcal{P}_F = \sum_{M=-F}^{F} |f_1 f_2; FM\rangle \langle f_1 f_2; FM| , \qquad \langle f_1 f_2; FM|f_1 f_2; F'M'\rangle = \delta_{FF'}\delta_{MM'}, \tag{D.9}$$

which is defined for the subspace $f_1 \otimes f_2$. The projection operator $\mathcal{P}_F$ applied on a state $|\Psi\rangle$ yields the contributing wave functions with total angular momentum F.

D.2.1 Distinguishable Particles

We start again with treating the case of distinguishable particles. With the help of the projection operator (D.9) we can write the identity operator $\mathbb{1}$ of the angular momentum subspace $f_1 \otimes f_2$ as

$$\mathbb{1} = \sum_{F=|f_1-f_2|}^{f_1+f_2} \mathcal{P}_F. \tag{D.10}$$

We introduce the operators of angular momentum

$$\mathbf{F}_i^2 \, |f_1 f_2; FM\rangle = f_i(f_i+1) \, |f_1 f_2; FM\rangle \qquad i = 1, 2 \tag{D.11}$$

and the corresponding operator for the total angular momentum

$$\mathbf{F}^2 \, |f_1 f_2; FM\rangle = F(F+1) \, |f_1 f_2; FM\rangle , \qquad \mathbf{F} = \mathbf{F}_1 + \mathbf{F}_2. \tag{D.12}$$

They satisfy the relation

$$\mathbf{F}_1 \cdot \mathbf{F}_2 = \frac{1}{2} \left(\mathbf{F}^2 - \mathbf{F}_1^2 - \mathbf{F}_2^2 \right). \tag{D.13}$$

Multiplying Eq. (D.13) from the right side with the unity operator (D.10) and using Eqs. (D.9), (D.11)–(D.13) leads to the identity

$$\mathbf{F}_1 \cdot \mathbf{F}_2 = \sum_{F=|f_1-f_2|}^{f_1+f_2} \lambda_F \mathcal{P}_F$$

with the coefficients

$$\lambda_F = \frac{1}{2} \Big[F(F+1) - f_1(f_1+1) - f_2(f_2+1) \Big]. \tag{D.14}$$

Using Eq. (D.9) we get the property $\mathcal{P}_F \mathcal{P}_{F'} = \mathcal{P}_F \delta_{FF'}$. Applying this relation to Eq. (D.14) yields the generalized result

$$(\mathbf{F}_1 \cdot \mathbf{F}_2)^n \;\; = \sum_{F=|f_1-f_2|}^{f_1+f_2} \lambda_F^n \mathcal{P}_F, \qquad n = 0, 1, 2, \ldots . \tag{D.15}$$

With (D.15) we have a set of linear equation which can be summarized in the following $k \times k$-matrix equation

$$\begin{pmatrix} (\mathbf{F}_1 \cdot \mathbf{F}_2)^{k-1} \\ (\mathbf{F}_1 \cdot \mathbf{F}_2)^{k-2} \\ \vdots \\ (\mathbf{F}_1 \cdot \mathbf{F}_2) \\ \mathbb{1} \end{pmatrix} = \mathbf{V} \begin{pmatrix} \mathcal{P}_{f_1+f_2} \\ \mathcal{P}_{f_1+f_2-1} \\ \vdots \\ \mathcal{P}_{|f_1-f_2|+1} \\ \mathcal{P}_{|f_1-f_2|} \end{pmatrix}, \tag{D.16}$$

where $k-1 = j_1 + j_2 - |j_1 - j_2|$ and $\mathbf{V}$ is a matrix of Vandermond's form

$$\mathbf{V} = \begin{pmatrix} \lambda_{f_1+f_2}^{k-1} & \lambda_{f_1+f_2-1}^{k-1} & \cdots & \lambda_{|f_1-f_2|}^{k-1} \\ \lambda_{f_1+f_2}^{k-2} & \lambda_{f_1+f_2-1}^{k-2} & \cdots & \lambda_{|f_1-f_2|}^{k-2} \\ \vdots & \vdots & \ddots & \vdots \\ \lambda_{f_1+f_2}^{1} & \lambda_{f_1+f_2-1}^{1} & \cdots & \lambda_{|f_1-f_2|}^{1} \\ 1 & 1 & \dots & 1 \end{pmatrix} \tag{D.17}$$

with the characteristic determinant (see Ref. [42])

$$\det \mathbf{V} = \prod_{i>j} (\lambda_i - \lambda_j). \tag{D.18}$$

According to Eq. (D.14) we always have $\lambda_i \neq \lambda_j$ for $i \neq j$; $i, j \geq 0$. Therefore, the Vandermond's determinant (D.18) is non-vanishing, hence the inverse $\mathbf{V}^{-1}$ exists. Thus, we are able to express the projectors $\mathcal{P}_n$ in terms of the operators $(\mathbf{F}_1 \cdot \mathbf{F}_2)^m$

$$\mathcal{P}_F = \sum_{F'=0}^{k-1} (\mathbf{V}^{-1})_{FF'} (\mathbf{F}_1 \cdot \mathbf{F}_2)^{F'}. \tag{D.19}$$

D.2.2 Identical Particles

We now regard a system of identical Bosons and Fermions, respectively. As discussed in Appendix D.1.2 we always have for a bosonic and fermonic system that $\mathcal{P}_F |\Psi\rangle = 0$ for F an even and odd number, respectively. Therefore, we can set the respective projectors in (D.15) equally zero. After removing the respective row from the matrix $\mathbf{V}$ we again obtain a matrix of the Vandermond's form, where we can use the arguments as done above.

We discuss the particular case of two identical bosons with spin one. The matrix equation (D.16) then reads

$$\begin{pmatrix} \mathbf{F}_1 \cdot \mathbf{F}_2 \\ \mathbb{1} \end{pmatrix} = \begin{pmatrix} \lambda_2 & \lambda_0 \\ 1 & 1 \end{pmatrix} \begin{pmatrix} \mathcal{P}_2 \\ \mathcal{P}_0 \end{pmatrix} \tag{D.20}$$

Solving for the projection operators leads to

$$\mathcal{P}_0 = \frac{1}{3}\left(\mathbb{1} - \mathbf{F}_1 \cdot \mathbf{F}_2\right), \tag{D.21}$$

$$\mathcal{P}_2 = \frac{1}{3}\left(2\mathbb{1} + \mathbf{F}_1 \cdot \mathbf{F}_2\right). \tag{D.22}$$

Considering now a delta potential of the following

$$V^{(\mathrm{int})}\left(\mathbf{x}_1 - \mathbf{x}_2\right) = \delta\left(\mathbf{x}_1 - \mathbf{x}_2\right)\Big(g_0\mathcal{P}_0 + g_2\mathcal{P}_2\Big) \tag{D.23}$$

then we can write this equally as

$$V^{(\mathrm{int})}\left(\mathbf{x}_1 - \mathbf{x}_2\right) = \delta\left(\mathbf{x}_1 - \mathbf{x}_2\right)\Big(c_0\mathbb{1} + c_2\mathbf{F}_1 \cdot \mathbf{F}_2\Big), \tag{D.24}$$

with the coefficients

$$c_0 = \frac{1}{3}(2g_2 + g_0), \tag{D.25}$$

$$c_2 = \frac{1}{3}(g_2 - g_0). \tag{D.26}$$

We can also consider a delta potential for spin two, spin three, or higher order particles. We treat the first two examples explicitly. For two particles identical particles with $f = 2$ the delta potential is given by

$$V^{(\mathrm{int})}\left(\mathbf{x}_1 - \mathbf{x}_2\right) = \delta\left(\mathbf{x}_1 - \mathbf{x}_2\right)\Big(g_0\mathcal{P}_0 + g_2\mathcal{P}_2 + g_4\mathcal{P}_4\Big). \tag{D.27}$$

The transformed potential then reads

$$V^{(\mathrm{int})}(\mathbf{x}_1, \mathbf{x}_2) = \delta(\mathbf{x}_1 - \mathbf{x}_2)\Big[c_0 + c_2\mathbf{F}_1 \cdot \mathbf{F}_2 + c_4(\mathbf{F}_1 \cdot \mathbf{F}_2)^2\Big] \tag{D.28}$$

with the coefficients

$$\begin{aligned} c_0 &= \frac{9}{35}g_4 + \frac{8}{7}g_2 - \frac{2}{5}g_0, \\ c_2 &= \frac{9}{70}g_4 - \frac{2}{21}g_2 - \frac{1}{30}g_0, \\ c_4 &= \frac{1}{70}g_4 - \frac{1}{21}g_2 + \frac{1}{30}g_0. \end{aligned}$$

Such a system has been realized for ^{87}Rb [27, 31]. In contrast to a spinor condensate with spin one, the Gross-Pitaevskii equations of the spin 2 system are not integrable anymore, because of the large number of degrees of freedom. On the contrary, it shows a chaotic behavior.

Analogously, we find for identical particles with spin three

$$V^{(\mathrm{int})}\left(\mathbf{x}_1 - \mathbf{x}_2\right) = \delta\left(\mathbf{x}_1 - \mathbf{x}_2\right)\Big(g_0\mathcal{P}_0 + g_2\mathcal{P}_2 + g_4\mathcal{P}_4 + g_6\mathcal{P}_6\Big) \tag{D.29}$$

and therefore

$$V^{(\mathrm{int})}(\mathbf{x}_1,\mathbf{x}_2) \;=\; \delta(\mathbf{x}_1-\mathbf{x}_2)\Big[c_0+c_2\mathbf{F}_1\cdot\mathbf{F}_2+c_4(\mathbf{F}_1\cdot\mathbf{F}_2)^2+c_6(\mathbf{F}_1\cdot\mathbf{F}_2)^3\Big] \qquad \text{(D.30)}$$

with

$$\begin{aligned}
c_0 &= -\frac{4}{231}g_6+\frac{27}{77}g_4-\frac{1}{7}g_2+\frac{20}{21}g_0,\\
c_2 &= -\frac{1}{231}g_6+\frac{117}{770}g_4-\frac{1}{7}g_2-\frac{1}{210}g_0,\\
c_4 &= \frac{5}{4158}g_6+\frac{3}{385}g_4-\frac{13}{378}g_2+\frac{8}{315}g_0,\\
c_6 &= -\frac{1}{4158}g_6-\frac{1}{770}g_4+\frac{1}{378}g_2-\frac{1}{630}g_0.
\end{aligned} \qquad \text{(D.31)}$$

A system with particles of spin three, namely ^{52}Cr has already successfully be Bose-Einstein condensed [66], but so far only within a magnetical trap, i.e., most of the spin degrees of freedom are frozen out. On the other hand, for higher spins the magnetic dipole moment of the atoms, become so strong, that the latter delta potential has to be modified by a respective dipole correction.

List of Figures

Bibliography

[1] S. N. Bose, *Plancks Gesetz und Lichtquantenhypothese*, Z. Phys. **26**, 178 (1924).

[2] A. Einstein, *Quantentheorie des einatomigen idealen Gases*, Sitzungsb. Kgl. Preuss. Akad. Wiss., 261 (1924).

[3] A. Einstein, *Quantentheorie des einatomigen idealen Gases. Zweite Abhandlung*, Sitzungsb. Kgl. Preuss. Akad. Wiss., 3 (1925);
Internet: `http://www.lorentz.leidenuniv.nl/history/Einstein_archive/`

[4] M. H. Anderson, J. R. Ensher, M. R. Matthews, C. E. Wiemann, and E. A. Cornell, *Observation of Bose-Einstein Condensation in a Dilute Atomic Vapor*, Science **269**, 198 (1995).

[5] C. C. Bradley, C. A. Sackett, J. J. Tollett, and R. G. Hule, *Evidence of Bose-Einstein Condensation in an Atomic Gas with Attractive Interactions*, Phys. Rev. Lett. **75**, 1687 (1995).

[6] K. B. Davis, M.-O. Mewes, M. R. Andrews, N. J. van Druten, D. S. Durfee, D. M. Kurn, and W. Ketterle, *Bose-Einstein Condensation in a Gas of Sodium Atoms*, Phys. Rev. Lett. **75**, 3969 (1995).

[7] S. Chu, *Nobel Lecture: The Manipulation of Neutral Particles*, Rev. Mod. Phys. **70**, 685 (1998).

[8] C. N. Cohen-Tannoudji, *Nobel Lecture: Manipulating Atoms with Photons*, Rev. Mod. Phys. **70**, 707 (1998).

[9] W. D. Philips, *Nobel Lecture: Laser Cooling and Trapping of Neutral Atom*, Rev. Mod. Phys. **70**, 721 (1998).

[10] W. Ketterle and N. J. van Druten, *Evaporative Cooling of Trapped Atoms*, Adv. Atom. Mol. Opt. Phys. **37**, 181 (1996).

[11] H. Feshbach, *Unified Theory of Nuclear Reactions*, Ann. Phys. (N.Y.) **5**, 357 (1958).

[12] S. Inouye, M. R. Andrews, J. Stenger, H.-J. Miesner, D. M. Stamper-Kurn, and W. Ketterle, *Observation of Feshbach Resonances in a Bose-Einstein Condensate*, Nature **392**, 151 (1998).

[13] E. A. Donley, N. R. Claussen, S. T. Thompson, and C. E. Wieman, *Atom-Molecule Coherence in a Bose-Einstein Condensate*, Nature **417**, 529 (2002).

[14] M. W. Zwierlein, C. A. Stan, C. H. Schunck, S. M. Raupach, S. Gupta, Z. Hadzibabic, and W. Ketterle, *Observation of Bose-Einstein Condensation of Molecules*, Phys. Rev. Lett. **91**, 250401 (2003).

[15] M. Greiner, C. A. Regal, and D. S. Jin, *Emergence of a Molecular Bose-Einstein Condensate from a Fermi Gas*, Nature **426**, 537 (2003).

[16] M. Bartenstein, A. Altmeyer, S. Riedl, S. Jochim, C. Chin, J. H. Denschlag, and R. Grimm, *Crossover from a Molecular Bose-Einstein Condensate to a Degenerate Fermi Gas*, Phys. Rev. Lett. **92**, 120401 (2004).

[17] M. P. A. Fisher, P. B. Weichman, G. Grinstein, and D. S. Fisher, *Boson Localization and the Superfluid-Insulator Transition*, Phys. Rev. B **40**, 1 (1989).

[18] D. Jaksch, C. Bruder, J. I. Cirac, C. W. Gardiner, and P. Zoller, *Cold Bosonic Atoms in Optical Lattices*, Phys. Rev. Lett. **81**, 15 (1998).

[19] M. Greiner, O. Mandel, T. Esslinger, T. W. Hänsch, and I. Bloch, *Quantum Phase Transition from a Superfluid to a Mott Insulator in a Gas of Ultracold Atoms*, Nature **415**, 39 (2002).

[20] I. Bloch, T. Hänsch, and T. Esslinger, *Atom Laser with a CW Output Coupler*, Phys. Rev. Lett. **82**, 3008 (1999).

[21] F. S. Cataliotti, S. Burger, C. Fort, P. Maddaloni, F. Minardi, A. Trombettoni, A. Smerzi, and M. Inguscio, *Josephson Junction Arrays with Bose-Einstein Condensates*, Science **293**, 843 (2001).

[22] T.-L. Ho, *Spinor Bose Condensates in Optical Traps*, Phys. Rev. Lett. **81**, 742 (1998).

[23] T. Ohmi and K. Machida, *Bose-Einstein Condensation with Internal Degrees of Freedom in Alkali Atom Gases*, J. Phys. Soc. Jap. **67**, 1822 (1998).

[24] W. Ketterle, *Spinor Condensates and Light Scattering from Bose-Einstein Condensates*, Proceeding from Les Houches 1999 Summer School, Session LXXII,
E-Print: /cond-mat/0005001

[25] D. M. Stamper-Kurn, M. R. Andrews, A. P. Chikkatur, S. Inouye, H.-J. Miesner, J. Stenger, and W. Ketterle, *Optical Confinement of a Bose-Einstein Condensate*, Phys. Rev. Lett. **80**, 2027 (1998).

[26] M.-S. Chang, C. D. Hamley, M. D. Barrett, J. A. Sauer, K. M. Fortier, W. Zhang, L. You, and M. S. Chapman, *Observation of Spinor Dynamics in Optically Trapped ^{87}Rb Bose-Einstein Condensates*, Phys. Rev. Lett. **92**, 140403 (2004).

[27] H. Schmaljohann, M. Erhard, J. Kronäger, M. Kottke, S. van Staa, L. Cacciapuoti, J. J. Arlt, K. Bongs, and K. Sengstock, *Dynamics of $F = 2$ Spinor Bose-Einstein Condensates*, Phys. Rev. Lett. **92**, 040402 (2004).

[28] L. Santos and T. Pfau, *Spin-3 Chromium Bose-Einstein Condensates*, Phys. Rev. Lett. **96**, 190404 (2006).

[29] Z. Hadzibabic, C. A. Stan, K. Dieckmann, S. Gupta, M. W. Zwierlein, A. Görlitz, and W. Ketterle, *Two-Species Mixture of Quantum Degenerate Bose and Fermi Gases*, Phys. Rev. Lett. **88**, 160401 (2002).

[30] G. Roati, F. Riboli, G. Modugno, and M. Inguscio, Fermi-Bose, *Quantum Degenerate ^{40}K–^{87}Rb Mixture with Attractive Interaction*, Phys. Rev. Lett. **89**, 150403 (2002).

[31] T. Kuwamoto, T. Araki, T. Eno, and T. Hirano, *Magnetic Field Dependence of the Dynamics of ^{87}Rb Spin-2 Bose-Einstein Condensates*, Phys. Rev. A **69**, 063604 (2004).

[32] J. M. McGuirk, H. J. Lewandowski, D. M. Harber, T. Nikuni, J. E. Williams, and E. A. Cornell, *Spatial Resolution of Spin Waves in an Ultracold Gas*, Phys. Rev. Lett. **89**, 090402 (2002).

[33] Q. Gu, K. Bongs, and K. Sengstock, *Spin Waves in Ferromagnetically Coupled Spinor Bose Gases*, Phys. Rev. A **70**, 063609 (2004).

[34] C. K. Law, H. Pu, and N. P. Bigelow, *Quantum Spins Mixing in Spinor Bose-Einstein Condensates*, Phys. Rev. Lett. **81**, 5257 (1998).

[35] H. Pu, C. K. Law, S. Raghavan, J. H. Eberly, and N. P. Bigelow, *Spin-Mixing Dynamics of a Spinor Bose-Einstein Condensate*, Phys, Rev. A **60**, 1463 (1999).

[36] M.-S. Chang, Q. Qin, W. Zhang, L. You, and M. S. Chapman, *Coherent Spinor Dynamics in a Spin-1 Bose Condensate*, Nat. Phys. **1**, 111 (2005).

[37] J. Kronjäger, C. Becker, M. Brinkmann, R. Walser, P. Navez, K. Bongs, and K. Sengstock, *Evolution of a Spinor Condensate: Coherent Dynamics, Dephasing, and Revivals*, Phys. Rev. A **72**, 063619 (2005).

[38] A. Widera, F. Gerbier, S. Fölling, T. Gericke, O. Mandel, and I. Bloch, *Coherent Collisional Spin Dynamics in Optical Lattices*, Phys. Rev. Lett. **95**, 190405 (2005).

[39] A. E. Leanhardt, T. A. Pasquini, M. Saba, A. Schirotzek, Y. Shin, D. Kielpinski, D. E. Pritchard, and W. Ketterle, *Cooling Bose-Einstein Condensates Below 500 Picokelvin*, Science **301**, 1513 (2003).

[40] E. Arimondo, M. Inguscio, and P. Violino, *Experimental Determinations of the Hyperfine Structure in the Alkali Atoms*, Rev. Mod. Phys. **49**, 31 (1977).

[41] R. Grimm, M. Weidemüller, and Y. B. Ovchinnikov, *Optical Dipole Trap for Neutral Atoms*, Adv. At. Mol. Opt. Phys. **42**, 95 (2000).

[42] F. R. Gantmacher, *Matrizentheorie* (Springer-Verlag, Berlin, 1986).

[43] A. L. Fetter and J. D. Walecka, *Quantum Theory of Many-Particle Systems* (McGraw-Hill, New York, 1971).

[44] J. W. Negele and H. Orland, *Quantum Many-Particle Systems* (AddisonWesley, New York, 1988).

[45] K. Huang, *Statistical Mechanics*, Second Edition (John Wiley & Sons, New York, 1987).

[46] H. Kleinert, *Collective Quantum Fields*, Fortschr. Phys. **26**, 565 (1978);
Internet: `http://www.physik.fu-berlin.de/~kleinert/55/55.pdf`

[47] H. Kleinert, *Path Integrals in Quantum Mechanics, Statistics, Polymer Physics, and Financial Markets*, Forth Edition (World Scientific Publishing Co., Singapore, 2006);
Internet: `http://www.physik.fu-berlin.de/~kleinert/lecture-notes.html`

[48] H. Kleinert and V. Schulte-Frohlinde, *Critical Properties of* Φ^4*–Theories* (World Scientific, Singapore, 2001).

[49] S. Coleman and E. Weinberg, *Radiative Corrections as the Origin of Spontaneous Symmetry Breaking*, Phys. Rev. D **7**, 1888 (1973).

[50] R. Jackiw, *Functional Evaluation of the Effective Potential*, Phys. Rev. D **9**, 1686 (1974).

[51] H. T. C. Stoof, *Lecture Notes for Les Houches Summer School on Coherent Atom Waves*, E-Print: /cond-mat/9910441

[52] T. P. Meyrath, F. Schreck, J. L. Hanssen, C.-S. Chu, and M. G. Raizen, *Bose-Einstein Condensate in a Box*, Phys. Rev. A **71**, 041604(R) (2005).

[53] W. Nolting, *Quantenmechanik. Teil 1 / 2* (Springer-Verlag, Berlin, 2004).

[54] E. P. Gross, *Structure of a Quantized Vortex in Boson Systems*, Nuovo Cimento **20**, 454 (1961)

[55] L. P. Pitaevskii *Vortex Lines in an Imperfect Bose Gas*, Soviet Phys. JETP **13**, 2 (1961).

[56] T. Isoshima, T. Ohmi, and K. Machida, *Double Phase Transitions in Magnetized Spinor Bose-Einstein Condensation*, J. Phys. Soc. Jap. **69**, 3864 (2000).

[57] R. P. Feynman and H. Kleinert, *Effective Classical Partition Functions*, Phys. Rev. A **34**, 5080 (1986).

[58] G. C. Wick, *The Evaluation of the Collision Matrix*, Phys. Rev. **80**, 2 (1950).

[59] A. Pelster and K. Glaum, *Many-Body Vacuum Diagrams and Their Recursive Graphical Construction*, Phys. Stat. Sol. B **237**, 72 (2003).

[60] S. Giorgini, L. P. Pitaevskii, and S. Stringari, *Condensate Fraction and Critical Temperature of a Trapped Interacting Bose Gas*, Phys. Rev. A **54**, R4633 (1996).

[61] P. Arnold and B. Tomášik, *T_c for Trapped Dilute Bose Gases: A Second-Order Result*, Phys. Rev. A **64**, 053609 (2001).

[62] F. Gerbier, J. H. Thywissen, S. Richard, M. Hugbart, P. Bouyer, and A. Aspect, *Critical Temperature of a Trapped, Weakly Interacting Bose Gas*, Phys. Rev. Lett. **92**, 030405 (2004).

[63] E. G. M. van Kempen, S. J. J. M. F. Kokkelmans, D. J. Heinzen, and B. J. Verhaar, *Interisotope Determination of Ultracold Rubidium Interactions from Three High-Precision Experiments*, Phys. Rev. Lett. **88**, 093201 (2002).

[64] A. Crubellier, O. Dulieu, F. Masnou-Seeuws, M. Elbs, H. Knöckel, and E. Tiemann, *Simple Determination of Na2 Scattering Lengths Using Observed Bound Levels at the Ground State Asymptote*, Eur. Phys. J. D **6**, 211 (1999).

[65] W. Zhang, Su Yi, and L. You, *Bose-Einstein Condensation of Trapped Interacting Spin-1 Atoms*, Phys. Rev. A **70**, 043611 (2004).

[66] A. Griesmaier, J. Werner, S. Hensler, J. Stuhler, and T. Pfau, *Bose-Einstein Condensation of Chromium*, Phys. Rev. Lett. **94**, 160401 (2005).

[67] F. Dalfovo, S. Giorgini, L. P. Pitaevskii, and S. Stringari, *Theory of Bose-Einstein Condensation in Trapped Gases*, Rev. Mod. Phys. 71, 463 (1999).

[68] A. Pelster, *Lecture Notes on Bose-Einstein Condensation* (in german); Internet: `http://www.theo-phys.uni-essen.de/tp/ags/pelster~dir/SS04/skript.pdf`

[69] L. Pitaevskii and S. Stringari, *Bose-Einstein Condensation* (Clarendon Press, Oxford, 2003).

[70] C. V. Ciobanu, S.-K. Yip, and T.-L. Ho, *Phase diagrams of F=2 spinor Bose-Einstein condensates*, Phys. Rev. A **61**, 033607 (2000).

[71] S. Yi, L. You, and H. Pu, *Quantum Phases of Dipolar Spinor Condensates*, Phys. Rev. Lett. **93**, 040403 (2004).

[72] B. H. Bransden and C. J. Joachain, *Physics of Atoms and Molecules* (Longman, New York, 1983).

[73] K. Huang and C. N. Yang, *Quantum-Mechanical Many-Body Problem with Hard-Sphere Interaction*, Phys. Rev. **105**, 767 (1957).

Danksagung

Zuallererst möchte ich mich vielmals bei Prof. Dr. Hagen Kleinert dafür bedanken, dass er es mir ermöglicht hat in seiner Gruppe meine Diplomarbeit abzulegen. Herr Kleinert stand immer mit seinem unglaublich breitem Wissen über die Physik mit Rat und Tat zur Seite.

Zu sehr großem Dank bin ich auch Herrn PD Dr. Pelster verpflichtet, der etliche Stunden damit aufopferte, mich durch die Untiefen der feldtheoretischen Quanten-Statistik zu manövrieren, ohne dabei merklich an Geduld zu verlieren. Im Besonderen hat mich seine beständig hohe Motivation und Aufopferungsbereitschaft beeindruckt, mit der es meist schaffte nicht nur mich zu begeistern und zu motivieren.

Als nächstes gilt mein Dank Konstantin Glaum, der sich immer ausgiebig für einen Zeit nahm, wenn man ihn gebraucht hat. Ausserdem hat er das Wunder vollbracht, mein ganzes Diplom vollständig durchzulesen und dabei auch noch die kleinsten Fehler aus den Formeln "herauszuholen", wofür ich ihm wirklich sehr dankbar bin.

Mein Dank geht auch an Aristeu Lima, der mir bei der Korrektur des Diploms hilfreich zur Seite stand.

Für die überaus angenehme Atmosphäre in der Gruppe danke ich zunächst meinen Zimmergenossen Walja Korolevski, Sonja Overesch und Moritz Schütte. Ausserdem den restlichen Leuten aus der Gruppe: Steffen Röthel, Sebastian Kling, Tim, Alexander Hoffmann und Francisco Santos. Nicht zu vergessen sind auch Flavio Nogueira und den immer gut gelaunten Jürgen Dietel.

Ein ganz großes Dankeschön an Jo, welche während der ganzen Zeit immer für mich da war.

Der größte Dank gilt meiner Mutter und meinem Vater, welche mich immer in jeglicher Hinsicht unterstützt haben und für mich da sind.